2017

Elucidation of regulatory mechanisms of the ITK and its substrate PLCγ1

Sujan Devkota
Iowa State University

Elucidation of regulatory mechanisms of the ITK and its substrate PLCγ1

by

Sujan Devkota

A dissertation submitted to the graduate faculty

in partial fulfillment of the requirements for the degree of

DOCTOR OF PHILOSOPHY

Major: Biochemistry

Program of Study Committee:
Amy H. Andreotti, Major Professor
Aragula Gururaj Rao
Richard Honzatko
Scott Nelson
Vincenzo Venditti

The student author and the program of study committee are solely responsible for the content of this dissertation. The Graduate College will ensure this dissertation is globally accessible and will not permit alterations after a degree is conferred.

Iowa State University

Ames, Iowa

2017

TABLE OF CONTENTS

ACKNOWLEDGMENTS

I would like to express my thanks to my major professor, Dr. Amy Andreotti, who has provided me with invaluable guidance and mentorship throughout my Ph.D. I would like to thank her for teaching me to be critical and detail oriented. It was tremendous learning experience for me working with her. Her mentorship has provided me with the opportunity to grow a scientific researcher and as person as well.

I would also like to thank all the past and present members of in the Dr. Amy Andreotti's lab. I would especially like to thank Dr. Raji Joseph for training me to carryout various experiments. She has helped me tremendously to grow as experimental scientist. I would also like to thank Dr. Bruce Fulton from NMR facility at Iowa State University, for helping me to understand NMR experiments as well as helping me to set up NMR experiments.

I would also like to thank my family, and friends for providing me with support and encouragement throughout the course of my Ph.D.

ABSTRACT

This dissertation studies the regulatory mechanism of IL-2 inducible tyrosine kinase (ITK) and its substrate phospholipase C γ1 (PLCγ1). ITK and PLCγ1 are key mediators of the signaling pathway downstream of the T cell receptor that results in the T cell part of the adaptive immune response. In T cells, ITK is phosphorylated and activated by LCK. ITK then phosphorylates PLCγ1 at tyrosine 783 and activates phospholipase activity. This phosphorylation is dependent upon various coordinated intermolecular and intramolecular interactions within and between ITK and PLCγ1. This dissertation identifies and characterizes various regulatory interactions in ITK and its substrate PLCγ1 that regulates ITK mediated phosphorylation of PLCγ1.

For ITK, this thesis explores the function of the N-terminal Pleckstrin homology (PH) domain in regulating the activation of the ITK. The ITK PH domain engages in direct interaction with ITK kinase domain and the region of the kinase domain interaction is mapped in the ITK PH domain. Mutations in ITK PH domain, that disrupts its interaction with kinase domain, lead to the increase in the activity of ITK. The ITK interaction surface mapped on the ITK PH domain lies adjacent to its phosphatidylinositol (3,4,5)-triphosphate (PI (3,4,5) P_3) binding pocket. Hence, IP_4, the soluble head group of (PI (3,4,5) P_3) competes with the ITK kinase domain for ITK PH domain binding. Also, PI (3,4,5) P_3 binding of ITK PH domain increases the catalytic activity of the ITK. In addition, PI (3,4,5) P_3 binding increases the activation loop Y511

accessibility for LCK phosphorylation. This study expanded our knowledge on regulation of ITK by its N terminal PH domain (Chapter 3).

ITK is a key modulator of immune response and has therefore been very attractive target for small molecule intervention for immunity related diseases such as autoimmune disease and asthma. The key novel regulatory ITK PH/kinase site can be a plausible allosteric target for small molecule discovery efforts. Part of this thesis contributes to assay development to detect the ITK PH/Kinase interaction in cells. Bimolecular Fluorescence complementation (BiFC) assay confirms that the ITK PH/Kinase interaction occurs in cell (Chapter 4). This assay can now be used to screen for small molecules that modulate the ITK PH/Kinase interaction.

For PLCγ1, this thesis studies the mechanism of disruption of its autoinhibitory conformation. The PLCγ1 autoinhibitory conformation is characterized by an intramolecular interaction between the C terminal SRC homology 2 (SH2C) domain and the adjacent linker containing Y783. This conformation makes the crucial phosphorylation target (Y783) inaccessible to ITK. I have described the mechanism on how this autoinhibitory interaction is broken (Chapter 2). Our results suggest that the scaffold protein SLP-76 disrupts the autoinhibitory PLCγ1 conformation. More specifically, SLP-76 phosphotyrosine 173 (Y173) binds the SH2C domain of the PLCγ1, competing with the autoinhibitory conformation of PLCγ1 and releasing the linker, making the Y783 more accessible to ITK. Our results identify the new role of the scaffold protein SLP-76 adding to its previously described role in co-localizing the enzyme and

substrate pair. This role is defined as the substrate priming as SLP-76 primes PLCγ1, the substrate for ITK for efficient phosphorylation. Our results provide further understanding of the regulation of ITK mediated phosphorylation of PLCγ1 and create a foundation for small molecule discovery efforts that should yield new ways to either enhance or diminish T cell function.

CHAPTER 1

GENERAL INTRODUCTION

Signal transduction in cells is mediated by protein phosphorylation, carried out by enzymes known as kinases. Protein kinases specifically transfer the γ-phosphate from adenosine triphosphate (ATP) to hydroxyl containing side chains of the substrate protein. Tyrosine kinases are responsible for phosphorylating tyrosine residues on their substrates and are divided into two categories, receptor tyrosine kinases and non-receptor tyrosine kinases. Kinases play crucial roles in various cellular processes like signal transduction, cell cycle, metabolism and apoptosis (1, 2). Links between abnormal regulation of protein phosphorylation and diseases have been found, and hence highlight the need to study the complex mechanism of regulation of kinases and their substrates (3, 4).

Our lab studies non-receptor tyrosine kinases belonging to TEC family, more specifically, two homologs, Interleukin-2 inducible tyrosine kinase (ITK) and Bruton's tyrosine kinase (BTK), which are primarily expressed and mediate signal transduction in T-cells and B-cells, respectively (5). ITK and BTK phosphorylate the substrate Phospholipase C γ1 (PLCγ1) and Phospholipase C γ2 (PLCγ2) respectively, and activate these lipases. Proper regulation of both ITK and BTK is crucial for normal signal transduction within these immune cells. Deregulation of these kinases causes a failure in T and B cells to develop normally, resulting in compromised immunity, making individuals vulnerable to severe infections (3). Mutations in Btk are the cause of X-linked agammaglobulinemia (XLA), a disease characterized by failure to develop appropriate

immune responses (6). These mutations, causes loss of BTK activity resulting in significant decrease mature B cells in blood and reduced immunoglobulins, leading to a severely compromised immune response. Similarly, loss of function mutations in ITK leads to fatal Epstein-Barr virus induced lymphoproliferative diseases (EBV-LPD) (7). As well, ITK has also been shown to play a role in HIV infectivity and replication (3, 8, 9). In addition, ITK has been linked to autoimmune diseases like multiple sclerosis and inflammatory bowel diseases (10). The connections between ITK and various immunological diseases make ITK an attractive drug target. However, better understanding of the specific molecular regulatory mechanisms that control ITK enzyme activity is essential. Hence this dissertation deciphers the regulatory mechanisms of ITK and its substrate PLCγ1 that govern the activity of the ITK.

ITK and PLCγ1 are both modular proteins regulated by complex intramolecular interactions within their domains. In addition, PLCγ1 phosphorylation takes place in the context of larger signalosome complex formed by the scaffold proteins SRC homology 2 domain containing leucocyte protein of 76 kDa (SLP-76), linker of activation of T cells (LAT) and GRB2-related adapter protein (GADS) (11). This dissertation investigates the intermolecular interactions between ITK, PLCγ1 and the adaptor protein SLP-76 that is necessary for selective phosphorylation of PLCγ1 by ITK. In addition, it also investigates the autoregulation mechanism of ITK. We have identified a specific intramolecular interaction within ITK that maintains ITK in its autoinhibited state. Also, this dissertation describes the mechanism of transition from the ITK autoinhibited state to the ITK activated state required for proper T cell signaling.

Literature Review

1. ITK, PLCγ1 and SLP-76 in the T cell signaling pathway

ITK, PLCγ1 and SLP-76 are involved in signal transduction downstream of the T-cell receptor (TCR). The T cell receptor is activated when antigen bound by the Major Histocompatibility Complex I (MHC I) is engaged by the TCR (12). This process is also called TCR ligation. TCR ligation is followed by rapid activation of LCK and ZAP-70 tyrosine kinases. These kinases then phosphorylate different molecules. LCK phosphorylates and activates phosphoinositide 3-kinase, which in turn phosphorylates phosphatidylinositol (4,5)-diphosphate making phosphatidylinositol (3,4,5)-triphosphate (13). Zap-70 phosphorylates the scaffold proteins LAT and SLP-76. These phosphorylated scaffold proteins lack intrinsic catalytic activity but form the backbone of the TCR signaling complex, as they serve as a platform for the assembly of other molecules into the signaling complex. Both ITK and its substrate PLC γ1 are co-localized in the signaling complex by binding to LAT and SLP-76. ITK also gets targeted into the membrane via the interaction between its PH domain and phosphatidylinositiol (3,4,5)-triphosphate (13). Within this complex ITK is phosphorylated by LCK leading to ITK activation. Other molecules that are part of this signaling complex are GRB2, GADS, ADAP, VAV and NCK (12, 14). This signaling complex imparts signals into three major pathways, leading to gene expression, actin reorganization and cell adhesion (14-16).

Gene expression is mediated by ITK when it phosphorylates PLCγ1 at tyrosine 783 (Y783), which leads to PLCγ1 activation (17). Activated PLCγ1 hydrolyzes the membrane lipid phosphatidylinositol-4, 5-bisphosphate (PIP_2) producing two key second

messengers, inositol-1, 4, 5-triphosphate (IP_3) and diacylglycerol (DAG). IP_3 binds to receptors on the endoplasmic reticulum and trigger the release of intracellular Ca^{2+} ions, which then stimulates Ca^{2+} release activated Ca^{2+} channels (CRAC) leading to influx of extracellular Ca^{2+} (18-20). The calcium binding protein Calmodulin binds with Ca^{2+} ions and activates the phosphatase Calcineurin, which dephosphorylates the transcription factor NFAT, inducing the translocation of transcription factor NFAT into the nucleus (21). Calcium bound calmodulin also binds ITK, enhancing the recruitment of ITK to the membrane. DAG on the other hand plays a role in the activation of both PKC and MAPK/Erk pathways, which promotes transcription factors NFκB (22). These transcription factors regulate the expression of various cytokines like IL-2 for appropriate immune response.

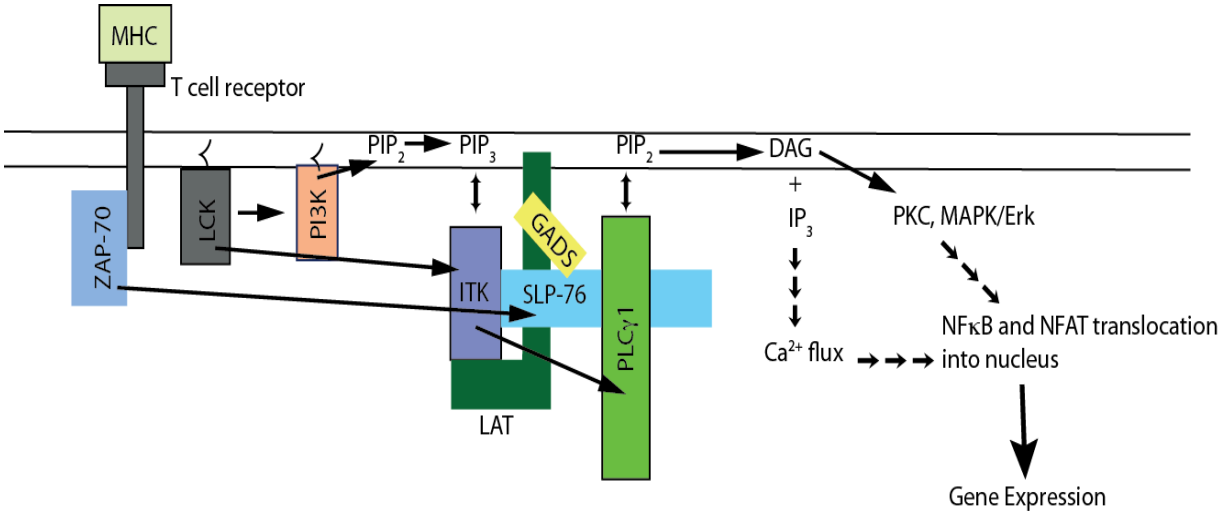

Figure 1. ITK, its substrate PLCγ1 and adaptor protein SLP-76 in TCR signaling pathway. ITK phosphorylates PLCγ1 within of signaling complex formed by scaffold proteins including SLP-76, ultimately leading this pathway for gene expression.

2. ITK

ITK is a member of TEC family of non- receptor tyrosine kinase along with BTK, BMX, TEC and TXK. TEC family kinases are expressed in hematopoietic cells and regulate the development, activation and differentiation of lymphocytes (17). ITK is a 72-kDa protein, primarily expressed in T cells and, as already described, is a key mediator of the T cell signaling pathway. The domain structure of ITK along with other TEC family kinases, with the exception of TXK, is unique among non-receptor tyrosine kinases because of the presence of the amino terminal Pleckstrin homology (PH domain) (23). The PH domain is followed by Zn^{2+} binding Tec Homology (TH) motif, a proline rich region (PRR), Src homology 3 (SH3) domain, Src homology 2 (SH2) domain and kinase domain. The domain organization is illustrated in Figure 2. The function of the PH domain is to bind Phosphatidylinositol (3,4,5)-trisphosphate (PIP_3) in the membrane, hence co-localizing ITK with other proteins in the signaling complex. The SH3 domain is known to bind proline-rich sequences and the SH2 domain recognizes and binds phosphotyrosine containing motifs. The kinase domain is the catalytic domain, which carries out the transfer of the γ-phosphate from ATP to tyrosine residues of the substrates. Like all other kinase domain, the ITK kinase domain is a bilobal structure with a smaller N lobe and a larger C lobe. The N lobe consist of five beta strands and one critical α helix called αC helix. The C lobe is composed of mainly α helices. The active site where phosphate transfer occurs is formed within the cleft between the N lobe and C lobe.

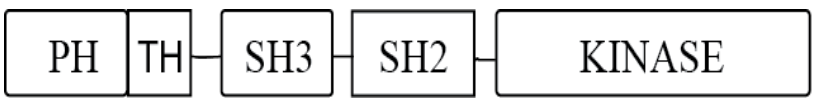

Figure 2. Domain organization of ITK

3. PLCγ1

PLCγ1 is a phospholipase, which catalyzes the hydrolysis of PIP_2 to IP_3 and DAG. In T cells, PLCγ1 is the key substrate of ITK. ITK phosphorylates PLCγ1 and activates its lipase activity. PLCγ1 is among 13 mammalian isozymes, which are divided into six groups: PLCβ, PLCγ, PLCδ, PLCε, PLCζ, and PLCη (24). PLC enzymes are key enzymes in signal transduction pathways, linking various cell receptors and downstream effectors proteins that are involved in regulation of various cellular processes. PLCγ isozymes (γ1 and γ2) are activated through phosphorylation mediated by receptor and non-receptor tyrosine kinases. PLCγ1 is expressed ubiquitously and is involved in signaling pathway downstream of receptors like platelet-derived growth factor (PDGF), fibroblast growth factor (FGF), epidermal growth factor (EGF), nerve growth factor (NGF) and T cell receptor, while PLCγ2 is expressed in B cells and is involved in signal transmission downstream of B cell receptor (25).

PLCγ1 and PLCγ2 both have the same domain arrangement, which consist of a core set of domains (PLC-core) and an array of regulatory modules called γ-specific array (γ-SA) unique to PLCγ isozymes. PLC core consists of N terminal Pleckstrin homology (PH) domain, EF-hands, catalytic triosephosphate isomerase (TIM) barrel fold and a C2 domain. The two halves (X and Y boxes) of the TIM barrel is separated by γ-SA. The γ-SA consists of a split PH domain, two Src homology domains (SH2N and SH2C for N and C terminal respectively) and an Src homology 3 (SH3) domain. The domain organization of PLCγ1 is shown in Figure 3.

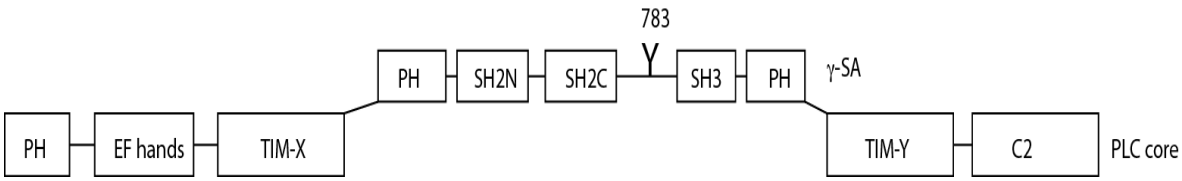

Figure 3. Domain organization of PLCγ1

4. SH2 domains and its role in regulating PLCγ1

The SH2 domain is present in molecules involved in signaling and mediates protein-protein interactions by binding to a phosphotyrosine ligand. All SH2 domains have a conserved three-dimensional structure with a central beta sheet flanked by a helix on each side (26). The SH2-pY mode of binding is shown in figure 4. The conserved arginine in the pY pocket of the SH2 domain interacts with the phosphotyrosine ligand phosphate (26). The hydrophobic pocket also known as pY+3 pocket, accommodates mostly hydrophobic residue (pY+3) in the peptide ligand.

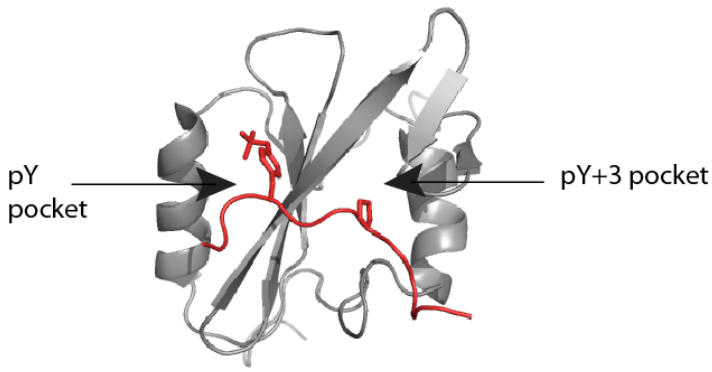

Figure 4. The structure of PLCγ1 SH2 domain adapted from reference number (27). The phosphotyrosine ligand is shown in red. PDB ID: 2PLD

SH2 domains of the PLCγ1 plays important role in its regulation. PLCγ1 has two SH2 domains SH2N and SH2C. Both SH2 domains are the part of γ-SA region and this γ-SA region of the PLCγ1 helps regulate the enzymatic activity. Deletion of the γ-SA regions leads to 20- to 100- fold increase in PLCγ1 activity (28). However, lack of high-resolution structural data for full-length PLCγ1, makes it difficult to study the precise mechanism on how the γ-SA region regulates PLCγ1 activation. However, lower resolution small angle light scattering data and NMR titration experiments pinpoint the role of SH2C domain that inhibits lipase activity. SH2C domain involve in binding PLC core containing split catalytic domain maintaining PLCγ1 in inactivated state (29). ITK phosphorylation of PLCγ1 is required to release the inactivated state.

SH2C not only regulates PLCγ1 lipase activity by directly interacting with the PLC core, it also regulates PLCγ1 phosphorylation by ITK. The phosphorylation target tyrosine 783 (Y783) is within the 33 amino acid long linker placed between SH2C domain and SH3 domain (Figure 3). Studies from our laboratory have also shown that PLCγ1 SH2C and ITK kinase domain directly interact (30). The interaction surface on both ITK kinase domain and PLCγ1 C terminal SH2 domain have been mapped and are shown as red residues in Figure 5. In ITK kinase domain, interaction is mediated by G helix in the C lobe while in SH2 domain various loop residues are critical for the interaction. This interaction is also defined as a substrate docking interaction, since it confers specificity and selectivity of the substrate. This specific interaction facilitates efficient phosphorylation of tyrosine 783 located in the long linker adjacent to the SH2 domain in PLCγ1 (30-32). The importance of this interaction is underscored by the fact

mutation that disrupts the docking interaction surface results in diminished Ca^{2+} in Jurkat T cells (31).

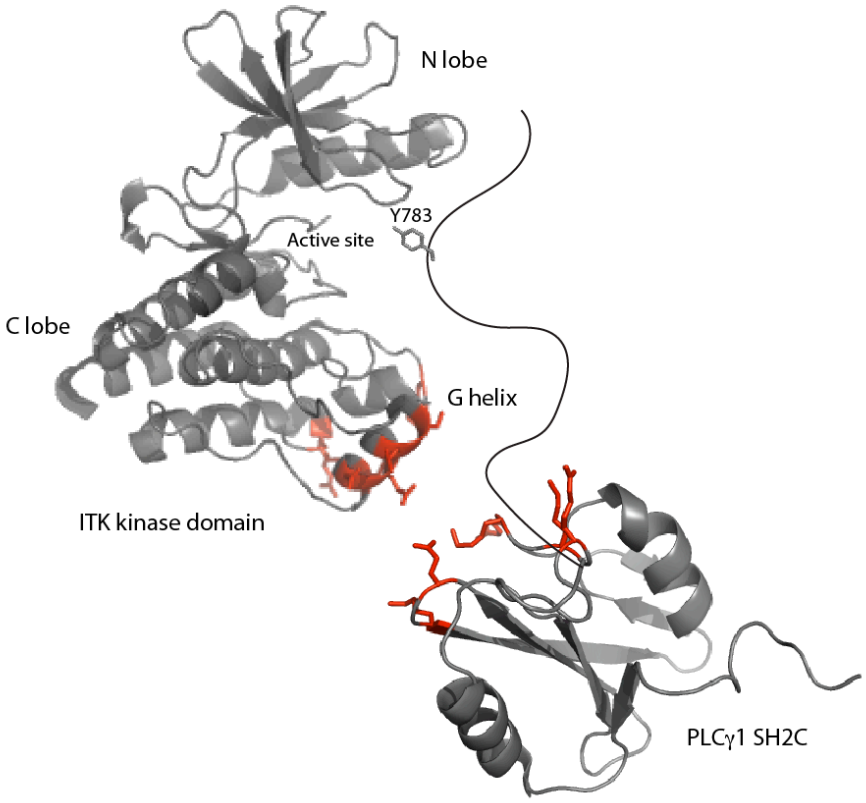

Figure 5. Structures of ITK kinase domain (PDB:1SNU) and PLCγ1 SH2C (PDB: 2PLD) domain with residues shown in red, that are involved in substrate docking interaction.

After ITK phosphorylation of PLCγ1 at Y783, phosphorylated linker undergoes intramolecular interactions with its SH2C domain. The crystal structure of the SH2N-SH2C-linker fragment reveals that PLCγ1 Y783, when phosphorylated, interacts with the SH2C domain in canonical fashion, where pY783 is accommodated in pY pocket and pY+3 residue is accommodated in pY+3 pocket. (Figure 6a). This intramolecular

interaction of SH2C domain and phosphorylated linker disrupts the SH2C domain interaction with the PLC core hence releases PLCγ1 inactivated state described above.

However, another crystal structure of the PLCγ1 SH2N-SH2C-linker fragment reveals that the SH2-linker interacts with the SH2 domain even when PLCγ1 Y783 is not phosphorylated (Figure 6b) (29). The linker conformation for unphosphorylated form is very similar to phosphorylated form except for the tyrosine 783 is pointed outward and does not occupy the pY pocket in SH2C (Figure 5b). This conformation of the PLCγ1 is thought to be autoinhibitory in nature because the Y783 is inaccessible to ITK for phosphorylation. This autoinhibitory interaction adds another regulatory layer, where Y783 cannot be phosphorylated, unless this interaction is disrupted. However, confirmation of this intramolecular interaction is necessary because artifact from crystal packing could also lead to this conformation.

So we asked, whether this interaction is real and takes place in solution and if so, whether this makes Y783 in linker inaccessible to ITK and how this interaction is disrupted so that ITK can readily phosphorylate the Y783. Chapter 2 of this thesis precisely addresses these questions. We explore the possible role of scaffold protein SLP-76, on disrupting the autoinhibitory PLCγ1 interaction in chapter 2.

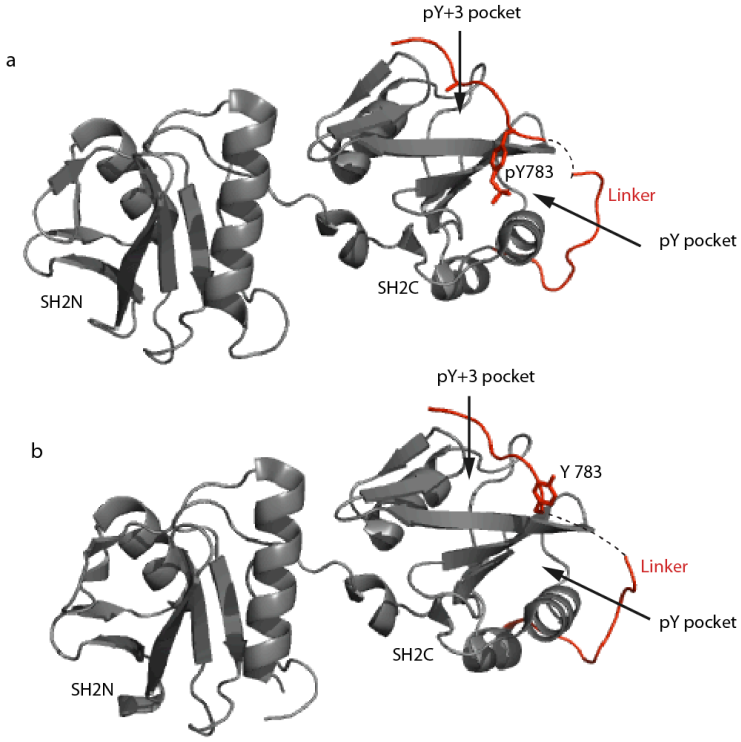

Figure 6. Crystal structure of SH2N-SH2C-linker, phosphorylated form (a) (PDB:4FBN) and unphosphorylated form (b) (PDB:4EY0). The linker with ITK phosphorylation site is shown in red. Missing part of linker is shown as dashed line.

5. SLP-76

SLP-76 is a scaffold protein, mostly expressed in hematopoietic cell types. It consists of three modular domains: N terminal acidic region with four phosphotyrosine motifs, central proline rich domain and a C-terminal SH2 domain (33) (Figure 6). These domains with their distinct ligand binding properties help regulate the assembly and localization of different proteins to form signaling complexes. SLP-76 on its N terminal acidic domain contains three tyrosine phosphorylation sites (Y113, Y128, Y145) that are known to be phosphorylated by ZAP-70 (34). These phosphorylated tyrosine mediate

interactions with the guanine nucleotide exchange factor VAV, the adapter NCK, and ITK (35, 36). ITK has been shown to bind to pY145 of SLP-76 (36). Binding of ITK SH2 to SLP-76 pY145 helps localize ITK to a larger signaling complex resulting in the phosphorylation and activation of its substrate.

Recently, a new phosphorylation site (Y173) has been discovered in SLP-76 and this specific tyrosine unlike the other phosphorylation sites on SLP-76 is phosphorylated by ITK and not by ZAP-70 (34). Mutation of Y173F in SLP-76 leads to abrogation of phosphorylation of PLCγ1 at Y783 (34). However, the detail mechanism on how Y173 is involved in phosphorylation of PLCγ1 Y783 is not known. In chapter 2, we describe the how pY173 is involved in disrupting PLCγ1 autoinhibitory conformation (described above) leading to the efficient phosphorylation of Y783 by ITK.

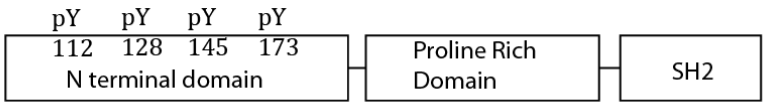

Figure 6. Domain organization of SLP-76

6. ITK regulation

Multiple layers of molecular mechanisms regulate activation of ITK. After T cell activation, ITK is localized to membrane via its PH domain binding PI(3,4,5)P3. Phosphorylation at a specific residue within the activation loop is required for the activation of most kinases including those of the TEC family. ITK is phosphorylated on

the activation loop tyrosine (Y511) in the kinase domain by the SRC family kinase LCK (37). Phosphorylation on the ITK activation loop enhances the catalytic activity of the ITK (37). Phosphorylation in the activation loop causes conformational changes within kinase domain that allow for catalysis to occur. More specifically, after activation loop phosphorylation, the activation loop moves out of the active site allowing for the αC helix containing a conserved glutamate residue to swing in towards the active site and form a crucial salt bridge between the αC helix glutamate side chain and a conserved lysine side chain in the N lobe.

Following T cell activation, ITK also associates with signaling complex formed by adaptor proteins LAT and SLP-76 localizing ITK with its substrate PLCγ1. Specifically, ITK SH2 and SH3 domain binds the scaffold protein SLP-76 phosphotyrosine 145 and proline rich region respectively. Within this signaling complex ITK, associates with its substrate PLCγ1 by substrate docking mechanism as described above and phosphorylates it.

These intermolecular interactions, likely rearrange the tertiary structure of the ITK leading to its activation. Previous studies have shown that the rearrangement of the tertiary structure of the protein controls the activation status of the kinases (38, 39). For example crystal structures of SRC kinases in the inactive conformation shows that the SH2 domain binds to a conserved C-terminal regulatory phosphotyrosine on the Kinase tail (40). TEC family kinases, however are likely to be regulated differently because they lack the conserved tyrosine in the C terminal kinase tail but instead contain N terminal

PHTH domain which is absent in SRC family kinases. Full-length crystal structures of the TEC kinases are currently unavailable. However, a recent crystal structure of Tec family member kinase BTK reveals intramolecular interactions in autoinhibited state of the protein. In BTK, the crystal structure of the SH2-SH3-Kinase fragment reveals the intramolecular interaction between domains and mutation in interaction interface causes increase in the catalytic activity of BTK (41). However, ITK full-length structure is not available, but deletion mutation studies suggest the inhibitory role of SH3, SH2 and PHTH domain on catalytic activity of the ITK (42). Deletion of PH domain alone increases the k_{cat} of ITK by 5 fold (42). Part of this thesis work is dedicated to the thorough investigation of role of PH domain on ITK kinase activity (Chapter 3).

7. PH domain

PH domains are approximately 120 amino acid lipid-binding modules found in many proteins involved in signal transduction pathways and cytoskeletal regulation (43). This domain binds phosphoinositide within cell membranes. All PH domains are structurally conserved but lack primary sequence similarity (44). Three-dimensional structures of several PH domains reveal that they share common three-dimensional features consisting of two perpendicular anti-parallel beta sheets and C-terminal alpha helix (45).

Several structures of PH domains belonging to TEC family kinase (BTK, TEC) have been determined and show that the C-terminal Zn^{2+} binding TH domain is crucial for the structural integrity of the PH domain (46, 47). The structure of ITK PH domain

has not been solved to date. PH domain of TEC family kinases specifically binds to PIP_3 in the plasma membrane hence recruiting the kinase to the membrane (48). The crystal structure of BTK PH domain bound to IP_4 the soluble head group of PIP_3 is shown in Figure 8.

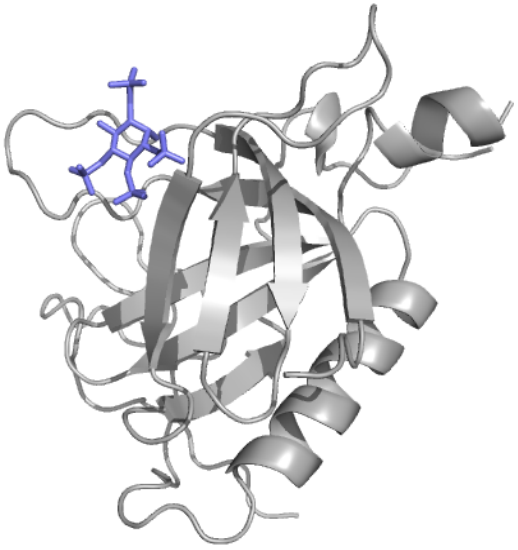

Figure 8. Crystal structure of BTK PH domain complex IP_4 (blue), the soluble headgroup of PIP_3, PDB ID: 1B55

Along with the canonical role of targeting proteins to the membrane via phosphatidylinositol (3,4,5)-triphosphate (PI (3,4,5) P_3) binding, PH domains have also been implicated in other non- canonical functions, such as mediating protein-protein interactions and regulating the activity of the enzymes. Some examples of PH domain mediated protein-protein interactions include BTK PH domain interaction with the βγ subunit of G protein coupled receptors (49, 50), filamentous actin (51) and Protein kinase C (52). Examples of PH domain regulating enzymatic activity include BTK (41) and Protein kinase B (PKB/Akt) (53, 54). In both cases, the PH domain is known to interact

with kinase domain intramolecularly to autoinhibit the kinase and disruption of this interaction is known to enhance the enzymatic activity of both enzymes.

Thesis Organization

This thesis dissertation includes five chapters. Chapter 1 provides the general introduction and literature review on T cell kinase ITK its substrate PLCγ1 and scaffold protein SLP-76 and their roles in T cell receptor signaling. It also reviews the regulatory mechanisms of ITK and PLCγ1. Chapter 2, which has been published in the *Journal of Molecular Biology*, focuses on role of the adaptor protein SLP-76 on regulating the conformation of PLCγ1 for efficient phosphorylation by ITK. Using in vitro experiments and NMR titrations, fluorescence titrations, pull down assays and activity assays; we were able to describe the mechanism by which SLP-76 pY173 regulates the phosphorylation of PLCγ1 by ITK. The results suggest that SLP-76 pY173 interacts with the SH2C domain of PLCγ1 regulating the accessibility of Y783 in the linker, for ITK. This mechanism is described as a substrate priming mechanism whereby SLP-76 primes the PLCγ1 for efficient phosphorylation by ITK.

Chapter 3 is a revised manuscript currently under consideration in *Biochemistry*. The data focus on the characterization of the intramolecular interaction between the ITK kinase domain and PH domain and the role of this interaction in regulating ITK kinase activity. We have defined a new binding surface on the ITK PH domain that directly interacts with the kinase domain and demonstrate that mutations leading to the disruption of this regulatory interaction activate ITK. Chapter 4 is a preliminary study of the ITK

PH domain and ITK Kinase domain interactions in vivo, using a bimolecular fluorescence complementation (BiFC) assay. This study will eventually lead to the development of an in vivo screen for small molecules targeting the ITK PH/Kinase binding interface. The general conclusion chapter (chapter 5) includes a summary of the research work and future directions

Motivation

This thesis aims to contribute to our understanding the complex regulation mechanism of ITK and its substrate PLCγ1. For ITK, this thesis is focused on its N terminal PH domain and its role in regulating the ITK enzyme. For PLCγ1, this thesis is focused on how PLCγ1 autoinhibitory conformation is disrupted by SLP-76. Understanding the regulatory mechanism of this enzyme/substrate pair is valuable for targeting these molecules for therapeutic purposes to treat diseases that are linked to ITK. Significant effort has been invested for small molecules discovery that target the active site of the ITK and other kinases (55-57). However, the common chemical and structural environment in the active site of all kinases pose specificity problems. To combat these problem, specific allosteric regulatory sites within ITK that govern ITK activity can also be targeted. Hence, the study of regulatory interactions that influence the catalytic activity of the ITK is crucial. Non-catalytic domains in ITK regulate the ITK kinase activity but due to the lack of full length structure, exact mechanism of these regulatory domains on how they influence the activity of the ITK are not clear. Hence the motivation of this dissertation is to define and characterize the crucial interactions of ITK, both intermolecular regulatory interactions (Chapter 2) and intramolecular

regulatory interactions (Chapter 3), using a variety of biochemical and biophysical techniques.

References

1. Pines J (1994) Protein kinases and cell cycle control. *Semin Cell Biol* 5(6):399-408.
2. Johnson LN (2009) The regulation of protein phosphorylation. *Biochem Soc Trans* 37(Pt 4):627-641.
3. Hussain A, *et al.* (2011) TEC family kinases in health and disease - loss-of-function of BTK and ITK and the gain-of-function fusions ITK-SYK and BTK-SYK. *Febs J* 278(12):2001-2010.
4. Shchemelinin I, Sefc L, & Necas E (2006) Protein kinases, their function and implication in cancer and other diseases. *Folia Biol-Prague* 52(3):81-100.
5. Tomlinson MG, *et al.* (2004) Expression and function of Tec, Itk, and Btk in lymphocytes: evidence for a unique role for Tec. *Mol Cell Biol* 24(6):2455-2466.
6. Tsukada S, *et al.* (1993) Deficient expression of a B cell cytoplasmic tyrosine kinase in human X-linked agammaglobulinemia. *Cell* 72(2):279-290.
7. Huck K, *et al.* (2009) Girls homozygous for an IL-2-inducible T cell kinase mutation that leads to protein deficiency develop fatal EBV-associated lymphoproliferation. *J Clin Invest* 119(5):1350-1358.
8. Readinger JA, *et al.* (2008) Selective targeting of ITK blocks multiple steps of HIV replication. *Proc Natl Acad Sci U S A* 105(18):6684-6689.

9. Tarafdar S, Poe JA, & Smithgall TE (2014) The accessory factor Nef links HIV-1 to Tec/Btk kinases in an Src homology 3 domain-dependent manner. *J Biol Chem* 289(22):15718-15728.

10. Waite JC & Skokos D (2012) Th17 response and inflammatory autoimmune diseases. *Int J Inflam* 2012:819467.

11. Qi Q & August A (2007) Keeping the (kinase) party going: SLP-76 and ITK dance to the beat. *Sci STKE* 2007(396):pe39.

12. Smith-Garvin JE, Koretzky GA, & Jordan MS (2009) T cell activation. *Annu Rev Immunol* 27:591-619.

13. Yang WC, Ching KA, Tsoukas CD, & Berg LJ (2001) Tec kinase signaling in T cells is regulated by phosphatidylinositol 3-kinase and the Tec pleckstrin homology domain. *J Immunol* 166(1):387-395.

14. Takesono A, Finkelstein LD, & Schwartzberg PL (2002) Beyond calcium: new signaling pathways for Tec family kinases. *J Cell Sci* 115(Pt 15):3039-3048.

15. Brownlie RJ & Zamoyska R (2013) T cell receptor signalling networks: branched, diversified and bounded. *Nat Rev Immunol* 13(4):257-269.

16. Grasis JA & Tsoukas CD (2011) Itk: the rheostat of the T cell response. *J Signal Transduct* 2011:297868.

17. Berg LJ, Finkelstein LD, Lucas JA, & Schwartzberg PL (2005) Tec family kinases in T lymphocyte development and function. *Annu Rev Immunol* 23:549-600.

18. Chang CL & Liou J (2016) Homeostatic regulation of the PI(4,5)P2-Ca(2+) signaling system at ER-PM junctions. *Biochim Biophys Acta* 1861(8 Pt B):862-873.

19. Freedman BD (2006) Mechanisms of calcium signaling and function in lymphocytes. *Crit Rev Immunol* 26(2):97-111.

20. Lewis RS (2001) Calcium signaling mechanisms in T lymphocytes. *Annu Rev Immunol* 19:497-521.

21. Rao A, Luo C, & Hogan PG (1997) Transcription factors of the NFAT family: regulation and function. *Annu Rev Immunol* 15:707-747.

22. Altman A & Villalba M (2003) Protein kinase C-theta (PKCtheta): it's all about location, location, location. *Immunol Rev* 192:53-63.

23. Smith CI*, et al.* (2001) The Tec family of cytoplasmic tyrosine kinases: mammalian Btk, Bmx, Itk, Tec, Txk and homologs in other species. *Bioessays* 23(5):436-446.

24. Vines CM (2012) Phospholipase C. *Adv Exp Med Biol* 740:235-254.

25. Koss H, Bunney TD, Behjati S, & Katan M (2014) Dysfunction of phospholipase Cgamma in immune disorders and cancer. *Trends Biochem Sci* 39(12):603-611.

26. Liu BA, Engelmann BW, & Nash PD (2012) The language of SH2 domain interactions defines phosphotyrosine-mediated signal transduction. *FEBS Lett* 586(17):2597-2605.

27. Pascal SM*, et al.* (1994) Nuclear magnetic resonance structure of an SH2 domain of phospholipase C-gamma 1 complexed with a high affinity binding peptide. *Cell* 77(3):461-472.

28. Horstman DA, DeStefano K, & Carpenter G (1996) Enhanced phospholipase C-gamma1 activity produced by association of independently expressed X and Y domain polypeptides. *Proc Natl Acad Sci U S A* 93(15):7518-7521.

29. Bunney TD*, et al.* (2012) Structural and functional integration of the PLCgamma interaction domains critical for regulatory mechanisms and signaling deregulation. *Structure* 20(12):2062-2075.

30. Joseph RE, Min L, Xu R, Musselman ED, & Andreotti AH (2007) A remote substrate docking mechanism for the tec family tyrosine kinases. *Biochemistry* 46(18):5595-5603.

31. Min L, Joseph RE, Fulton DB, & Andreotti AH (2009) Itk tyrosine kinase substrate docking is mediated by a nonclassical SH2 domain surface of PLCgamma1. *Proc Natl Acad Sci U S A* 106(50):21143-21148.

32. Xie Q, Joseph RE, Fulton DB, & Andreotti AH (2013) Substrate recognition of PLCgamma1 via a specific docking surface on Itk. *J Mol Biol* 425(4):683-696.

33. Koretzky GA, Abtahian F, & Silverman MA (2006) SLP76 and SLP65: complex regulation of signalling in lymphocytes and beyond. *Nat Rev Immunol* 6(1):67-78.

34. Sela M*, et al.* (2011) Sequential phosphorylation of SLP-76 at tyrosine 173 is required for activation of T and mast cells. *EMBO J* 30(15):3160-3172.

35. Jordan MS*, et al.* (2006) Functional hierarchy of the N-terminal tyrosines of SLP-76. *J Immunol* 176(4):2430-2438.

36. Bunnell SC*, et al.* (2000) Biochemical interactions integrating Itk with the T cell receptor-initiated signaling cascade. *J Biol Chem* 275(3):2219-2230.

37. Heyeck SD, Wilcox HM, Bunnell SC, & Berg LJ (1997) Lck phosphorylates the activation loop tyrosine of the Itk kinase domain and activates Itk kinase activity. *J Biol Chem* 272(40):25401-25408.

38. Boggon TJ & Eck MJ (2004) Structure and regulation of Src family kinases. *Oncogene* 23(48):7918-7927.

39. Engen JR*, et al.* (2008) Structure and dynamic regulation of Src-family kinases. *Cell Mol Life Sci* 65(19):3058-3073.

40. Xu W, Doshi A, Lei M, Eck MJ, & Harrison SC (1999) Crystal structures of c-Src reveal features of its autoinhibitory mechanism. *Mol Cell* 3(5):629-638.

41. Wang Q*, et al.* (2015) Autoinhibition of Bruton's tyrosine kinase (Btk) and activation by soluble inositol hexakisphosphate. *Elife* 4.

42. Joseph RE, Min L, & Andreotti AH (2007) The linker between SH2 and kinase domains positively regulates catalysis of the Tec family kinases. *Biochemistry* 46(18):5455-5462.

43. Rebecchi MJ & Scarlata S (1998) Pleckstrin homology domains: a common fold with diverse functions. *Annu Rev Biophys Biomol Struct* 27:503-528.

44. Lemmon MA (2007) Pleckstrin homology (PH) domains and phosphoinositides. *Biochem Soc Symp* (74):81-93.

45. Riddihough G (1994) More meanders and sandwiches. *Nat Struct Biol* 1(11):755-757.

46. Vihinen M, Nilsson L, & Smith CI (1994) Tec homology (TH) adjacent to the PH domain. *FEBS Lett* 350(2-3):263-265.

47. Baraldi E*, et al.* (1999) Structure of the PH domain from Bruton's tyrosine kinase in complex with inositol 1,3,4,5-tetrakisphosphate. *Structure* 7(4):449-460.

48. August A, Sadra A, Dupont B, & Hanafusa H (1997) Src-induced activation of inducible T cell kinase (ITK) requires phosphatidylinositol 3-kinase activity and the Pleckstrin homology domain of inducible T cell kinase. *Proc Natl Acad Sci U S A* 94(21):11227-11232.

49. Touhara K, Inglese J, Pitcher JA, Shaw G, & Lefkowitz RJ (1994) Binding of G protein beta gamma-subunits to pleckstrin homology domains. *J Biol Chem* 269(14):10217-10220.

50. Tsukada S, Simon MI, Witte ON, & Katz A (1994) Binding of beta gamma subunits of heterotrimeric G proteins to the PH domain of Bruton tyrosine kinase. *Proc Natl Acad Sci U S A* 91(23):11256-11260.

51. Yao L*, et al.* (1999) Pleckstrin homology domains interact with filamentous actin. *J Biol Chem* 274(28):19752-19761.

52. Yao L, Kawakami Y, & Kawakami T (1994) The pleckstrin homology domain of Bruton tyrosine kinase interacts with protein kinase C. *Proc Natl Acad Sci U S A* 91(19):9175-9179.

53. Wu WI*, et al.* (2010) Crystal structure of human AKT1 with an allosteric inhibitor reveals a new mode of kinase inhibition. *PLoS One* 5(9):e12913.

54. Alessi DR & Cohen P (1998) Mechanism of activation and function of protein kinase B. *Curr Opin Genet Dev* 8(1):55-62.

55. Sahu N & August A (2009) ITK inhibitors in inflammation and immune-mediated disorders. *Curr Top Med Chem* 9(8):690-703.

56. Vargas L, Hamasy A, Nore BF, & Smith CI (2013) Inhibitors of BTK and ITK: state of the new drugs for cancer, autoimmunity and inflammatory diseases. *Scand J Immunol* 78(2):130-139.

57. Fabbro D, Cowan-Jacob SW, & Moebitz H (2015) Ten things you should know about protein kinases: IUPHAR Review 14. *Br J Pharmacol* 172(11):2675-2700.

CHAPTER 2

SCAFFOLD PROTEIN SLP-76 PRIMES PLCγ1 FOR ACTIVATION BY ITK MEDIATED PHOSPHORYLATION

A paper published in the *Journal of Molecular Biology* (Vol. 427, Issue 17, pp. 2734-2747, April 2015)

Sujan Devkota[1], Raji E. Joseph, Lie Min, D. Bruce Fulton and Amy Andreotti*

[1]Primary author

*Corresponding author

Abstract

Activation of the phospholipase, PLCγ1, is critical for proper T cell signaling following antigen receptor engagement. In T cells, the Tec family kinase, ITK, phosphorylates PLCγ1 at tyrosine 783 (Y783) leading to activation of phospholipase function and subsequent production of the second messengers IP_3 and DAG. In this work we demonstrate that PLCγ1 can be primed for ITK mediated phosphorylation on Y783 by a specific region of the adaptor protein, SLP-76. The SLP-76 phosphotyrosine containing sequence, pY^{173}IDR, does not conform to the canonical recognition motif for an SH2 domain yet binds with significant affinity to the C-terminal SH2 domain of PLCγ1 (SH2C). The SLP-76 pY^{173} motif competes with the autoinhibited conformation

surrounding the SH2C domain of PLCγ1 leading to exposure of the ITK recognition element on the PLCγ1 SH2 domain and release of the target tyrosine, Y783. These data contribute to the evolving model for the molecular events occurring early in the T cell activation process.

Introduction

Activation of phospholipase Cγ1 (PLCγ1) by phosphorylation of Y783 is mediated by Interleukin-2 induced tyrosine kinase (ITK) and is a key event following T-cell receptor (TCR) stimulation (58, 59). Once active, PLCγ1 hydrolyzes phosphatidylinositol-4,5-bisphosphate (PIP_2) to produce inositol 1,4,5-triphosphate (IP_3) and diacylglycerol (DAG); second messengers that control calcium flux from the endoplasmic reticulum and activation of Protein kinase C, respectively (60). A number of additional signaling molecules participate in activation of PLCγ1, in particular the scaffolding functions of SLP-76 (SH2 domain-containing leucocyte protein of 76 kDa) (61), LAT (linker for activation of T cells) (62) and Gads (Grb2-related adaptor downstream of Shc) (63) play important roles in co-localization of ITK and PLCγ1 (33). Specific contacts among the proteins in this T cell signaling complex have been identified and characterized providing glimpses into the molecular mechanisms by which TCR signals are propagated.

ITK and PLCγ1 are both multi-domain containing proteins that have Src homology 2 (SH2) and Src homology 3 (SH3) domains in addition to their catalytic domains (Fig. 1a). Binding sites for the SH2 and SH3 adaptor domains of ITK and

PLCγ1 have been identified on both SLP-76 and LAT. Specifically, the PLCγ1 SH3 domain and N-terminal SH2 domain (SH2N) bind to the proline-rich region of SLP-76 and the LAT phosphotyrosine 132 (pY132), respectively (64, 65). The ITK SH2 domain binds one of three well-characterized phosphotyrosine sites (35) in the N-terminal half of SLP-76 (Fig. 1); pY145 is the target of ITK SH2 (36, 66) while SLP-76 pY112 and pY128 bind to SH2 domains within the signaling molecules, Vav and Nck (67-70). In addition to these canonical Src homology domain mediated interactions, a direct substrate docking interaction between ITK and PLCγ1 occurs via a phosphotyrosine independent mechanism involving the C-terminal SH2 domain (SH2C) of PLCγ1 and the ITK kinase domain (30). The PLCγ1 SH2C domain docks onto the C-lobe of the ITK kinase domain creating an enzyme/substrate recognition complex required for efficient phosphorylation of PLCγ1 Y783 (31, 32). Clearly, a large number of distinct protein-protein interactions (Fig. 1b) are present within the complex web of signaling interactions required for proper signal transduction in the T cell (71-73) and it is likely that additional interactions, including those not yet described, also contribute to the pathway. Indeed, a recent finding points to another regulatory phosphorylation site in the N-terminal region of SLP-76 at Y173 (34); this newly recognized phosphotyrosine is adjacent to the pY112, pY128 and pY145 sites.

Sela *et al.* (34) demonstrate that phosphorylation at Y173 within SLP-76 is required for TCR induced phosphorylation of PLCγ1. A detailed mechanistic explanation for this observation is currently lacking but the authors in the original work speculate that SLP-76 pY173 may bind to the SH2C domain of PLCγ1 to facilitate

docking of PLCγ1 onto the ITK domain (34). The kinase docking site and phosphotyrosine binding pocket form distinct surfaces on the PLCγ1 SH2C domain and it is therefore possible that binding of SLP-76 pY173 to PLCγ1 SH2C may enhance ITK/PLCγ1 docking. We have previously shown, however, that the interaction of PLCγ1 SH2C with the ITK kinase domain is unaffected by phosphopeptide binding to PLCγ1 SH2C (31) and so an allosteric role for SLP-76 pY173 facilitating docking can be ruled out. Co-localization of ITK and PLCγ1 at adjacent sites on SLP-76 may enhance ITK mediated phosphorylation of PLCγ1 at Y783 but PLCγ1 makes multiple contacts within the signaling complex (PLCγ1 SH3/SLP-76; PLCγ1 SH2N/LAT) and Sela et al. show that mutation of Y173 does not reduce association of ITK or PLCγ1 with SLP-76 in T cells (34). Moreover, it has been observed that a loss of function mutation in the SH2C domain within full length PLCγ1 does not significantly affect recruitment of PLCγ1 to the SLP-76 signaling complex yet PLCγ1 Y783 phosphorylation, and hence PLCγ1 activity, is decreased significantly (74).

Here we pursue a detailed model to explain the role of SLP-76 pY173 in T cell signal transduction. We test the hypothesis that SLP-76 pY173 alters the inhibitory conformation of PLCγ1 (75) thereby priming PLCγ1 for activation by ITK. Our findings show that, in spite of a non-classical SH2 binding motif, the SLP-76 derived phosphopeptide surrounding pY173 binds to PLCγ1 SH2C, disrupting an intramolecular PLCγ1 inhibitory complex, leading to release of PLCγ1 Y783 for more efficient phosphorylation by ITK. The data provided here add to our evolving view of the molecular events controlling antigen receptor stimulated activation of PLCγ1.

Results

The unphosphorylated Y783 containing linker in PLCγ1 associates intramolecularly with the adjacent SH2C domain in solution.

The structure of the SH2N-SH2C-linker fragment of PLCγ1 has been recently solved (29) and reveals a specific intramolecular contact between the PLCγ1 linker region that contains Y783 and the SH2C domain (Fig. 2a). A large stretch of the PLCγ1 linker region is not defined by the electron density, but Y783 and the following six amino acids (Y^{783}VEANPM) are defined and form contacts with the pY+3 binding pocket of SH2C (Fig. 2a). We first wished to assess the extent to which the Y783 linker region associates with PLCγ1 SH2C in solution. Using NMR spectroscopy, we acquired ^{1}H-^{15}N HSQC data for the PLCγ1 SH2C domain alone and the longer PLCγ1 SH2C-linker protein (Fig 2b). Extensive differences in the chemical shifts of the SH2C NMR resonances are observed upon comparing spectra of PLCγ1 SH2C and SH2C-linker, consistent with association between the linker region and the SH2C domain. Linewidths (and therefore rotational correlation times) are very similar for both proteins indicating the linker region contacts SH2C in an intramolecular manner. Thus, solution NMR data appears consistent with the SH2C/linker association observed in the crystal structure.

Extensive chemical shift differences between the backbone amide resonances of SH2C and SH2C-linker are observed (Fig. 2b). It is likely that, in addition to intramolecular contacts between linker and SH2C, covalent extension of the C-terminus of SH2C to form SH2C-linker contributes to the observed spectral differences. Nevertheless, we can unequivocally identify the SH2C resonances that do not change

when compared to SH2C-linker and the remaining SH2C resonances are therefore either directly or indirectly affected by the presence of the Y783 containing linker. Mapping the spectral changes onto the SH2C domain within the PLCγ1 SH2N-SH2C-linker crystal structure shows that the most contiguous regions giving rise to spectral differences upon linker association correspond to regions of the SH2C domain that directly contact the linker in the crystal structure (Fig. 2c).

To further examine the solution conformation of PLCγ1 SH2C-linker, we probed the contribution of specific residues C-terminal to Y783 since these side chains make contacts to SH2C in the crystal structure (Fig. 2a). We constructed an SH2C-linker variant where N787, P788 and M789 are mutated to alanine (PLCγ1 SH2C-linker NPM_AAA) and acquired ^{1}H-^{15}N HSQC data. The SH2C-linker resonances shift significantly in the mutant protein to positions that are nearly coincident with the resonances of PLCγ1 SH2C alone (Fig. 2d and supplementary figure 1) suggesting that the C-terminal residues of SH2C-linker ($N^{787}P^{788}M^{789}$) stabilize linker association in solution. Finally, using size exclusion chromatography, we find that the retention time of the mutant PLCγ1 SH2C-linker ($N^{787}P^{788}M^{789}$_AAA) is less than wild type SH2C-linker, suggesting the NPM to AAA mutation releases the linker from the SH2C interaction, increasing the apparent size of the SH2C-linker protein (Fig. 2e). Together, these data provide evidence that the SH2C-linker region in PLCγ1 adopts an intramolecular complex in solution that resembles that observed in the available crystal structure.

Intramolecular SH2C-linker association limits docking of the PLCγ1 substrate to the ITK kinase domain.

Efficient PLCγ1 phosphorylation by ITK in T cells depends on a docking interaction between PLCγ1 SH2C and the ITK kinase domain; PLCγ1 SH2C binds to the C-lobe of the ITK kinase domain in a phosphotyrosine independent manner via side chains in the CD loop and C-terminus of SH2C (Fig. 3a). The PLCγ1 linker region associates with SH2C in a region that is nearly coincident with the kinase-docking site we have mapped previously (31). The proximity of PLCγ1 linker bound to SH2C and the recognition motif required for ITK docking prompted us to test the effect of the PLCγ1 linker on ITK kinase domain/PLCγ1 SH2C domain association. In a pull down experiment using immobilized GST fusions of PLCγ1 SH2C and SH2C-linker, we find that the ITK kinase/PLCγ1 SH2C domain interaction is stronger in the absence of the PLCγ1 linker sequence (Fig. 3b). Taken together with the data supporting the intramolecular complex seen in the PLCγ1 crystal structure, we interpret these data to suggest that the intramolecular association between SH2C and linker region competes with binding of PLCγ1 SH2C to the ITK kinase domain.

Despite unusual flanking sequence, the SLP-76 pY173 peptide binds to the PLCγ1 SH2C domain.

Like the PLCγ1/ITK substrate/kinase docking interaction, the intramolecular interaction between the Y783 linker and SH2C domain is independent of tyrosine phosphorylation. In spite of the absence of phosphorylation on Y783, the interaction of the linker with SH2C bears a resemblance to the structure of a canonical phosphotyrosine

ligand bound to the PLCγ1 SH2C domain (Figs. 2a, 3c). The bound linker and pY containing peptide are nearly superimposable and in both cases the 'specificity pocket' or pY+3 pocket of SH2C mediates direct contacts with residues C-terminal to the tyrosine (pY or Y783) (Fig. 3d). A difference between the two complexes occurs at the pY-binding pocket. In the SH2/phosphopeptide structure this pocket is filled by the pY side chain of the peptide ligand but the SH2C pY pocket remains empty in the structure of PLCγ1 SH2N-SH2C-linker without Y783 phosphorylation (Fig. 3d, inset).

Given the overlap in binding sites on the PLCγ1 SH2C domain for the unphosphorylated linker and a phosphopeptide ligand, we hypothesize that the pY173 containing phosphopeptide derived from SLP-76 competes with intramolecular linker binding to destabilize the autoinhibited form of PLCγ1. The SLP-76 sequence, pY^{173}-I-D-R, contains an arginine instead of the canonical/preferred hydrophobic residue in the pY+3 position (76) and so we first tested binding of the SLP-76 sequence to PLCγ1 SH2C. Titration of unlabeled SLP-76 peptide, N-S-M-pY^{173}-I-D-R-P-P-T-G-K, into ^{15}N labeled PLCγ1 SH2C was carried out with acquisition of ^{1}H-^{15}N HSQC spectra at each point in the titration (Fig. 4a). Chemical shift changes are measured for each amide NH resonance in the SH2C domain (Fig. 4b) and the largest changes are visualized on the structure of PLCγ1 SH2C (Fig. 4c). The resonance changes induced by addition of the SLP-76 peptide localize to the pY and pY+3 pockets as would be expected for a canonical interaction between phosphotyrosine peptide and SH2 domain (Fig. 4c). The unusual presence of arginine in the pY+3 position prompted us to model this residue into the structure of PLCγ1 SH2C bound to a canonical phosphopeptide. Superposition of the

Cα-Cβ bond of arginine onto that of proline in the structure shown in Figure 3c suggests that the hydrophobic residues lining the pY+3 pocket may create favorable interactions with the aliphatic portion of the arginine side chain much as they do with the proline in the pY+3 position (Fig. 4d). In addition, the model suggests the possibility of favorable cation-pi interactions (77) between the guanidinium group of the arginine side chain and two adjacent tyrosines, Y740 and Y741, deep in the pY+3 pocket of SH2C (Fig. 4d). Experimental structure determination will be needed to confirm this model but it is interesting to speculate that certain SH2 domains may be capable of broader ligand recognition within the pY+3 pocket. The only other report of an arginine occupying the pY+3 position in an SH2 domain phospholigand comes from a large proteomics study testing the binding propensity of predicted ligands to various SH2 domains (Supp Fig S4 in (78)). The sequence pYDTR binds to the Crk SH2 domain, which contains FY at the position corresponding to Y740 and Y741 in PLCγ1 SH2C. It is also notable that only a subset of SH2 domains contain the YY or FY motif, suggesting the potential for a specific recognition mechanism for pY target sequences with arginine in pY+3 position (79). Finally, to quantify the affinity of the unusual SLP-76 pY173 peptide binding to PLCγ1 SH2C, we measured fluorescence as a function of increasing pY173 peptide concentration and determined a dissociation constant of 1.6 μM (Fig. 4e).

Binding of SLP-76 pY173 to PLCγ1 SH2C releases the Y783 containing linker and unmasks the kinase docking site on SH2C.

Having determined that the Slp76 derived pY173 phosphopeptide binds to the PLCγ1 SH2C domain, we next examined the effect of this phosphopeptide on the

intramolecular PLCγ1 SH2C/linker association. Using dynamic light scattering, we compared the size distribution for PLCγ1 SH2C-linker and SH2C-linker plus the SLP-76 pY173 peptide. The mutant SH2C-linker ($N^{787}P^{788}M^{789}$_AAA) is used as a control for near complete linker displacement based on the data in Figure 2. Of the three PLCγ1 fragments, SH2C-linker, peptide bound SH2C-linker and the mutant SH2C-linker, the PLCγ1 SH2C-linker protein is the most compact structure with an average hydrodynamic radius of 2.0 nm (Fig. 5a). The size distributions for both the mutant SH2C-linker ($N^{787}P^{788}M^{789}$_AAA) and SH2C-linker plus SLP-76 pY173 peptide shift to larger particle size; an increase of 12-25% over the SH2C-linker protein (average hydrodynamic radii of 2.25 and 2.5 nm). These data suggest that the pY173 peptide displaces the linker in a manner similar to mutation of the linker itself leading to a more disengaged stretch of amino acids surrounding PLCγ1 Y783. In a separate experiment, addition of increasing SLP-76 pY173 peptide to the ^{15}N-labeled sample of PLCγ1 SH2C-linker (Fig. 5b) reveals NMR chemical shift changes toward the resonances of the pY173 peptide bound SH2C spectrum (Fig. 5c). Thus, the SLP_76 pY173 peptide ligand binds to PLCγ1 SH2C-linker in a manner that is nearly identical to the isolated SH2C domain albeit with slightly lower affinity, K_d = 2.9 μM compared to a K_d = 1.6 μM for the pY173/SH2C interaction (Fig. 5d, 4e). All of these data are consistent with a model where SLP-76 phosphopeptide binding to PLCγ1 SH2C directly competes with and releases the PLCγ1 linker region containing Y783 resulting in exposure of the kinase docking site on PLCγ1 SH2C and increased accessibility of PLCγ1 Y783 for the ITK kinase.

SLP-76 pY173 enhances the ITK phosphorylation of PLCγ1

To assess the effect of SLP-76 pY173 on the ITK mediated phosphorylation of PLCγ1 Y783, we carried out an in vitro kinase assay subjecting full length PLCγ1 to phosphorylation by full length ITK. An antibody specific to PLCγ1 pY783 is used to detect phosphorylation at the PLCγ1 783 position following incubation of the PLCγ1 substrate with active ITK (Fig. 6). Consistent with PLCγ1 adopting an autoinhibited form, we find that in vitro phosphorylation efficiency of Y783 in full length PLCγ1 is quite poor; pY783 levels are not different than background levels detected for the PLCγ1 substrate alone (Fig. 6a, lanes 2 & 3). The same in vitro kinase assay is next carried out with increasing concentration of the SLP-76 derived phosphopeptide, N-S-M-pY^{173}-I-D-R-P-P-T-G-K (Fig. 6a, lanes 4-7). Quantification of the pY783 levels shows that increasing SLP-76 pY173 peptide increases the extent of PLCγ1 pY783 phosphorylation by ITK (Fig. 6b). Smaller fragments of PLCγ1, P-SH2N-SH2C-linker-SH3-H and SH2C-linker, show the same trend (Fig. 6c-f). Increased concentration of the SLP-76 pY173 peptide causes an increase in ITK mediated PLCγ1 phosphorylation on Y783. For the smallest Y783 containing PLCγ1 fragment, SH2C-linker, we tested the importance of the pY binding pocket by mutation of R694 to alanine (Fig. 6e,f). Disruption of the PLCγ1 SH2C binding pocket by mutation results in no increase in Y783 phosphorylation by ITK upon addition of the SLP-76 pY173 peptide (Fig. 6e,f). These data directly implicate the PLCγ1 SH2C domain in the observed enhancement and show that addition of the SLP-76 pY173 peptide to the kinase assay is not simply activating ITK (by binding to the ITK SH2 domain). This latter point is consistent with our previous observations that pY containing peptides do not increase ITK kinase activity toward a generic peptide

substrate (unpublished data). Collectively, our findings point to a SLP-76 dependent priming model for PLCγ1 activation by ITK. The SLP-76 pY173 sequence binds to the PLCγ1 SH2C domain, disfavoring the autoinhibited conformation, which renders PLCγ1 a better substrate for ITK.

Discussion

ITK mediated phosphorylation of Y783 in PLCγ1 occurs in the context of a multi-component signaling cluster that includes the scaffold protein SLP-76 in addition to a number of others proteins (LAT, Vav, Nck, GADS) (Fig. 7). Our data provide support for an autoinhibited conformation of PLCγ1 in solution that is consistent with the reported crystal structure of the SH2N-SH2C-linker region of PLCγ1 (29). We find that the autoinhibited form of PLCγ1 shields the kinase-docking site on the PLCγ1 SH2C domain (31) and limits access to the substrate tyrosine, Y783 (Fig. 7a). Our data also suggest that the most recently characterized phosphorylation site on SLP-76, pY173, can prime PLCγ1 for phosphorylation by ITK. The SLP-76 pY173 containing phosphopeptide can bind to the PLCγ1 SH2C domain (in spite of the non-canonical arginine in the pY+3 position), releasing the PLCγ1 linker region from SH2C to reveal both the ITK kinase-docking site on PLCγ1 SH2C and the substrate tyrosine, Y783 (Fig. 7a,b). These conformational changes away from the autoinhibited form of PLCγ1 would predispose the PLCγ1 molecule for efficient phosphorylation by ITK. Once PLCγ1 is phosphorylated, an intramolecular interaction between pY783 and SH2C (80, 81) can compete with the PLCγ1 SH2C/SLP-76 pY173 interaction and displace PLCγ1 from the SLP-76/ITK signaling complex allowing another round of ITK mediated catalysis to

proceed (Fig. 7c). This final step is consistent with recent observations that activated PLCγ1 rapidly moves away from the ITK/LAT/SLP-76 complex to the TCR cluster (82). Also, the affinity we measured for PLCγ1 SH2C and SLP-76 pY173 interaction is relatively weaker for SH2 interaction and this weaker interaction possibly makes PLCγ1 SLP-76 interaction more transient and activated PLCγ1 can dislocate rapidly from ITK/LAT/SLP-76 complex. The extent to which the other adaptor domains (PH, SH2N, SH3, C2) within PLCγ1 also play a role in mediating release of active PLCγ1 from the ITK/SLP-76/LAT complex is not clear and must be considered in any evolving model of T cell activation. Finally, it is notable that complete loss of the SLP-76 pY173 site has no measureable effect on assembly of the signaling complex in T cells yet has a profound effect on the extent to which PLCγ1 is activated. Our biochemical results underscore the importance of *how* a substrate is presented to its cognate kinase; signaling molecules must not only assemble into a productive complex but must also be able to access the precise conformational state required for productive signal transduction.

The SLP-76 phosphoprotein combines its well-known scaffold function with a regulatory role in the form of conformational priming of PLCγ1. Previously published findings suggested that SLP-76 is required to activate ITK by maintaining an active conformation of the kinase (83). While interactions between SLP-76 pY145 and the ITK SH2 domain are required for proper T cell signaling (36), we have never been able to observe any direct effect of SLP-76 derived phosphopeptides on the in vitro kinase activity of ITK (unpublished data, A.H.A. and Xiaoguang Qu). Since the previously mentioned experiments pointing to a role for SLP-76 in activating ITK (83) made use the

PLCγ1 SH2N-SH2C-linker-SH3 substrate to probe ITK catalytic activity, it is possible that the activating effect that was observed is due to the role of SLP-76 in priming PLCγ1 for phosphorylation rather than activation of ITK catalytic activity per se.

There are numerous additional domain interactions that mediate formation of the signaling complexes involving PLCγ1 and ITK and so the evolving picture for PLCγ1 SH2C and SLP-76 pY173 must be considered as part of a larger set of regulatory interactions. A newly described protein-protein interaction regulating B-cell signaling implicates calcium dependent binding of the PLCγ2 C2 domain and pY119 in Slp-65 (the B-cell scaffolding protein related to the T cell expressed SLP-76) (84). Given the sequence similarities surrounding Slp-65 pY119 (EpY^{119}IDNR) and SLP-76 pY173, (MpY^{173}IDRP), the finding in B cells prompted us to consider whether the conformational priming of PLCγ1 we have characterized here could involve the PLCγ1 C2 domain. First we note that the SLP-76 driven amplification of PLCγ1 phosphorylation occurs even for the smallest fragments of PLCγ1 containing just SH2C and linker suggesting that C2 is not mediating the observed increase in pY783 levels (Fig. 6). It is also of note that the Slp-65 derived phosphopeptide does not bind full length PLCγ1 (84) suggesting that the Slp-65 phosphotyrosine motif, pYIDN, does not bind the PLCγ1 C2 domain and may not even bind well to PLC SH2 domain(s) leaving this Slp-65 site available to regulate B cell signaling in a manner quite different from the related site in SLP-76. Our data further suggest that the motif surrounding pY173 in SLP-76 (pYIDR) is tuned to bind specific SH2 domains; in particular the unusual presence of arginine in the pY+3 position may steer the SLP-76 phosphotyrosine motif toward binding SH2

domains (such as PLCγ1 SH2C) that can accommodate the long and positively charged arginine in this position. Thus, despite what appear to be sequence similarities in the proteins that regulate T- and B-cell signaling cascades, we are finding that very different mechanistic rules may apply to these distinct immune signaling systems.

Substrate priming has not, to our knowledge, been previously ascribed to the SLP-76 molecule. Since its identification in 1995 (85), SLP-76 has been well characterized as a scaffold protein and its role in recruiting and co-localizing multiple signaling proteins in T cells is undisputed. Our findings now suggest that SLP-76 may also play a role in directly regulating the apparent enzymatic activity emanating from the T cell receptor proximal Tec kinase, ITK. Substrate priming has been well described in other systems. One example is glycogen synthase; hierarchical phosphorylation events prime glycogen synthase for phosphorylation (and activation) by glycogen synthase kinase (86-88). Another example involves the RING ubiquitin ligases; a conformational shift away from an autoinhibited state coupled with tyrosine phosphorylation comprise integral components of the regulatory mechanisms controlling ubiquitin transfer (89-92). Dissecting the biochemical steps within the trio of T cell signaling proteins, SLP-76, ITK and PLCγ1, has uncovered a possible role for SLP-76 pY173 in promoting PLCγ1 activation in T cells by conformational priming. The next stage in advancing our understanding of how productive signaling complexes are formed in T cells will require significant effort in reconstituting larger, multi-component complexes that can recapitulate the signaling steps present in the cell.

Materials and Methods

Constructs

Baculoviral expression constructs of full-length ITK (mouse) and rat full-length PLCγ1 (rat) have been described previously (93). The fragments of PLCγ1 SH2C, SH2C-linker and P-SH2N-SH2C-linker-SH3-H were amplified by polymerase chain reaction and cloned to pGEX-4T-1 expression vector (GE Healthcare). The SH2C R694A mutation was introduced by site directed mutagenesis (Stratagene). All sequences were verified by sequencing at the Iowa State University DNA synthesis and sequencing facility.

Protein/peptide Production and Purification

Full-length ITK and PLCγ1 were expressed in S*f*9 cells and were purified as described previously (93). Similarly, PLCγ1 SH2C and SH2C-linker were expressed in *E. coli* BL21 cells and purified as described previously (30). For P-SH2N-SH2C-linker-H, bacterial cell pellets were re-suspended in lysis buffer consisting of 50mM Tries, pH 8 and 150 mM NaCl and lysed by treating with lysozyme (0.5 mg/ml). Cleared lysate was applied to a Glutathione Sepharose column (GE Healthcare) equilibrated with lysis buffer. The GST-tagged P-SH2N-SH2C-linker-H protein was eluted with lysis buffer containing 10 mM glutathione and the GST tag was cleaved by treatment with Thrombin (Sigma) for 5 minutes at room temperature. The cleavage reaction was stopped with 1mM PMSF, and the cleaved protein was applied to a HiLoad Superdex 200 prep grade column to separate GST from the desired PLCγ1 P-SH2N-SH2C-linker-H protein. The SLP-76 pY173 peptide with sequence Ac-NSMpY^{173}IDRPPTGK-NH_2 was synthesized and purified by GenScript.

NMR Spectroscopy

NMR spectra were collected on a Bruker AVII 700 spectrometer with a 5mm HCN z-gradient cryoprobe operating at a ^{1}H frequency 700.13 MHz at 298K. NMR titration experiments were carried out by acquiring ^{1}H-^{15}N HSQC spectra of 250 μM SH2C or SH2C-linker within increasing SLP-76 pY173 peptide concentration: 0, 39.9, 79.9, 159.1, 238, 355.7, 722.18, 1273, 1982 μM. The chemical shift changes in PLCγ1 SH2C induced by addition the SLP-76 pY173 peptide were quantified by using the following equation: $\Delta\delta_{ave} = \{[½\ [(\Delta\delta H)^2 + (0.2\Delta\delta N)^2]\}^{1/2}$ (94). Residues with chemical shift changes above the mean plus one standard deviation were considered significant. Buffer composition used to solubilize the SLP-76 pY173 peptide is identical to the protein buffer (50mM KH_2PO_4, pH 6.4, 150 mM NaCl, 2mM DTT and 0.02% NaN_3).

Fluorescence Spectroscopy

Tryptophan fluorescence for 3 μM PLCγ1 SH2C or SH2C-linker with increasing concentration of the SLP-76 pY173 peptide was measured using a Cary eclipse spectrophotometer at 25^0C. The wavelength used for tryptophan excitation was 295nm while emission was recorded between 300-400 nm. All measurements were carried out in triplicate. The maximum fluorescence intensity for each titration point was plotted against ligand concentration and the dissociation constant (K_d) was calculated by fitting the data in MATLAB using the equation: $I = I_0 + \Delta I * [[(K_d + P + L) - \{(K_d+P+L)^2 - 4P*L\}^{1/2}]/2P]$ (95), where I is fluorescence intensity, I_0 is fluorescence intensity of

protein without any ligand, ΔI is change in fluorescence intensity on ligand binding, K_d is dissociation constant, P is protein concentration and L is ligand concentration.

Dynamic light scattering

Hydrodynamic radii of 50 μM PLCγ1 SH2C-linker, 1:1 ratio of SH2C-linker + SLP-76 pY173 peptide, and SH2C-linker NPM_AAA mutant in buffer containing 50mM KH_2PO_4 pH 6.4, 150 mM NaCl, 2mM DTT and 0.02% NaN_3 were measured using a DynaPro® NanoStar™ light scattering instrument (Wyatt Technology) at 25^0C.

Kinase assays and western blotting

In vitro kinase assays were performed using full-length ITK and various substrate constructs of PLCγ1 (0.1 μM Full length PLCγ1, 0.1 μM P–SH2N-SH2C-linker-SH3-H, 1 μM SH2C-linker, 1 μM SH2C-linker R694A) with the increasing concentration of synthetic SLP-76 pY173 peptide. Kinase assay buffer consisted of 50mM HEPES pH 7,10mM $MgCl_2$, 1 mM DTT, 1mg/ml BSA, 1mM Pefabloc, and 200 μM ATP. PLCγ1 substrates and SLP-76 pY173 peptide were preincubated for 20 minutes prior to addition of the ITK enzyme. Kinase reactions were carried out for one minute for full length PLCγ1 and P–SH2N-SH2C-linker-SH3-H substrates and five minutes for SH2C-linker and SH2C-linker R694A. Upon completion of the kinase reaction, samples were boiled, separated by SDS-PAGE and western blotted with the anti pY783 antibody (EMD Millipore) for the detection of pY783 levels in each PLCγ1 substrate. Anti ITK (2F12) (Thermo Scientific) and Strep Tag II Monoclonal antibody (EMD Millipore)

were used to detect total level of ITK and full length PLCγ1 respectively. Smaller fragments of PLCγ1 were detected by Coomassie staining.

Acknowledgements

This work is supported by grants from the National Institutes of Health (National Institute of Allergy and Infectious Diseases, AI43957 & AI075150) to A.H.A. and by the Gary Roewe Research Award to S. Devkota. We also acknowledge technical assistance from Thamothanaran Subbiah in DNA construction and protein purification for the PLCγ1 P–SH2N-SH2C-linker-SH3-H fragment.

References

1. Houtman JC, Houghtling RA, Barda-Saad M, Toda Y, Samelson LE. (2005). Early phosphorylation kinetics of proteins involved in proximal TCR-mediated signaling pathways. *J Immunol* 175: 2449-2458.
2. Perez-Villar JJ, Kanner SB. (1999). Regulated association between the tyrosine kinase Emt/Itk/Tsk and phospholipase-C gamma 1 in human T lymphocytes. *J Immunol* 163: 6435-6441.
3. Readinger JA, Mueller KL, Venegas AM, Horai R, Schwartzberg PL. (2009). Tec kinases regulate T-lymphocyte development and function: new insights into the roles of Itk and Rlk/Txk. *Immunol Rev* 228: 93-114.
4. Wu JN, Koretzky GA. (2004). The SLP-76 family of adapter proteins. *Semin Immunol* 16: 379-393.

5. Yablonski D, Weiss A. (2001). Mechanisms of signaling by the hematopoietic-specific adaptor proteins, SLP-76 and LAT and their B cell counterpart, BLNK/SLP-65. *Adv Immunol* 79: 93-128.

6. Yoder J, Pham C, Iizuka YM, Kanagawa O, Liu SK, McGlade J, Cheng AM. (2001). Requirement for the SLP-76 adaptor GADS in T cell development. *Science* 291: 1987-1991.

7. Koretzky GA, Abtahian F, Silverman MA. (2006). SLP76 and SLP65: complex regulation of signalling in lymphocytes and beyond. *Nat Rev Immunol* 6: 67-78.

8. Deng L, Velikovsky CA, Swaminathan CP, Cho S, Mariuzza RA. (2005). Structural basis for recognition of the T cell adaptor protein SLP-76 by the SH3 domain of phospholipase Cgamma1. *J Mol Biol* 352: 1-10.

9. Paz PE, Wang S, Clarke H, Lu X, Stokoe D, Abo A. (2001). Mapping the Zap-70 phosphorylation sites on LAT (linker for activation of T cells) required for recruitment and activation of signalling proteins in T cells. *Biochem J* 356: 461-471.

10. Jordan MS, Sadler J, Austin JE, Finkelstein LD, Singer AL, Schwartzberg PL, Koretzky GA. (2006). Functional hierarchy of the N-terminal tyrosines of SLP-76. *J Immunol* 176: 2430-2438.

11. Bunnell SC, Diehn M, Yaffe MB, Findell PR, Cantley LC, Berg LJ. (2000). Biochemical interactions integrating Itk with the T cell receptor-initiated signaling cascade. *J Biol Chem* 275: 2219-2230.

12. Su YW, Zhang Y, Schweikert J, Koretzky GA, Reth M, Wienands J. (1999). Interaction of SLP adaptors with the SH2 domain of Tec family kinases. *Eur J Immunol* 29: 3702-3711.

13. Wu J, Motto DG, Koretzky GA, Weiss A. (1996). Vav and SLP-76 interact and functionally cooperate in IL-2 gene activation. *Immunity* 4: 593-602.

14. Wunderlich L, Farago A, Downward J, Buday L. (1999). Association of Nck with tyrosine-phosphorylated SLP-76 in activated T lymphocytes. *Eur J Immunol* 29: 1068-1075.

15. Raab M, da Silva AJ, Findell PR, Rudd CE. (1997). Regulation of Vav-SLP-76 binding by ZAP-70 and its relevance to TCR zeta/CD3 induction of interleukin-2. *Immunity* 6: 155-164.

16. Fang N, Motto DG, Ross SE, Koretzky GA. (1996). Tyrosines 113, 128, and 145 of SLP-76 are required for optimal augmentation of NFAT promoter activity. *J Immunol* 157: 3769-3773.

17. Joseph RE, Min L, Xu R, Musselman ED, Andreotti AH. (2007). A remote substrate docking mechanism for the tec family tyrosine kinases. *Biochemistry* 46: 5595-5603.

18. Min L, Joseph RE, Fulton DB, Andreotti AH. (2009). Itk tyrosine kinase substrate docking is mediated by a nonclassical SH2 domain surface of PLCgamma1. *Proc Natl Acad Sci U S A* 106: 21143-21148.

19. Xie Q, Joseph RE, Fulton DB, Andreotti AH. (2013). Substrate recognition of PLCgamma1 via a specific docking surface on Itk. *J Mol Biol* 425: 683-696.

20. Chakraborty AK, Weiss A. (2014). Insights into the initiation of TCR signaling. *Nat Immunol* 15: 798-807.

21. Sherman E, Barr V, Samelson LE. (2013). Super-resolution characterization of TCR-dependent signaling clusters. *Immunol Rev* 251: 21-35.

22. Samelson LE. (2011). Immunoreceptor signaling. *Cold Spring Harb Perspect Biol* 3: pii: a011510. doi: 10.1101/cshperspect.a011510.

23. Sela M, Bogin Y, Beach D, Oellerich T, Lehne J, Smith-Garvin JE, Okumura M, Starosvetsky E, Kosoff R, Libman E, Koretzky G, Kambayashi T, Urlaub H, Wienands J, Chernoff J, Yablonski D. (2011). Sequential phosphorylation of SLP-76 at tyrosine 173 is required for activation of T and mast cells. *EMBO J* 30: 3160-3172.

24. Braiman A, Barda-Saad M, Sommers CL, Samelson LE. (2006). Recruitment and activation of PLCgamma1 in T cells: a new insight into old domains. *Embo J* 25: 774-784.

25. DeBell K, Graham L, Reischl I, Serrano C, Bonvini E, Rellahan B. (2007). Intramolecular regulation of phospholipase C-gamma1 by its C-terminal Src homology 2 domain. *Mol Cell Biol* 27: 854-863.

26. Bunney TD, Esposito D, Mas-Droux C, Lamber E, Baxendale RW, Martins M, Cole A, Svergun D, Driscoll PC, Katan M. (2012). Structural and functional integration of the PLCgamma interaction domains critical for regulatory mechanisms and signaling deregulation. *Structure* 20: 2062-2075.

27. Kaneko T, Joshi R, Feller SM, Li SS. (2012). Phosphotyrosine recognition domains: the typical, the atypical and the versatile. *Cell Commun Signal* 10: 32.

28. Crowley PB, Golovin A. (2005). Cation-pi interactions in protein-protein interfaces. *Proteins* 59: 231-239.

29. Liu BA, Jablonowski K, Shah EE, Engelmann BW, Jones RB, Nash PD. (2010). SH2 domains recognize contextual peptide sequence information to determine selectivity. *Mol Cell Proteomics* 9: 2391-2404.

30. Campbell SJ, Jackson RM. (20030. Diversity in the SH2 domain family phosphotyrosyl peptide binding site. *Protein Eng* 16: 217-227.

31. Hajicek N, Charpentier TH, Rush JR, Harden TK, Sondek J. (2013). Autoinhibition and phosphorylation-induced activation of phospholipase C-gamma isozymes. *Biochemistry* 52: 4810-4819.

32. Gresset A, Hicks SN, Harden TK, Sondek J. (2010). Mechanism of phosphorylation-induced activation of phospholipase C-gamma isozymes. *J Biol Chem* 285: 35836-35847.

33. Cruz-Orcutt N, Vacaflores A, Connolly SF, Bunnell SC, Houtman JC. (2014). Activated PLC-gamma1 is catalytically induced at LAT but activated PLC-gamma1 is localized at both LAT- and TCR-containing complexes. *Cell Signal* 26: 797-805.

34. Bogin Y, Ainey C, Beach D, Yablonski D. (2007). SLP-76 mediates and maintains activation of the Tec family kinase ITK via the T cell antigen

receptor-induced association between SLP-76 and ITK. *Proc Natl Acad Sci U S A* 104: 6638-6643.

35. Engelke M, Oellerich T, Dittmann K, Hsiao HH, Urlaub H, Serve H, Griesinger C, Wienands J. (2013). Cutting edge: feed-forward activation of phospholipase Cgamma2 via C2 domain-mediated binding to SLP65. *J Immunol* 191: 5354-5358.

36. Jackman JK, Motto DG, Sun Q, Tanemoto M, Turck CW, Peltz GA, Koretzky GA, Findell PR. (1995). Molecular cloning of SLP-76, a 76-kDa tyrosine phosphoprotein associated with Grb2 in T cells. *J Biol Chem* 270: 7029-7032.

37. Ali A, Hoeflich KP, Woodgett JR. (2001). Glycogen synthase kinase-3: properties, functions, and regulation. *Chem Rev* 101: 2527-2540.

38. Williams DD, Marin O, Pinna LA, Proud CG. (1999). Phosphorylated seryl and threonyl, but not tyrosyl, residues are efficient specificity determinants for GSK-3beta and Shaggy. *FEBS Lett* 448: 86-90.

39. Dajani R, Fraser E, Roe SM, Young N, Good V, Dale TC, Pearl LH. (2001). Crystal structure of glycogen synthase kinase 3 beta: structural basis for phosphate-primed substrate specificity and autoinhibition. *Cell* 105: 721-732.

40. Dou H, Buetow L, Hock A, Sibbet GJ, Vousden KH, Huang DT. (2012). Structural basis for autoinhibition and phosphorylation-dependent activation of c-Cbl. *Nat Struct Mol Biol* 19: 184-192.

41. Dou H, Buetow L, Sibbet GJ, Cameron K, Huang DT. (2013). Essentiality of a non-RING element in priming donor ubiquitin for catalysis by a monomeric E3. *Nat Struct Mol Biol* 20: 982-986.

42. Ozkan E, Yu H, Deisenhofer J. (2005). Mechanistic insight into the allosteric activation of a ubiquitin-conjugating enzyme by RING-type ubiquitin ligases. *Proc Natl Acad Sci U S A* 102: 18890-18895.

43. Plechanovova A, Jaffray EG, Tatham MH, Naismith JH, Hay RT. (2012). Structure of a RING E3 ligase and ubiquitin-loaded E2 primed for catalysis. *Nature* 489: 115-120.

44. Joseph RE, Fulton DB, Andreotti AH. (2007). Mechanism and functional significance of itk autophosphorylation. *J Mol Biol* 373: 1281-1292.

45. Chang YG, Song AX, Gao YG, Shi YH, Lin XJ, Cao XT, Lin DH, Hu HY. (2006). Solution structure of the ubiquitin-associated domain of human BMSC-UbP and its complex with ubiquitin. *Protein Sci* 15: 1248-1259.

46. Bodenreider C, Beer D, Keller TH, Sonntag S, Wen D, Yap L, Yau YH, Shochat SG, Huang D, Zhou T, Caflisch A, Su XC, Ozawa K, Otting G, Vasudevan SG, Lescar J, Lim SP. (2009). A fluorescence quenching assay to discriminate between specific and nonspecific inhibitors of dengue virus protease. *Anal Biochem* 395: 195-204.

Figure Captions:

Figure 1. Domain structures and schematic of interactions for the signaling proteins that assemble downstream of the T cell receptor. (a) ITK, PLCγ1 and SLP-76 domain maps,

PLCγ1 Y783 is indicated within the 33-residue linker between the SH2C and SH3 domains of PLCγ1. The fourth phosphorylation site on SLP-76, Y173, is circled and the Proline-Rich Region of SLP-76 is indicated as PRR (SLP-76 Y112, Y128 and Y145 have been previously characterized and serve as binding sites for Vav, Nck and Itk when phosphorylated). (b) Schematic of the T cell signaling complex involving the proteins in the current study: ITK, PLCγ1 and SLP-76 as well as LAT, Vav, Nck and Gads (not included in this study). The dashed double-headed arrow indicates the SLP-76 pY173/ PLCγ1 SH2C interaction described in the current study. Solid, double-headed arrows indicate characterized interactions between specific domains of ITK, PLCγ1, SLP-76 and LAT that are discussed in the text. Asterisks (*) denote canonical SH3 or SH2 mediated interactions involving proline-rich (PXXP) or phosphotyrosine (pY) motifs, respectively. The lighter gray arrow indicates the phosphotyrosine-independent docking interaction between PLCγ1 SH2C and ITK kinase domains that is required for phosphorylation of PLCγ1 by ITK.

Figure 2. Solution data is consistent with the autoinhibited PLCγ1 conformation observed in the crystal structure. (a) Crystal structure of the PLCγ1 SH2N-SH2C-linker fragment (PDB ID: 4FBN). The SH2N and SH2C domains are gray and the linker region is cyan. The resolved linker residues surrounding and including Y783 are labeled. The N-terminal region of the PLCγ1 linker is also resolved and adopts a helical segment. The intervening eleven residues in the linker are not resolved in the crystal structure and are indicated by a dashed line. (b) Superposition of ^{1}H-^{15}N HSQC spectra for PLCγ1 SH2C (blue) and PLCγ1 SH2C-linker (cyan). (c) Structure of the PLCγ1 SH2C-linker region

extracted from the structure shown in (a). Linker is cyan, black indicates SH2C residues for which no chemical shift difference is observed and light gray shows SH2C residues for which chemical shift changes are observed when spectra of SH2C and SH2C-linker are compared (see (b)). (d) Superposition of three ^{1}H-^{15}N HSQC spectra: PLCγ1 SH2C-linker (cyan), mutant PLCγ1 SH2C-linker NPM_AAA (red), and PLCγ1 SH2C (blue). The resonances for two representative residues highlighted in green in PLCγ1 SH2N-SH2C-linker structure in a, (H714 and G727) are shown to illustrate the similarity between spectra of the mutant PLCγ1 SH2C-linker NPM_AAA and the isolated SH2C domain. (e) Size exclusion chromatography (*top*) showing the elution volume for PLCγ1 SH2C (solid line), SH2C-linker (dotted line) and mutant SH2C-linker NPM_AAA (dashed line). SDS-PAGE (*bottom*) showing the purity of the wild type and mutant SH2C-linker proteins.

Figure 3. Kinase docking site and intramolecular linker association site on PLCγ1 SH2C are partially coincident. (a) Surface rendition of PLCγ1 SH2N-SH2C-linker showing the kinase docking site on SH2C (orange, comprised of the CD loop and C-terminal region of the SH2 domain) required for ITK mediated phosphorylation of PLCγ1 Y783, location of the intramolecular linker association with SH2C (cyan), and the SH2N domain (receding). (b) Duplicate pull-down experiments showing diminished association of the FLAG tagged ITK kinase domain with PLCγ1 SH2C-linker compared to PLCγ1 SH2C. Anti-FLAG antibody shows level of associated ITK kinase domain and Ponceau S shows total levels of GST-SH2C and GST-SH2C-linker. (c) Ribbon structure of PLCγ1 SH2C domain bound to a canonical phosphotyrosine containing peptide (PDB ID: 2PLD).

Phosphopeptide ligand is red and the pY and pY+3 residues are labeled. (d) Overlay of the phospholigand bound SH2C structure shown in (c) and the SH2C-linker portion of the PLCγ1 SH2N-SH2C-linker structure. The phosphopeptide, pYIIP, is red and the PLCγ1 linker region containing Y783 is cyan. The pY+3 pocket is circled and the pY pocket is boxed and enlarged in the inset showing the different conformations of the pY and Y783 side chains.

Figure 4. The SLP-76 pY173 containing peptide binds the PLCγ1 SH2C domain. (a) Superposition of HSQC spectra from the NMR titration of PLCγ1 SH2C with increasing concentration of the SLP-76 pY173 peptide. Spectra are overlaid with light to dark blue scheme with increasing SLP-76 pY173 peptide concentration. (b) Chemical shift deviations (Δδ) for each of the PLCγ1 SH2C domain residues upon binding of pY173 phosphopeptide. The average deviation (0.1 ppm) is indicated by the horizontal dashed line. (c) Residues for which $\Delta\delta > 0.1$ ppm are indicated in red on the structure of PLCγ1 SH2C domain. (d) left panel shows the pY+3 pocket in the structure of PLCγ1 SH2C bound to a peptide containing proline at the pY+3 position (PDB ID: 2PLD, peptide ligand is cyan). Right, model of SH2C/peptide complex containing arginine in place of proline in the pY+3 position. Y740 and Y741 are labeled. (e) Fluorescence titration curve of the SLP-76 pY173 phosphopeptide binding to PLCγ1 SH2C.

Figure 5. (a) Dynamic light scattering data for PLCγ1 SH2C-linker (filled diamonds, solid line), mutant SH2C-linker NPM_AAA (filled squares, dotted line) and SH2C-linker + SLP-76 pY173 peptide (filled triangles, dashed line). (b) Superposition of HSQC

spectra from the NMR titration of PLCγ1 SH2C-linker with increasing concentration of the SLP-76 pY173 peptide. Spectra are overlaid with light to dark blue scheme with increasing SLP-76 pY173 peptide concentration (c) Peaks corresponding to the residues of SH2C in the context of SH2C-linker with increasing concentration of SLP-76 pY173 peptide (light to dark) superimposed with peak of same residue (red) when SH2C is fully bound to SLP-76 pY173 peptide. (d) Fluorescence titration curve of the SLP-76 pY173 phosphopeptide binding to PLCγ1 SH2C-linker.

Figure 6. SLP-76 pY173 enhances ITK mediated phosphorylation of PLCγ1 at Y783. (a) Lanes 1 and 2 contain enzyme alone and substrate alone, respectively. Phosphorylation of full length PLCγ1 by full length ITK in the absence of SLP-76 pY173 peptide (lane 3) and in the presence of increasing concentration of the SLP-76 pY173 peptide (lanes 4-7). In (a), (c) and (e), phosphorylation of Y783, ITK enzyme levels and substrate levels are detected using anti pY783, anti ITK, and either anti Strep antibody (a) or Coomassie stain (c,e). (b) Histogram representation of pY783 level from three independent experiments and error bar for pY783 level indicates the standard deviation. Intensity of pY783 level in the kinase reaction that lacks SLP-76 pY173 is normalized to 1. (c) Kinase assay using the smaller PLCγ1substrate fragment, P-SH2N-SH2C-linker-SH3-H, with increasing concentration of SLP-76 pY173 peptide as in (a). (d) Histogram representation of pY783 level from three independent experiments using PLCγ1 P-SH2N-SH2C-linker-SH3-H as substrate. (e) Comparison of pY783 level in PLCγ1 SH2C-linker (wt) and the SH2-linker R694A mutant with increasing concentration of the SLP-76 pY173 peptide. (f) Histogram

representation of pY783 level from three independent experiments using SH2C-linker wild type and SH2C-linker (R694A) mutant.

Figure 7. Model for priming of PLCγ1 by SLP-76 for phosphorylation and activation by ITK. (a) PLCγ1 is depicted in its autoinhibited conformation where the linker between SH2C and SH3 domains is intramolecularly engaged with SH2C, shielding Y783 and the kinase docking site on SH2C. T cell activation leads to phosphorylation of SLP-76 tyrosines such as Y145 creating a binding site for the ITK SH2 domain. Subsequent phosphorylation of SLP-76 Y173 occurs (possibly by ITK) creating a putative binding site for PLCγ1 SH2C. Additional protein-protein associations involving Nck, Vav, LAT and GADS occur and are included here for context. (b) Binding of PLCγ1 SH2C to SLP-76 pY173 would open the autoinhibited form of PLCγ1, revealing the kinase docking site on PLCγ1 SH2C and priming Y783 for phosphorylation by ITK. (c) Phosphorylated pY783 could compete in an intramolecular fashion with SLP-76 pY173 for the PLCγ1 SH2C binding pocket disengaging the SH2C with catalytic core and displacing activated PLCγ1 from SLP-76 and creating an open pY173 binding site for priming another molecule of PLCγ1.

Figures

Figure 1

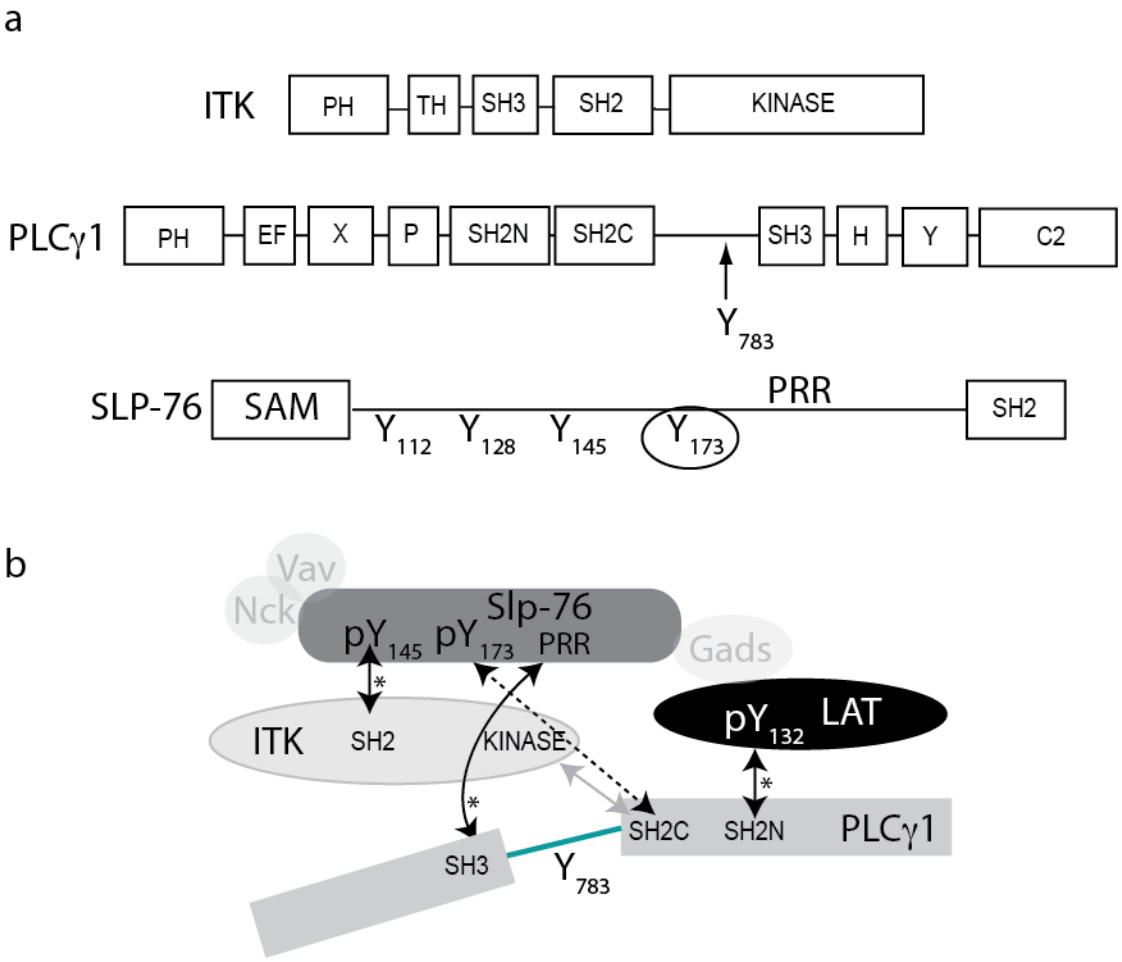

Figure 2

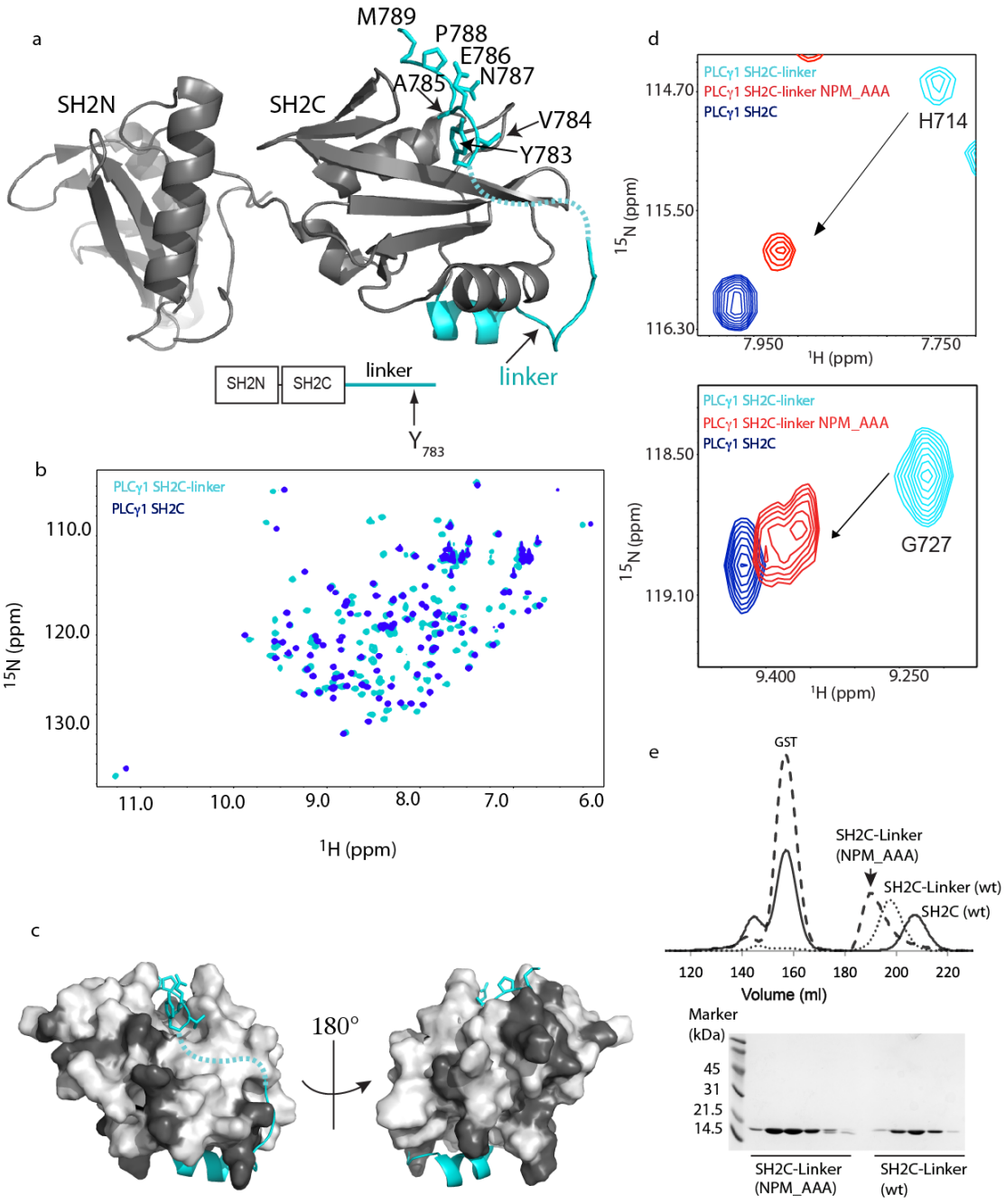
a
M789
P788
E786
N787
A785
V784
Y783
SH2N
SH2C
linker
linker
Y783
b
PLCγ1 SH2C-linker
PLCγ1 SH2C
15N (ppm)
1H (ppm)
c
180°
d
PLCγ1 SH2C-linker
PLCγ1 SH2C-linker NPM_AAA
PLCγ1 SH2C
H714
G727
15N (ppm)
1H (ppm)
e
GST
SH2C-Linker (NPM_AAA)
SH2C-Linker (wt)
SH2C (wt)
Volume (ml)
Marker (kDa)
45
31
21.5
14.5
SH2C-Linker (NPM_AAA)
SH2C-Linker (wt)

Figure 3

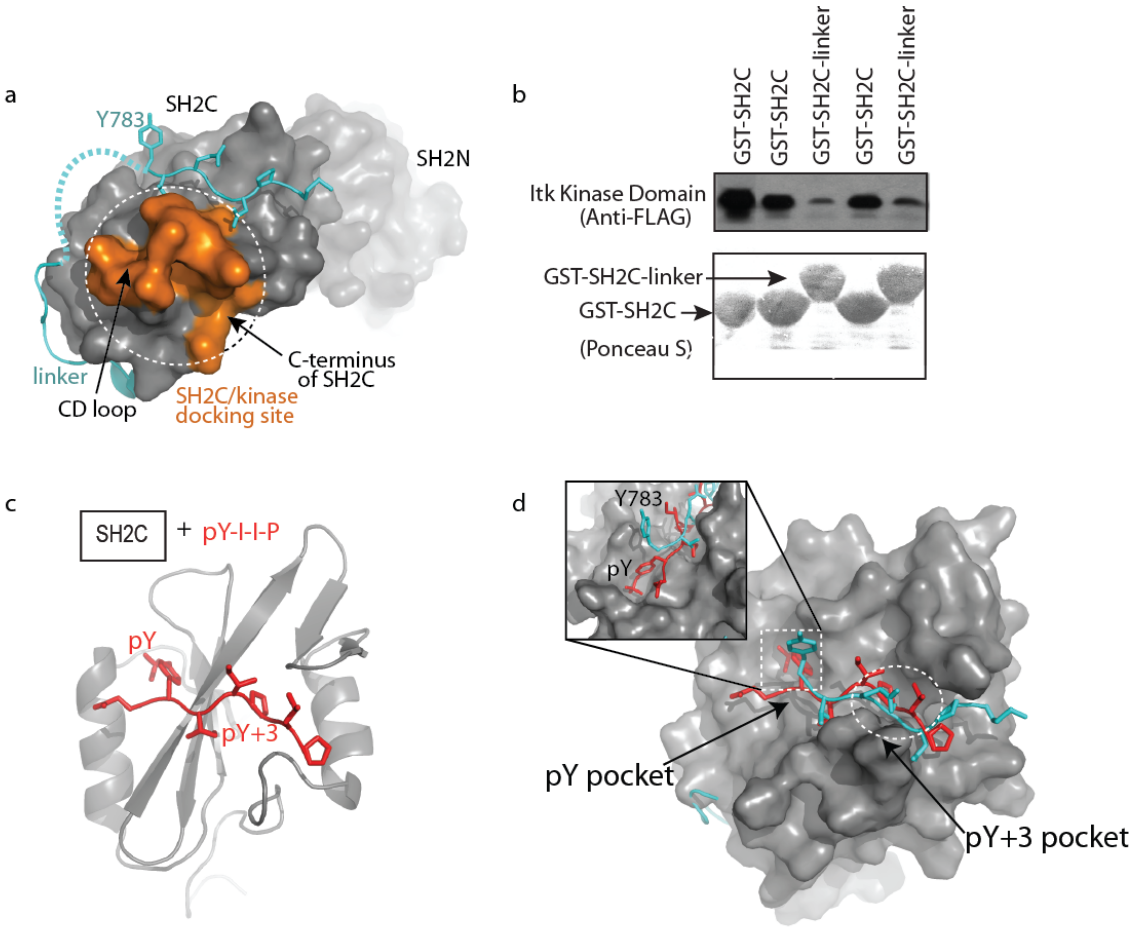
a
SH2C
Y783
SH2N
linker
CD loop
C-terminus
of SH2C
SH2C/kinase
docking site
b
GST-SH2C
GST-SH2C
GST-SH2C-linker
GST-SH2C
GST-SH2C-linker
Itk Kinase Domain
(Anti-FLAG)
GST-SH2C-linker
GST-SH2C
(Ponceau S)
c
SH2C
+ pY-I-I-P
pY
pY+3
d
Y783
pY
pY pocket
pY+3 pocket

Figure 4

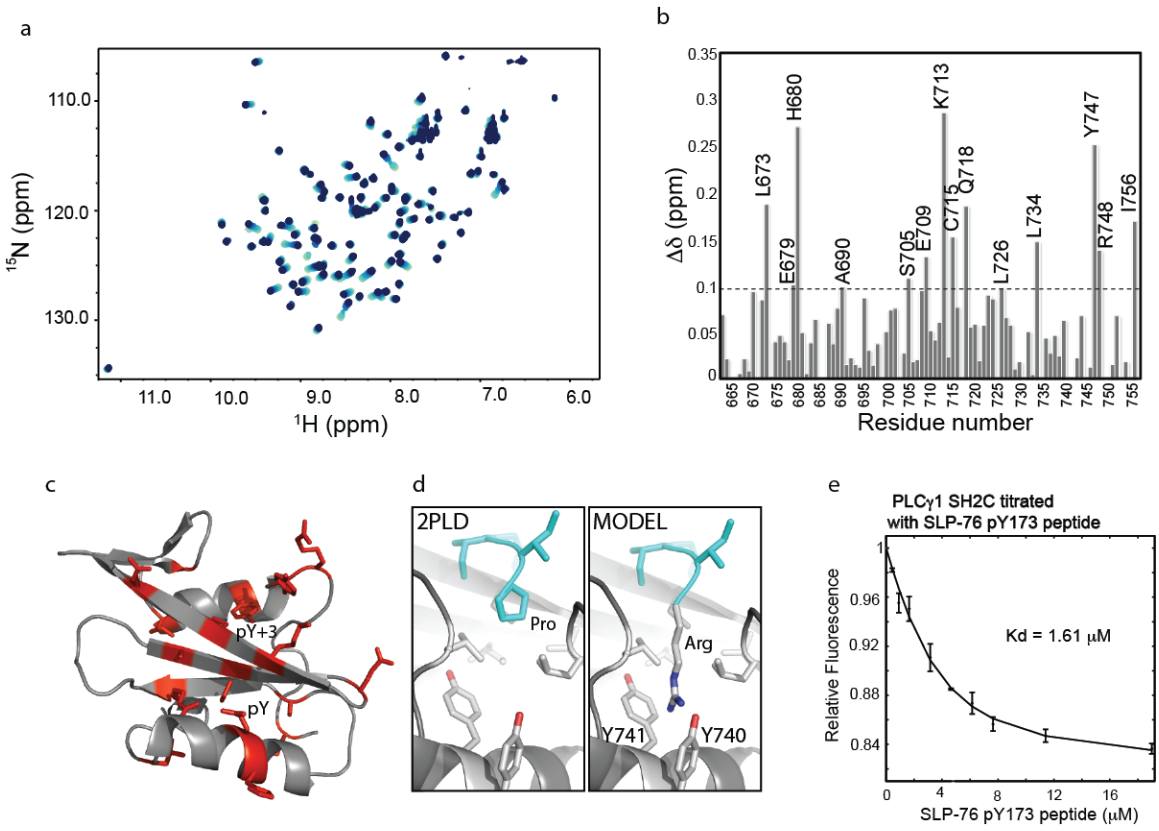
a
110.0
120.0
130.0
15N (ppm)
11.0
10.0
9.0
8.0
7.0
6.0
1H (ppm)
b
0.35
0.3
0.25
0.2
0.15
0.1
0.05
0
Δδ (ppm)
L673
H680
E679
A690
S705
E709
K713
C715
Q718
L726
L734
R748
Y747
I756
665
670
675
680
685
690
695
700
705
710
715
720
725
730
735
740
745
750
755
Residue number
c
pY+3
pY
d
2PLD
Pro
MODEL
Arg
Y741
Y740
e
PLCγ1 SH2C titrated
with SLP-76 pY173 peptide
1
0.96
0.92
0.88
0.84
Relative Fluorescence
Kd = 1.61 μM
0
4
8
12
16
SLP-76 pY173 peptide (μM)

Figure 5

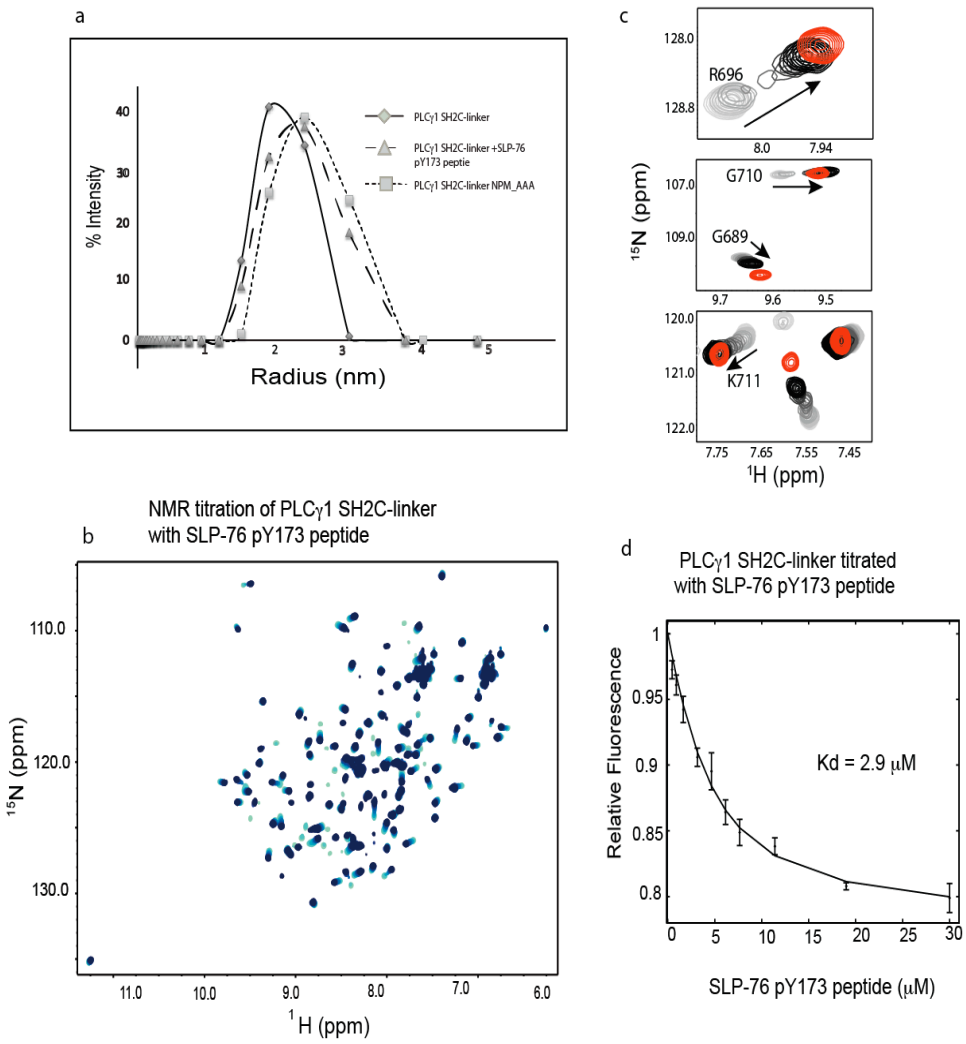
a
% Intensity
Radius (nm)
PLCγ1 SH2C-linker
PLCγ1 SH2C-linker +SLP-76 pY173 peptie
PLCγ1 SH2C-linker NPM_AAA
c
R696
G710
G689
K711
15N (ppm)
1H (ppm)
b
NMR titration of PLCγ1 SH2C-linker with SLP-76 pY173 peptide
15N (ppm)
1H (ppm)
d
PLCγ1 SH2C-linker titrated with SLP-76 pY173 peptide
Relative Fluorescence
Kd = 2.9 μM
SLP-76 pY173 peptide (μM)

Figure 6

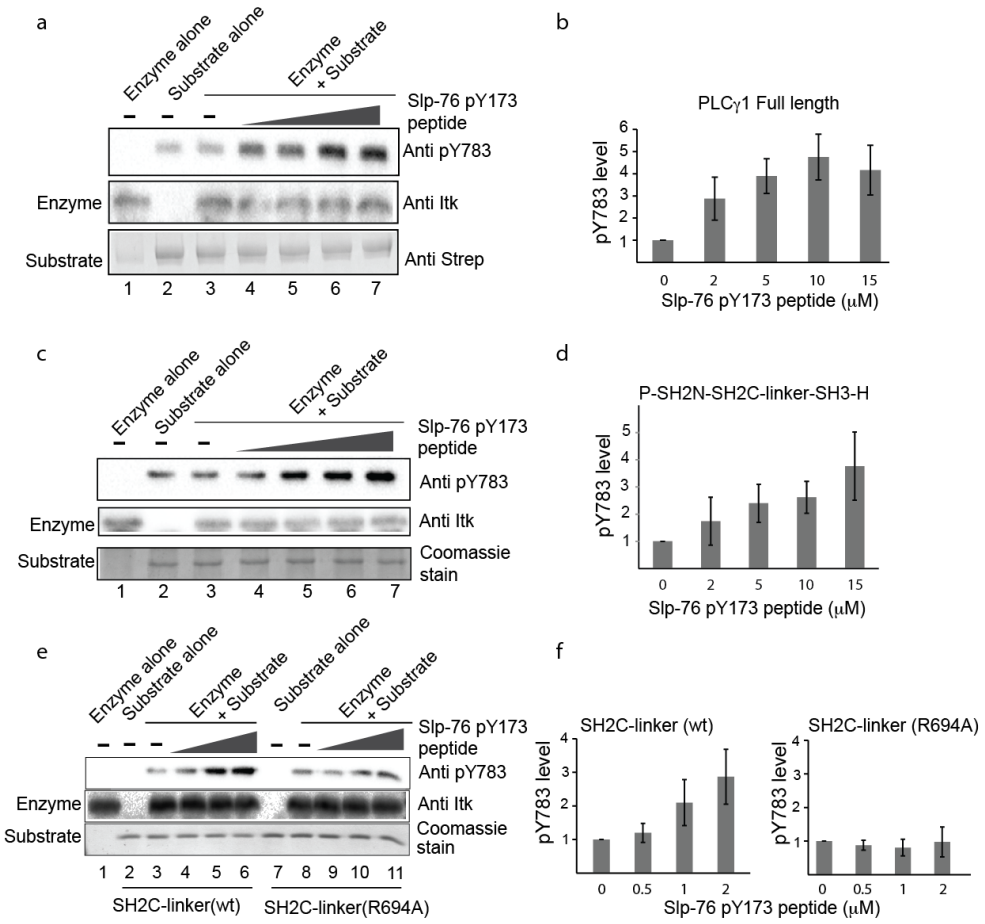
a
Enzyme alone
Substrate alone
Enzyme + Substrate
Slp-76 pY173 peptide
Anti pY783
Enzyme
Anti Itk
Substrate
Anti Strep
1 2 3 4 5 6 7
b
PLCγ1 Full length
pY783 level
Slp-76 pY173 peptide (μM)
c
Coomassie stain
d
P-SH2N-SH2C-linker-SH3-H
e
SH2C-linker(wt)
SH2C-linker(R694A)
f
SH2C-linker (wt)
SH2C-linker (R694A)

Figure 7

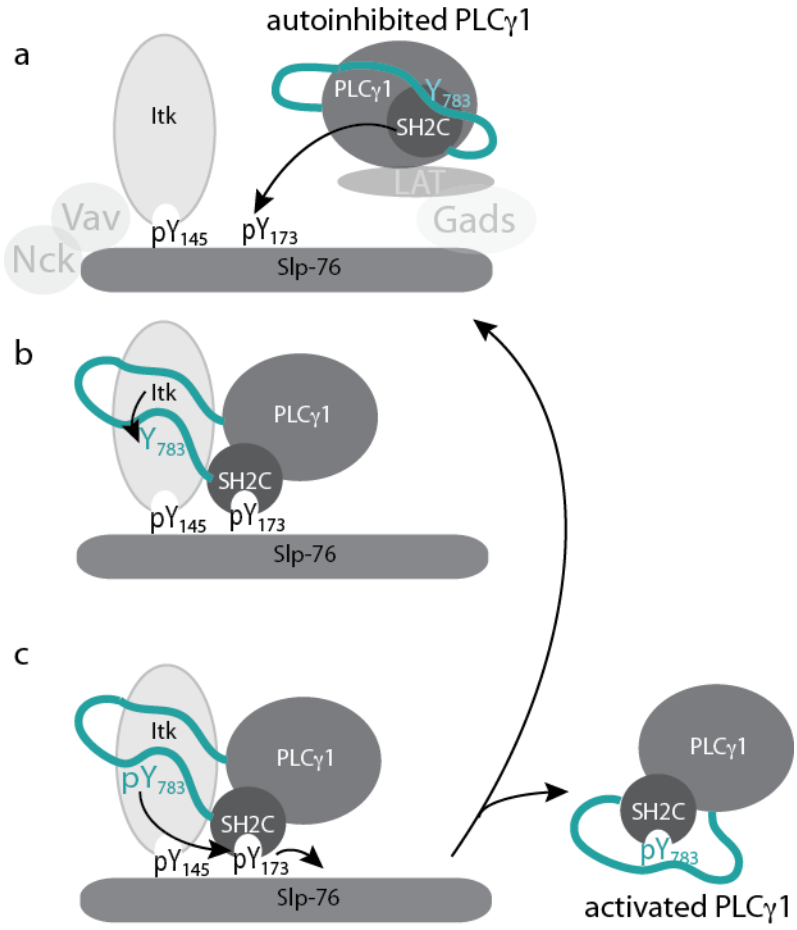
autoinhibited PLCγ1
a
Itk
PLCγ1
Y783
SH2C
LAT
Vav
Gads
Nck
pY145
pY173
Slp-76
b
Itk
PLCγ1
Y783
SH2C
pY145
pY173
Slp-76
c
Itk
PLCγ1
pY783
SH2C
pY145
pY173
Slp-76
PLCγ1
SH2C
pY783
activated PLCγ1

CHAPTER 3

AN AUTOINHIBITORY ROLE FOR THE PLECKSTRIN HOMOLOGY DOMAIN OF ITK AND ITS INTERPLAY WITH CANONICAL PHOSPHOLIPID RECOGNITION

A manuscript under revision in *Biochemistry*

Sujan Devkota[1], Raji E. Joseph, Scott E. Boyken, D. Bruce Fulton and Amy H. Andreotti*

[1]Primary author
*Corresponding author

Abstract

Pleckstrin homology (PH) domains are well known as phospholipid binding modules yet many PH domains across the proteome do not exhibit affinity for lipids suggesting that PH domain function extends beyond lipid recognition. In the current work, we characterize a protein binding function for the PH domain of Interleukin-2-inducible tyrosine kinase (ITK), an immune cell specific signaling protein that belongs to the TEC family of non-receptor tyrosine kinases. Its N-terminal Pleckstrin homology (PH) domain is a well characterized lipid-binding module that localizes ITK to the membrane via phosphatidylinositol (3,4,5)-trisphosphate (PIP_3) binding. Using a combination of NMR spectroscopy and mutagenesis, we have mapped an autoregulatory

protein interaction site on the ITK PH domain that makes direct contact with the catalytic kinase domain of ITK inhibiting the phospho-transfer reaction. Moreover, we have elucidated an important interplay between lipid binding by the ITK PH domain and the stability of the autoinhibitory complex formed by full length ITK. The ITK activation loop in the kinase domain becomes accessible to phosphorylation to the exogenous kinase LCK upon binding of the ITK PH domain to PIP_3. By clarifying the allosteric role of the ITK PH domain in controlling ITK function we have expanded the functional repertoire of the PH domain generally and opened the door to alternative strategies to target this specific kinase in the context of immune cell signaling.

Introduction

Protein kinase activity is tightly regulated before, during and after cellular signaling events(1). The molecular mechanisms responsible for controlling kinase catalytic activity are varied and can depend on the nature of the non-catalytic domains within a particular kinase family. For example, biochemical data and high resolution crystal structures revealed the regulatory role of the SRC Homology 2 and SRC Homology 3 (SH2 and SH3) domains within the SRC kinases (the largest family of non-receptor tyrosine kinases)(2). In the autoinhibited SRC kinase, these regulatory modules pack against the kinase domain in a manner that stabilizes the inactive conformation of the catalytic domain(3). Mutations, small molecules or peptides that displace the SH2 and/or SH3 domains from the kinase domain allow the catalytic domain to sample the active conformation leading to efficient phosphorylation of substrates.

The TEC kinases (ITK, BTK, TEC, BMX and TXK) are the second largest family of non-receptor tyrosine kinases and serve important signaling roles in hematopoietic cells during development as well as during activation of mature lymphocytes(4, 5). Dysregulation of TEC family members are associated with immunodeficiencies and malignancies(6, 7) and so a better understanding of the regulatory machinery of these kinases will aid therapeutic developments. A simple extrapolation of the SRC regulatory mechanism to the TEC family has not been possible, in part due to the presence of a Pleckstrin Homology (PH) domain and the fact that the SRC regulatory tail is absent from the TEC kinase family. PH domains are well known lipid-binding modules that exhibit specific binding to a range of phosphatidylinositol molecules(8-12). The TEC family PH domains bind specifically to phosphatidylinositol (3,4,5)-trisphosphate (PIP_3) that is transiently produced at the plasma membrane upon antigen receptor activation(13). PH domain mediated lipid binding co-localizes the TEC family kinases with the requisite adaptor proteins and substrate.

The PH domain of Interleukin-2 inducible tyrosine kinase (ITK) also appears to play an important regulatory role in controlling ITK catalytic activity. We have previously reported biochemical data that show a significant increase in turnover number upon deletion of the N-terminal PH domain of ITK(14). More recently, crystal structures of a tethered fragment of Bruton's tyrosine kinase (BTK) reveal contacts between the BTK PH and kinase domains(15). For the non-TEC family kinase, AKT, the regulatory role of the PH domain has also become clear through crystallography(16).

The full length T cell specific TEC kinase ITK has so far eluded crystallization and so we set out to characterize the regulatory role of the ITK PH domain in detail using a range of biochemical approaches and solution NMR spectroscopy. Our findings suggest that the ITK PH domain contacts the ITK kinase domain directly and exerts an inhibitory effect on ITK catalytic activity. We identify a specific surface of the ITK PH domain that mediates contacts with the ITK kinase domain and show that mutation of this region of the N-terminal PH domain activates ITK kinase activity. The soluble head group of PIP_3, inositol (1,3,4,5)-tetrakisphosphate (IP_4), competes with the regulatory interaction between ITK PH and kinase domains consistent with the long standing observation that PIP_3 production contributes to ITK activation in the activated T cell. Moreover, we find that PIP_3 containing liposomes activate full length ITK but not an ITK fragment that lacks the PH domain. Finally, we show that phospholipid engagement of the ITK PH domain exposes the activation loop tyrosine in the ITK kinase domain making it more accessible to phosphorylation by the SRC family kinase LCK. The negative regulatory interface we have identified on the ITK PH domain overlaps with the previously reported Ca^{2+}/Calmodulin (CaM) binding site on ITK, consistent with the observation that Ca^{2+}/CaM amplifies ITK signaling(17). The findings reported here provide further insight into the expanding repertoire of the PH domain beyond lipid recognition and sets the stage for targeting this newly described allosteric mechanism in developing therapeutic approaches that complement more traditional ATP inhibitors that bind to the kinase active site.

Materials and Methods

Constructs. Baculoviral constructs encoding FLAG-tagged full length ITK (WT and K390R) and SH3-SH2-kinase (K390R) fragment (P171-L619) of ITK has been described elsewhere(14). Similarly, bacterially expressed construct of His6-GB1 tagged ITK PHTH (C96E/T110I) domain has been described previously(18). The baculoviral construct of ITK kinase domain was produced using the Gateway cloning system (Invitrogen). Briefly, His6 tagged mouse ITK kinase domain (residues 356-619) was PCR amplified and cloned into pENTR/D-TOPO vector (Invitrogen). The pENTR/D-TOPO vector was then recombined with BaculoDirect C-Term Linear DNA (Invitrogen) using LR Clonase II (Invitrogen). The recombined linear DNA was then transfected into Sf9 cells using Cellfectin II reagent (Invitrogen). Baculovirus was selected and amplified for three rounds. All the mutations in the ITK PHTH domain and full length ITK were introduced by site directed mutagenesis (QuikChange Lightning Site-Directed mutagenesis kit, Agilent). N-terminal His6-GB1-tagged BTK PHTHSH3 domain (mouse, aa 1-270), or BTK PHTH domain (aa 1-176) were cloned into the pET20b vector (EMD-Millipore). C-terminally His6-tagged BTK kinase domain (mouse, aa 396-659) and linker-kinase domain (mouse, aa 382-659) were cloned into the pET28a vector (EMD-Millipore). In addition, both the BTK kinase domain and the BTK linker kinase domain constructs had a Y617P mutation which enabled soluble expression in bacteria. The mouse LCK kinase domain (aa Q230-P509) construct with an N-terminal 6His-tag in pET-28a vector was a kind gift from Dr. John Kuriyan. All constructs were verified by sequencing at the Iowa State University DNA Synthesis and Sequencing Facility.

Protein purification. Baculovirus production, expression and purification of all constructs of FLAG tagged full length ITK (WT and K390R), and FLAG tagged SH3-SH2-Kinase (K390R) fragment of ITK were carried out as described previously(14) with the exception of use of suspension High Five™ cells (Invitrogen) rather than adherent Sf9 cells for protein production. For His6 tagged ITK kinase domain production, High Five™ cells were infected with baculovirus and harvested 48 hours post infection. The cell pellet was resuspended in lysis buffer containing 20 mM Tris pH 8, 150 mM NaCl and 10 mM Imidazole. The cells were lysed by dounce homogenization and centrifuged at 16,000 rpm at 4°C for 1 hour. Glycerol was added to supernatant to a final volume of 10% and incubated with Ni-NTA resin overnight at 4°C on a rotary mixer. The resin was washed 5X with wash buffer containing 20 mM Tris pH 8, 150 mM NaCl, 20 mM Imidazole and 10% glycerol. Protein was eluted with elution buffer containing 20 mM Tris pH 8, 150 mM NaCl, 250 mM Imidazole and 10% glycerol. Eluted protein was passed through HiLoad 26/60 Superdex 75 prep grade column (GE Healthcare Life Sciences) pre-equilibrated with buffer 20 mM Tris pH 8, 150 mM NaCl and 10% glycerol. The pure protein containing fractions were pooled, concentrated and snap frozen and stored at -80°C. His6-GB1 tagged ITK PHTH domain, BTK PHTH domain, BTK PHTHSH3 domain, His6-tagged BTK kinase domain or His6-tagged BTK linker kinase domain proteins were expressed in *Escherichia coli* BL21 (DE3) cells and purified as described previously with some modifications(14, 18). After elution of protein from Ni-NTA column the protein was concentrated to 5 ml and injected onto a HiLoad 26/60 Superdex 75 prep grade column equilibrated with buffer composed of 50 mM KH_2PO_4 pH 7.5, 150 mM NaCl. The eluted protein was then concentrated and subjected to His6-

GB1 tag cleavage with Factor Xa (Novagen) for 16 hours at room temperature. The cleavage reaction was stopped with 1 mM PMSF and loaded onto a Ni NTA column to remove His6-GB1 and any uncleaved fusion protein. The flow-through was again passed through HiLoad 26/60 Superdex 75 prep grade column pre equilibrated with buffer containing Tris pH 8, 150 mM NaCl and 10% glycerol. His6 tagged LCK kinase domain was expressed and purified from ArcticExpress cells as described previously(19). The LCK protein was eluted with elution buffer containing 20 mM Tris pH 8, 150mM NaCl, 250mM Imidazole and 10% glycerol**.** The protein was flash frozen and stored at -80°C.

PHTH/Kinase domain interaction assay. Purified ITK His6-GB1 PHTH domain (2 μM or 4 μM) was immobilized on 20 μL (50% slurry) IgG Sepharose beads (GE Healthcare) and was incubated with purified His6-tagged ITK kinase domain (4 μM) in buffer containing 20 mM Tris pH 8, 150 mM NaCl and 10% glycerol at 4°C overnight. The samples were washed 5 times in the same buffer, suspended in 2X SDS loading buffer and boiled. Samples were run on a 12% SDS-PAGE gel for 120 minutes at 180 volts and transferred onto a PVDF membrane and western blotted with anti His6 antibody (Millipore). For pull down assays involving various soluble inositol phosphates (Echelon Biosciences and Cayman chemicals), purified ITK His6-GB1 PHTH (2 μM) was incubated with specified inositol phosphates for 20 minutes before adding His6-tagged ITK kinase domain.

NMR spectroscopy. NMR spectra for ITK PHTH domain in NMR buffer (50mM HEPES pH 8, 150mM NaCl, 10% glycerol) was obtained on a Bruker AVII 700

spectrometer with a 5 mm HCN z-gradient cryoprobe operating at ^{1}H frequency 700.13 MHz with sample temperature of 298K. NMR titration was carried out by collecting ^{1}H-^{15}N HSQC spectra of 200 μM ^{15}N labeled ITK PHTH domain with increasing concentration of unlabeled ITK kinase domain (0, 26, and 50 μM). Buffer with 10% glycerol was necessary to ensure the stability of ITK kinase domain. NMRviewJ(20) was used for NMR spectra visualization and analysis.

In vitro phosphorylation assay. 150 nM full length ITK wild type and mutants (K48D/R49D, V28E/F30Y) and 1μM PLCγ1 SH2C-linker substrate(21) were incubated in an in vitro kinase assay buffer composed of 50 mM HEPES pH 7, 10 mM $MgCl_2$, 1 mM DTT, 1 mg/ml BSA, 1 mM Pefabloc, and 200 μM ATP for various time points (0, 30, 60 and 120 minutes) at room temperature. The samples were boiled for 5 minutes, separated by SDS-PAGE and transferred into a PVDF membrane. The membranes were blotted with anti-BTK pY551 (BD Biosciences) to detect pY511 levels in ITK. Anti-BTK pY511 recognizes the Y511 phosphorylated form of ITK. Anti-ITK (2F12, Thermo Scientific) and PLCγ1 pY783 (EMD Millipore) monoclonal antibody were used to detect total enzyme levels and PLCγ1 pY783 levels, respectively. Total PLCγ1 level was probed by Coomassie staining. In kinase assays to test the effect of inositol lipids, ITK enzyme was pre incubated with soluble inositol phosphates or PIP_3 liposomes for ten minutes before starting the reaction.

For the ITK loop accessibility kinase assay using active LCK kinase domain, 1 μM full length ITK (K390R) or ITK SH3-SH2-kinase (K390R) fragment were incubated with 100 μM liposomes for 10 minutes prior to the addition of 200 nM LCK kinase

domain to start the reaction. The reaction was carried out for 5 minutes at room temperature. The pY511 level was detected as described above. Total ITK and ITK SH3-SH2-Kinase level was detected with an anti-FLAG antibody (Sigma) and total LCK level was detected with anti His6 antibody (Millipore).

Liposome preparation. 1,2-dioleoyl-sn-glycero-3-phosphocholine (DOPC), 1,2-dioleol-sn-glycero-3-[phospho-L-serine] (DOPS) and 1-stearoyl-2-arachidonoyl-sn-glycero-3[phosphoinsositol-3,4,5-triphosphate] (PIP_3) (Avanti polar lipids) were separately dissolved in chloroform. For liposomes containing PIP_3, all three lipids were mixed in 75:10:5 molar ratio (DOPC:DOPS:PIP_3). For control liposome (without PIP_3) DOPC and DOPS were mixed in 79:21 molar ratio (DOPC:DOPS). After mixing, chloroform was evaporated by gentle flow of nitrogen into the test tube containing the lipid mixture. The lipid mixture was then dried overnight at room temperature in a vacuum desiccator. The dried lipid films were hydrated for one hour at room temperature with buffer containing 50 mM HEPES (pH 7) such that the final liposome concentration is 12 mM. The hydrated lipid films were then subjected to five freeze thaw cycles using liquid nitrogen and a 37°C water bath. Unilamellar liposomes were created using the mini extrusion set (Avanti polar lipids) by passing through a 100 nM filter (Whatman). Liposomes were then stored at 4°C and used within 48 hours.

CD spectroscopy. CD spectra of 5 μM ITK PHTH wild type and mutants were acquired on a Jasco J-710 in the far UV region (190-240 nm). The samples were prepared in buffer containing 10 mM NaH_2PO_4 (pH 7.4). CD spectra were obtained at a scanning

rate of 100 nm/min with a spectral bandwidth of 2 nm and response time of 1 s. All CD spectra are the average of two scans and were converted from mdegree into molar residue ellipticity (deg cm^2 $dmol^{-1}$).

Results

Full length ITK kinase consists of three regulatory domains: PHTH, SH3, and SH2 that are positioned N-terminal to the catalytic kinase domain (Fig. 1a). It should be noted here that the TH (or TEC Homology) region of the TEC family kinases is considered an extension of the PH fold and so throughout this work we are using the larger ITK fragment that contains both PH and TH regions (ITK PHTH). Based on previous biochemical findings that suggest a role for the PHTH domain in controlling kinase activity(14), we set out to better understand how the ITK PHTH region exerts control over ITK mediated phosphorylation. We first expressed and purified His6-GB1 fused ITK PHTH domain and a separate His6 tagged ITK kinase domain (Fig. 1a).

The purified ITK N-terminal fragment, His6-GB1-PHTH (Fig. 1a) was immobilized using IgG sepharose and incubated with the ITK kinase domain. Following extensive washing of the sepharose beads, we find that the ITK kinase domain binds to the ITK PHTH fragment in a concentration dependent manner (Fig. 1b, lanes 7,8). Interestingly, the analogous interaction is not detected in similar experiments with the BTK PHTH and kinase domains (Fig. 1c,d, lanes 6,9). A large loop insertion in the BTK PHTH domain makes it similar in size to the BTK kinase domain and so we assessed the possibility of a direct interaction using the larger BTK His6-GB1-PHTH-SH3 fragment

and the BTK His6-Kinase as well as the BTK linker-kinase domain (Fig. 1c,d, lanes 7,10). No interaction is detected between these N-terminal and C-terminal domains of BTK (Fig. 1d) under the same conditions used to detect the ITK PHTH/kinase interaction (Fig. 1b). These data therefore suggest that ITK PHTH interacts in trans with the ITK kinase domain and a corresponding in trans interaction between the BTK PHTH and kinase domains is not detected in the assay.

To further characterize the ITK PHTH/kinase interaction we expressed and purified ^{15}N-labeled ITK PHTH for NMR spectroscopy. Using previously published assignments for an ITK PHTH variant harboring two mutations ((C96E/T110I) that improve expression and solubility(17, 18), we titrated unlabeled ITK kinase domain into the labeled ITK PHTH domain and acquired ^{1}H-^{15}N HSQC spectra at each point of the titration (Fig. 2a-c). Many of the PHTH amide NH resonances in the HSQC spectrum do not change throughout the course of the titration (Fig. 2b,c). A subset of ITK PHTH resonances, however, show selective disappearance as the concentration of ITK kinase domain is increased (Fig. 2b,c). Mapping these spectral changes onto a structural model of ITK PHTH shows the residues that are affected by binding of ITK kinase domain are primarily located in two regions: across β-strands 2-4 of the PH domain and one side of the long α-helix of the PH domain fold (Fig. 2d).

NMR spectral changes are sensitive to small changes in local environment and often map a surface or region that is larger than the actual interface between two proteins in a complex. We therefore used mutagenesis to refine the binding site on the ITK PHTH

domain that mediates the interaction with the ITK kinase domain. Based on NMR spectral changes, we first mutated residues within the beta strand region (β2-β4) as well as residues on the β3-β4 loop. Mutations were chosen to directly probe residues for which NMR spectral changes were observed (Fig. 2d) and to assess other residues in this beta-strand region that have surface exposed sidechains but lacked an observable spectral change either due to intramolecular hydrogen bonding, adverse conformational dynamics and/or lack of assignment. Specific amino acid mutations were based on either the corresponding residue in BTK, a charge reversal or mutation to alanine. The extent of interaction of wild type ITK PHTH and each PHTH mutant with the ITK kinase domain was assessed using the same pull down assay described in Figure 1 (Fig. 3a,b). A greater than 50% decrease in binding of the ITK kinase domain to ITK PHTH was observed upon mutation of four residues: (Fig. 3b; V28, F30, K48, and R49). Mutation of two additional residues, L51D and E56A, causes a 50% decrease in binding between the ITK kinase and PHTH domains (Fig. 3b). To further probe the ITK PHTH surface, we mutated additional surface residues across the entire ITK PHTH domain (including surface exposed side chains on the α-helix) and find only small changes in ITK kinase/PHTH binding (Fig. 3c,d) suggesting that these additional sidechains do not substantially contribute to the interaction between the two domains.

Mapping the mutagenesis results onto a model of the ITK PHTH domain shows that the residues that mediate binding of the ITK kinase domain to ITK PHTH cluster in one region of the PHTH domain and those residues that do not contribute to the interaction based on mutagenesis data are outside of this newly defined binding surface

(Fig. 3e-g). The secondary structural elements within PHTH involved in mediating the PHTH/kinase interaction include the beta strands β2 and β4 and the β3-β4 loop (Fig. 3e,f).

Our previous biochemical work assessing the activity of ITK deletions(14) suggested that the ITK PHTH region inhibits ITK kinase domain activity. Having mapped the surface on the ITK PHTH domain responsible for the interaction with the ITK kinase domain, we next introduced specific PHTH domain mutations into full length ITK and measured both ITK activation loop autophosphorylation (pY511) and phosphorylation of the ITK substrate PLCγ1 (pY783) to determine the extent to which specific PHTH domain residues affect ITK catalytic activity. Mutation of two pairs of PHTH domain residues, K48/R49 and V28/F30, caused the largest decrease in the ITK PHTH/kinase domain interaction (Fig. 3a,b) and so these residues were mutated in full length ITK. Using CD spectroscopy, we first established that these mutations do not alter the overall fold of the PHTH domain but retain the secondary structure of the wild type sequence (Fig. 4a). The kinase activity of full length wild type ITK was then compared to the full length double mutants, ITK K48D/R49D and ITK V28E/F30Y, ensuring that each enzyme is not phosphorylated on the activation loop tyrosine (Y511) at the beginning of the assay (Fig. 4b-d). Both sets of mutations in the PHTH domain affect ITK catalytic activity; activation loop phosphorylation levels (pY511) and phosphorylation of exogenous PLCγ1 are increased compared to wild type ITK (Fig. 4b-d). While both sets of mutations increase ITK activity, mutation of K48/R49, at the center of the newly defined binding surface on the ITK PHTH domain (Fig. 3e), has a greater

effect on the kinase activity of full length ITK than does the more peripheral V28E/F30Y mutation. Thus, mutations in the ITK PHTH domain that disrupt the interaction with the kinase domain appear to reduce autoinhibition and increase catalytic function of the ITK kinase domain.

In the context of cell signaling, the PHTH domain of ITK binds to phosphatidylinositol (3,4,5)-trisphosphate (PIP_3) at the membrane via a conserved binding pocket. The lipid binding pocket on ITK PHTH is adjacent to the cluster of amino acids we have identified here that mediate an autoinhibtory interaction with the ITK kinase domain (Fig. 5a). In fact, R29, which is located between V28 and F30 in the ITK PHTH domain, is the conserved arginine that mediates binding to the negatively charged lipid head group. Given the juxtaposition of this lipid binding residue between two residues that mediate the autoinhibitory PHTH/kinase interaction, we decided to avoid mutagenesis and instead test whether binding of the soluble head group of PIP_3, inositol (1,3,4,5)-tetrakisphosphate ($IP(1,3,4,5)P_4$), affects the interaction between ITK PHTH and ITK kinase domain. In this assay we compare the interaction between ITK PHTH and ITK kinase domain in the presence of increasing concentration of $IP(1,3,4,5)P_4$ and a control inositol (1,3,4,6)-tetrakisphosphate ($IP(1,3,4,6)P_4$) (Fig. 5b,c). The amount of ITK kinase domain that associates with ITK PHTH decreases in the presence of increasing inositol 1,3,4,5 tetrakisphosphate ligand concentration but not the inositol 1,3,4,6 tetrakisphosphate regioisomer (Fig. 5b,c). To further test specificity we examined a panel of inositol phosphates and find that the inositol tertakisphosphate (IP_4), specifically, inositol (1,3,4,5)-tetrakisphosphate is the only soluble lipid among eleven

tested that disrupts the ITK PHTH/kinase domain interaction to greater than 50% (Fig. 5d,e (lane 8)). This suggests that the ITK PHTH/kinase domain interaction is mutually exclusive with lipid binding to the ITK PHTH domain and is specific to the soluble lipid head group of PIP_3.

Since inositol (1,3,4,5)-tetrakisphosphate specifically interferes with the ITK PH/kinase interaction we next examined the effect of IP_4 on ITK kinase activity. Using the same kinase assay described in Figure 4b, ITK activation loop phosphorylation levels (pY511) were monitored in the presence of increasing concentration of $IP(1,3,4,5)P_4$ or the regioisomeric control compound $IP(1,3,4,6)P_4$. ITK activation loop phosphorylation decreases with increasing IP_4, whether the isomer corresponding to the soluble head group of the physiologically relevant PIP_3 ($IP(1,3,4,5)P_4$) or the regioisomer $IP(1,3,4,6)P_4$ is used in the assay (Fig. 6a,b). Previous findings showed no change in ITK mediated in vitro phosphorylation of a non-physiological peptide substrate(22) and so together these results suggest that either IP_4 by itself does not directly activate ITK in spite of interfering with the regulatory PHTH/Kinase interaction, or at the concentrations required to disrupt the PHTH/kinase interaction, IP_4 is incompatible with the in vitro kinase assay causing non-specific inhibition of ITK activity. The observation that the regioisomeric IP_4 compound decreases ITK activation loop phosphorylation to the same extent as the physiologically relevant IP_4 ($IP(1,3,4,5)P_4$) (Fig. 6b) but does not disrupt the ITK PHTH/kinase interaction (Fig. 5c) supports the conclusion that the in vitro ITK kinase assay is not a reliable measure of the effect of IP_4 on ITK function.

In an effort to circumvent the non-specific kinase inhibition caused by soluble IP_4, we expanded the ITK in vitro kinase assay to examine the effect of the ITK PHTH domain target, PIP_3; the plasma membrane bound phospholipid produced by phosphoinositide 3-kinase following T cell receptor activation(23). ITK activation loop phosphorylation levels (pY511) were monitored in the presence of PIP_3 containing liposomes as well as control liposomes that lack PIP_3. Unlike the equivocal effects of IP_4 on ITK activity, PIP_3 activates ITK as measured by phosphorylation on the activation loop tyrosine Y511 (Fig. 6c, lane 2, 6d) whereas control liposomes do not enhance activation loop phosphorylation (Fig. 6c, lane 3, 6d). This result is consistent with binding of the PIP_3 headgroup in a manner that competes with an autoregulatory interaction mediated by the ITK PHTH domain (Fig. 5a).

To gain additional insight into precisely how PIP_3 leads to increased phosphorylation on the ITK activation loop, we next carried out a combined kinase assay that makes use of kinase inactive full length ITK (K390R), the inactive ITK fragment lacking the PHTH domain (ITK SH3-SH2-Kinase (K390R)) and active LCK kinase domain, the SRC family kinase that is responsible for phosphorylation of ITK Y511 in activated T cells(24) (Fig. 7a). The catalytically inactive full length ITK (K390R) and ITK SH3-SH2-Kinase (K390R) are used in this assay to ensure that phosphorylation on ITK Y511 is solely due to LCK activity and not due to intrinsic ITK activity. Thus, the extent to which ITK Y511 is phosphorylated by exogenous LCK reveals the accessibility of the ITK activation loop under different conditions(25). Both full length ITK (K390R) and the ITK SH3-SH2-Kinase (K390R) fragment are subjected to phosphorylation by

active LCK in the presence and absence of PIP_3. In the absence of PIP_3 (either no liposomes or control liposomes (PC/PS) that do not contain PIP_3) we find the ITK SH3-SH2-Kinase (K390R) fragment is phosphorylated on Y511 to a greater extent than full length ITK (K390R) (Fig. 7b,c lanes 3 & 4 and 7 & 8) suggesting that the PHTH domain reduces accessibility of the ITK activation loop to LCK. For full length ITK (K390R) in the presence of PIP_3 containing liposomes (PC/PS/PIP_3), LCK dependent phosphorylation of the ITK activation loop tyrosine (pY511) is higher than full length ITK (K390R) in the absence of liposomes or in the presence of control liposomes (Fig. 7 b,c lane 6 versus 2, 4 & 8). In contrast, LCK mediated phosphorylation of the activation loop tyrosine Y511 in the ITK SH3-SH2-Kinase fragment that lacks PHTH is unaffected by the presence or absence of PIP_3 (Fig. 7b,c lanes 3,5,7). These observations suggest that binding of PIP_3 to the ITK PHTH domain 'activates' ITK by unmasking of the ITK activation loop making it more accessible to phosphorylation by LCK.

Discussion

The findings reported here support an autoregulatory role for the PHTH region in controlling the catalytic activity of ITK. The role of the PHTH domain in ITK regulation has been hinted at in previous deletion studies(14) but not previously dissected at the molecular level. In the context of the full length ITK enzyme, a specific surface on the PHTH domain encompassing the β3-β4 loop of the PH fold mediates a direct interaction with the ITK kinase domain resulting in diminished ITK catalytic activity. Mutation of ITK PHTH residues at this interface leads to activation of the remote catalytic domain in the full length ITK enzyme.

A structural model of the autoinhibited form of the related TEC family kinase, BTK, has recently been reported(15). Consistent with our observation that the BTK PHTH and BTK kinase domains do not interact in trans (Fig. 1d), crystallographic analysis of the BTK PHTH/kinase interaction required a tethered BTK PHTH-Kinase construct, which yielded a structure defining a PHTH/kinase interface centered on the base of the PH domain α-helix (Fig. 8a). R133 and Y134 in the BTK PH domain mediate primary sidechain contacts between BTK PH and kinase domains in the tethered BTK crystal structure(15) yet NMR resonances for the corresponding ITK residues, R111 and N112, as well as that of the neighboring residue N113, are unaffected by addition of unlabeled ITK kinase domain (Fig. 2b,c). Moreover, mutation of ITK R111 to glutamate does not affect the ITK PHTH/kinase interaction (Fig. 3d). These findings support the conclusion that the PHTH/kinase interface observed in the crystal structure of the tethered BTK PHTH-kinase construct is not the interface that mediates the autoregulatory ITK PHTH/kinase contact. Instead, ITK residues in the β3-β4 loop of the PHTH domain and not those on the α-helix are primarily responsible for mediating the ITK PHTH/kinase autoinhibitory interaction (Fig. 8a).

Typically protein kinases belonging to the same family are regulated by related mechanisms and yet our data describing ITK autoinhibition diverge from the available structural model of BTK. If autoinhibition of these related kinases are in fact mediated by a shared mechanism, it is possible that the alternative PHTH/kinase interaction evident in BTK(15) (Fig. 8a) might represent an intermediate state between fully autoinhibited and

active kinase that was captured as a result of tethering the BTK PHTH and kinase domains. Indeed, mutation of the BTK β3-β4 loop residues that correspond to the ITK PHTH domain surface we have defined here (BTK R49E and K52E (K48 and L51 in ITK)) was shown to activate BTK catalytic activity(15). Since these β3-β4 loop residues of the BTK PHTH domain are not located at the PHTH/kinase interface in the tethered BTK structural model, the authors of that work suggested that mutations in the BTK β3-β4 loop might alleviate electrostatic repulsion allowing transient dimerization (and hence autophosphorylation) to occur more favorably. Our data clearly support an ITK inhibitory contact between PHTH and kinase domains and it remains to be determined whether or not ITK is also regulated by PHTH domain mediated dimerization. By the same token, it is also possible that, like ITK, the β3-β4 loop of the BTK PH domain might mediate important autoinhibitory contacts with the BTK kinase domain not captured in the crystal structure of the tethered domains.

Regardless of the exact details of autoinhibition of ITK and BTK, differences do persist within this kinase family since we find that the ITK PHTH/kinase interaction can be readily detected intermolecularly while the BTK PHTH/kinase interaction cannot (Fig. 1). This observation suggests that the intramolecular regulatory interaction (regardless of details) is stronger in ITK than BTK, an idea that is consistent with earlier work suggesting that B cell proteins such as BTK and SYK are more easily activated than their T cell counterparts, ITK and ZAP-70(25, 26). The reason for differences in regulation of ITK and BTK may be related to the notion that, compared to B cells, T cell activation

needs to be under stricter control given the deleterious effects of over production of inflammatory cytokines(25).

The ITK PHTH binding residues in and around the β3-β4 loop are close to the binding site of the PIP_3 phospholipid head group (Fig. 8a) consistent with the observation that binding of the soluble head group of the PIP_3 ligand, $IP(1,3,4,5)P_4$, selectively disrupts the ITK PHTH/kinase interaction (Fig. 5). This finding may also be related to earlier observations that $IP(1,3,4,5)P_4$ itself promotes activation of ITK in T lymphocytes(22) and so $IP(1,3,4,5)P_4$ might, at least in part, pry open the autoinhibited form of ITK. However, the results of in vitro assays in the presence of inositol tetrakisphosphates suggest difficulty in directly measuring the effect of IP_4 on ITK kinase activity (Fig. 6a,b). It should also be noted that the autoinhibitory region of the ITK PH domain that we have identified here partially overlaps with a peripheral binding site identified on the BTK PH domain that binds IP_6(15). IP_6 binding to the BTK PH domain putatively stabilizes transient dimerization and subsequent BTK autophosphorylation(15). Yet, as the authors in that work note, the peripheral BTK IP_6 binding site is not conserved in ITK and so an IP_6 regulatory role for ITK seems unlikely.

The well characterized physiological ligand of the ITK PHTH domain, PIP_3, is a membrane bound phospholigand produced upon T cell activation. Using PIP_3 containing liposomes we find that phospholigand binding to the ITK PHTH domain leads to ITK activation by enhancing LCK mediated phosphorylation of the ITK activation loop tyrosine Y511 (Fig. 7). The data suggest that engagement of the ITK PHTH with

phospholipid ligand leads to release of the autoinhibitory PHTH/kinase contact (opening of the compact domain arrangement suggested in the BTK crystal structure) revealing the ITK activation loop tyrosine (ITK Y511) to the LCK active site (Fig. 8b).

Inspecting the electrostatic surface of the ITK kinase domain shows that there is a large acidic patch extending from the N-lobe over the activation loop that might provide a complementary binding surface for the positively charged amino acids in the ITK PHTH β3-β4 loop (Fig. 8c). Further structural work will definitively determine whether this acidic surface on the ITK kinase domain serves as the binding interface with the ITK PHTH domain in the autoinhibitory conformation. Like ITK, the BTK kinase domain shares the large negatively charged surface (Fig. 8d) yet this is not the surface contacted by the BTK PHTH domain in the structural model that emerged from tethering the two domains(15). The serine/threonine kinase belonging to the AGC superfamily, AKT, is also regulated by its PH domain and a crystal structure of that regulatory complex shows the AKT PH domain occludes the kinase active site by contacting the corresponding region of the AKT kinase domain that extends from the N-lobe across part of the activation loop(16). Certainly, a similar autoinhibitory mechanism for the TEC family kinases ITK and BTK that sterically precludes activation loop phosphorylation seems plausible and is supported by the ITK/LCK loop accessibility assay described here (Fig. 7).

The ITK PHTH β3-β4 loop has also been previously implicated in binding the calcium binding protein, Calmodulin(17). Binding of Ca^{2+}/Calmodulin to the ITK PHTH

domain (via β3-β4 loop residues) was shown to result in sustained ITK activation and potentiated calcium signaling in T cells. Based on the negative regulatory role we have now demonstrated for this region of ITK PHTH, it is possible that one of the consequences of Ca^{2+}/Calmodulin binding to ITK is to maintain an open, active state and prevent formation of the autoinhibitory state. Along these lines, it is interesting to note that the COSMIC (catalogue of somatic mutations in cancer) database lists several mutations in ITK that span the PHTH interface responsible for binding to the ITK kinase domain (Fig. 8e). It is possible that these mutations activate ITK kinase activity in much the same way that the targeted mutations studied here abolish the autoregulatory PHTH/kinase interaction (Fig. 3) and increase ITK mediated phosphorylation of PLCγ1 (Fig. 4). Similar oncogenic activation via PH domain mutations has been reported for AKT(27).

It is becoming increasingly clear that Pleckstrin Homology domains target non-lipid binding partners in addition to membrane-bound phospholipids. A recent review by Huang and co-workers(28) highlights the varied roles of the PH domain in lymphocyte signaling as well as the regulatory role of the PH domain in non-lymphocytic proteins generally. In one example, the DH-PH domain module of Dbs, a Cdc42 specific Guanine Exchange Factor, contacts Cdc42 via the β3-β4 loop of the Dbs PH domain(29). In another example, the guanine nucleotide exchange factor P-Rex2 recognizes its substrate G protein via the β3-β4 loop region of the PH domain(30). With our observations of a critical role for the same β3-β4 loop of ITK PHTH in binding the ITK kinase domain as well as Ca^{2+}/Calmodulin(17), it is possible that this region of the PH fold may serve as a

general protein recognition motif. It is noteworthy that binding mediated by the β3-β4 loop region of the PH domain seems sensitive to phospholipid binding at a nearby site suggesting significant interplay between lipid and protein recognition by this common signaling domain. The growing examples of PH domain mediated regulation also suggest that the specific protein interactions mediated by the PH fold are potential targets for allosteric regulation of signaling molecules via the activity of small molecules. Indeed, targeting AKT in this manner has already been demonstrated providing proof of principle for other systems such as the TEC family kinases.

Acknowledgements

This work was supported by a grant from the NIH, National Institute of Allergy and Infectious Diseases, AI043957. The authors would like to thank Thamotharan Subbiah for making the baculoviral ITK kinase domain construct.

References

1. Lee MJ & Yaffe MB (2016) Protein Regulation in Signal Transduction. *Cold Spring Harb Perspect Biol* 8(6).
2. Xu W, Harrison SC, & Eck MJ (1997) Three-dimensional structure of the tyrosine kinase c-Src. *Nature* 385(6617):595-602.
3. Xu W, Doshi A, Lei M, Eck MJ, & Harrison SC (1999) Crystal structures of c-Src reveal features of its autoinhibitory mechanism. *Mol Cell* 3(5):629-638.

4. Andreotti AH, Schwartzberg PL, Joseph RE, & Berg LJ (2010) T-cell signaling regulated by the Tec family kinase, Itk. *Cold Spring Harb Perspect Biol* 2(7):a002287.

5. Bradshaw JM (2010) The Src, Syk, and Tec family kinases: distinct types of molecular switches. *Cell Signal* 22(8):1175-1184.

6. Tsukada S*, et al.* (1993) Deficient expression of a B cell cytoplasmic tyrosine kinase in human X-linked agammaglobulinemia. *Cell* 72(2):279-290.

7. Huck K*, et al.* (2009) Girls homozygous for an IL-2-inducible T cell kinase mutation that leads to protein deficiency develop fatal EBV-associated lymphoproliferation. *J Clin Invest* 119(5):1350-1358.

8. Lemmon MA (2007) Pleckstrin homology (PH) domains and phosphoinositides. *Biochem Soc Symp* (74):81-93.

9. Moravcevic K, Oxley CL, & Lemmon MA (2012) Conditional peripheral membrane proteins: facing up to limited specificity. *Structure* 20(1):15-27.

10. Harlan JE, Hajduk PJ, Yoon HS, & Fesik SW (1994) Pleckstrin homology domains bind to phosphatidylinositol-4,5-bisphosphate. *Nature* 371(6493):168-170.

11. Vanhaesebroeck B, Stephens L, & Hawkins P (2012) PI3K signalling: the path to discovery and understanding. *Nat Rev Mol Cell Biol* 13(3):195-203.

12. Cantrell DA (2001) Phosphoinositide 3-kinase signalling pathways. *J Cell Sci* 114(Pt 8):1439-1445.

13. Okoh MP & Vihinen M (1999) Pleckstrin homology domains of tec family protein kinases. *Biochem Biophys Res Commun* 265(1):151-157.

14. Joseph RE, Min L, & Andreotti AH (2007) The linker between SH2 and kinase domains positively regulates catalysis of the Tec family kinases. *Biochemistry* 46(18):5455-5462.

15. Wang Q*, et al.* (2015) Autoinhibition of Bruton's tyrosine kinase (Btk) and activation by soluble inositol hexakisphosphate. *Elife* 4.

16. Wu WI*, et al.* (2010) Crystal structure of human AKT1 with an allosteric inhibitor reveals a new mode of kinase inhibition. *PLoS One* 5(9):e12913.

17. Wang X*, et al.* (2014) Calmodulin and PI(3,4,5)P(3) cooperatively bind to the Itk pleckstrin homology domain to promote efficient calcium signaling and IL-17A production. *Sci Signal* 7(337):ra74.

18. Boyken SE, Fulton DB, & Andreotti AH (2012) Rescue of the aggregation prone Itk Pleckstrin Homology domain by two mutations derived from the related kinases, Btk and Tec. *Protein Sci* 21(9):1288-1297.

19. Joseph RE & Andreotti AH (2008) Bacterial expression and purification of interleukin-2 tyrosine kinase: single step separation of the chaperonin impurity. *Protein Expr Purif* 60(2):194-197.

20. Johnson BA & Blevins RA (1994) NMR View: A computer program for the visualization and analysis of NMR data. *J Biomol NMR* 4(5):603-614.

21. Joseph RE, Min L, Xu R, Musselman ED, & Andreotti AH (2007) A remote substrate docking mechanism for the tec family tyrosine kinases. *Biochemistry* 46(18):5595-5603.

22. Huang YH*, et al.* (2007) Positive regulation of Itk PH domain function by soluble IP4. *Science* 316(5826):886-889.

23. August A, Sadra A, Dupont B, & Hanafusa H (1997) Src-induced activation of inducible T cell kinase (ITK) requires phosphatidylinositol 3-kinase activity and the Pleckstrin homology domain of inducible T cell kinase. *Proc Natl Acad Sci U S A* 94(21):11227-11232.

24. Heyeck SD, Wilcox HM, Bunnell SC, & Berg LJ (1997) Lck phosphorylates the activation loop tyrosine of the Itk kinase domain and activates Itk kinase activity. *J Biol Chem* 272(40):25401-25408.

25. Joseph RE*, et al.* (2013) Activation loop dynamics determine the different catalytic efficiencies of B cell- and T cell-specific tec kinases. *Sci Signal* 6(290):ra76.

26. Latour S, Chow LM, & Veillette A (1996) Differential intrinsic enzymatic activity of Syk and Zap-70 protein-tyrosine kinases. *J Biol Chem* 271(37):22782-22790.

27. Parikh C*, et al.* (2012) Disruption of PH-kinase domain interactions leads to oncogenic activation of AKT in human cancers. *Proc Natl Acad Sci U S A* 109(47):19368-19373.

28. Wang X, Hills LB, & Huang YH (2015) Lipid and Protein Co-Regulation of PI3K Effectors Akt and Itk in Lymphocytes. *Front Immunol* 6:117.

29. Rossman KL*, et al.* (2002) A crystallographic view of interactions between Dbs and Cdc42: PH domain-assisted guanine nucleotide exchange. *Embo J* 21(6):1315-1326.

30. Joseph RE & Norris FA (2005) Substrate specificity and recognition is conferred by the pleckstrin homology domain of the Dbl family guanine nucleotide exchange factor P-Rex2. *J Biol Chem* 280(30):27508-27512.

31. Roy A, Kucukural A, & Zhang Y (2010) I-TASSER: a unified platform for automated protein structure and function prediction. *Nat Protoc* 5(4):725-738.

32. Marquez JA*, et al.* (2003) Conformation of full-length Bruton tyrosine kinase (Btk) from synchrotron X-ray solution scattering. *Embo J* 22(18):4616-4624.

Figure Captions

Figure 1. The ITK PHTH domain interacts with the ITK kinase domain in trans**.** (a) Domain constructs of ITK used in this study. Full length ITK is shown above the His6-GB1-tagged PHTH domain fragment of ITK (residues 1-154) and the His6-tagged Kinase domain fragment (residues 356-619). (b) Coomassie gel showing ITK kinase domain (4 μM) associates with ITK PHTH domain (2 and 4 μM in lanes 7 and 8, respectively) immobilized on IgG sepharose beads. Lanes 1 shows the ITK kinase domain alone does not associate with IgG sepharose, lanes 2, 3 and 4 are loading controls. Lane 5 shows the ITK kinase domain and asterisks show the IgG heavy and light chains. Lane 6 shows that the ITK kinase domain does not associate with IgG sepharose bound His6-GB1 that lacks ITK PHTH. (c) Domain constructs of BTK used in this study. Full length BTK is shown above the His6-GB1-tagged PHTHSH3 (residues 1-270), the His6-GB1-tagged PHTH (residues 1-176) and the His6-tagged Kinase domain fragments of BTK (residues 396-

659 (Kinase domain) and residues 382-659 (Linker-Kinase domain)). (d) Coomassie gel showing that neither the BTK kinase domain (1 μM) or the BTK linker-kinase domain (1 μM) associates in this assay with either the BTK PHTH domain (2 μM) or the larger BTK PHTHSH3 construct (2 μM) immobilized on IgG sepharose beads (lanes 6,7,9 and 10). Protein alone loading controls are shown on the left side of the gel. As in (b) asterisks indicate IgG heavy and light chains.

Figure 2. NMR mapping of the ITK PHTH regulatory interface**.** (a) [^{15}N,^{1}H]- HSQC spectrum of uniformly ^{15}N-labeled ITK PHTH domain. (b,c) Addition of unlabeled ITK kinase domain to uniformly ^{15}N-labeled ITK PHTH domain results in significant broadening and in some cases chemical shift changes of selected peaks (boxed) in the overlay of [^{15}N, ^{1}H] HSQC spectra acquired during the titration. A large subset of ITK PHTH resonances do not change over the course of the titration. ITK R111, N112 and N113 (corresponding to R133, Y134 and N135 in BTK), do not change during the titration (circled). Black spectrum corresponds to ITK PHTH alone (200 μM), cyan spectrum acquired after addition of 26 μM unlabeled ITK kinase domain and red spectrum acquired after addition of 50 μM unlabeled ITK kinase domain. (d) Computational model of ITK PHTH based on crystal structures of the corresponding BTK domain fragment (PDB IDs: 1BTK and 1B55); threading was performed using I-TASSER(31). ITK PHTH residues for which spectral changes were observed in the NMR data shown in (a-c) are shown in red and labeled. The residues located on β-strands 2-4 are circled and those on the α-helix are boxed. All structural figures were made using PyMol(8).

Figure 3. NMR based mutagenesis refines the surface of the ITK PHTH domain that contacts the ITK kinase domain. (a,c) Anti-His6 blots showing ITK kinase domain (4μM) associates to different extents with wild type and mutant ITK PHTH domain (2μM) that is immobilized on IgG sepharose beads. (b,d) The fraction of ITK kinase domain bound to wild type and mutant ITK PHTH domains; bound kinase is normalized to His6-GB1 PHTH level in each lane and then compared to wild type (wt). The dotted line shows a decrease in ITK PHTH/kinase domain interaction of 50%. Data shown in (a) and (c) are representative of three independent experiments. (e,f) The binding surface determined from the data in (a) and (c) is mapped onto the ITK PHTH domain computational model, labeled and shown in red. The interface residues are located on the β4 and β2 strands as well as the β3-β4 loop. Those residues that, upon mutation, do not disrupt the ITK PHTH/kinase domain interaction are labeled and shown in cyan. In (f) R111 is circled as it corresponds to the BTK residue R133 that is at the interface of the tethered BTK PHTH and kinase domains for which a crystal structure was recently solved(15). (g) Two views of the ITK PHTH surface residues shown in (e) and (f) where red indicates involvement in the ITK PHTH/kinase interaction and cyan corresponds to those residues for which mutation does not affect the ITK PHTH/kinase interaction. The β3-β4 loop residues that are within the binding site identified here are colored pink but were not probed directly by mutagenesis.

Figure 4. Mutation of the ITK PHTH interface residues in full length ITK increases ITK catalytic activity**.** (a) Circular dichroism spectra for wild type ITK PHTH (blue), ITK PHTH (K48D/R49D) (green) and ITK PHTH (V28E/F30Y) (red). (b) Kinase assay

spanning 0-120 minutes showing ITK activation loop autophosphorylation (pY511) and phosphorylation of exogenous PLCγ1 (pY783) for full length, wild type ITK (150 nM) in lanes 1-4, full length ITK mutant K48D/R49D (150 nM) in lanes 5-8, and full length ITK mutant V28E/F30Y (150 nM) in lanes 9-12. Phosphorylation of ITK Y511 is detected using anti-BTK pY551 (labeled Anti pY511 for clarity throughout), PLCγ1 pY783 levels are detected using anti-pY783 antibody and total enzyme levels are detected using anti-ITK antibody. Total PLCγ1 substrate levels (SH2C-linker) are detected using Coomassie stain. (c,d) Histogram representation of normalized pY511 (c) and pY783 (d) levels from the ITK kinase assays shown in (b). The intensities of the band corresponding to pY511 and pY783 were divided by the total ITK enzyme level in each lane. The value of these ratios for ITK (K48D/R49D) at time point 120 minutes was set to 1. All other intensity ratios are shown relative to this value. Experiments were run in triplicate.

Figure 5. The ITK PHTH/Kinase interaction is selectively disrupted by binding of soluble inositol 1,3,4,5-tetrakisphosphate ($IP(1,3,4,5)P_4$). (a) Close up view of the ITK PHTH interface residues that mediate contact to the ITK kinase domain (labeled and in red) and the adjacent lipid binding site. The computational model of the ITK PHTH domain was aligned with the crystal structure of BTK PHTH domain bound to $IP(1,3,4,5)P_4$ (PDB ID: 1B55). BTK PHTH domain is not shown for clarity. The IP_4 head group of PIP_3 is shown bound to the PHTH domain and positions 1,3,4, and 5 are labeled. The position of the conserved arginine that binds IP_4 is indicated to show that it sits between two residues that mediate contacts to the ITK kinase domain (V28 and F30). (b) Anti-His6 blots showing ITK kinase domain (4μM) binding to the ITK PHTH domain (2μM)

immobilized on IgG sepharose beads in the presence of soluble inositol 1,3,4,5-tetrakisphosphate ($IP(1,3,4,5)P_4$) and the regioisomeric IP_4, inositol 1,3,4,6-tetrakisphosphate ($IP(1,3,4,6)P_4$). The first lane shows total ITK kinase domain input followed by increasing concentration of IP_4 compounds (0-10 μM). (c) Histogram representation of the fraction of ITK kinase domain bound to the ITK PHTH domain at 0, 0.5, 1, 2, 5 and 10 μM IP_4 (data for inositol 1,3,4,5-tetrakisphosphate is on the left and inositol 1,3,4,6-tetrakisphosphate is on the right). Bound kinase is normalized to His6-GB1 PHTH level in each lane and then compared to the amount of bound kinase in the absence of IP_4 (0 μM). (d,e) The same experiment described for panels (b) and (c) is carried out for a panel of inositol phosphates. Lane 1 (apo) contains no added inositol phosphate and the specific compound used in lanes 2-12 is indicated above the blot in (d). The concentration of all inositol phosphates is 5 μM. The IP_4 compound that is the soluble head group of the PIP_3 target of ITK in T cells (inositol 1,3,4,5-tetrakisphosphate) is labeled in red.

Figure 6. PIP_3 activates ITK catalytic activity**.** (a) In vitro ITK kinase assay (500 nM ITK) in the presence of 1, 10, and 100 μM inositol 1,3,4,5-tetrakisphosphate (lanes 2-4) and the regioisomer control inositol 1,3,4,6-tetrakisphosphate (1, 10, and 100 μM, lanes 5-7). Lane 1 contains no inositol phosphate. ITK activation loop autophosphorylation (pY511) is detected at 30 minutes using using anti-BTK pY551 and total enzyme levels are detected using anti-ITK antibody. (b) Histogram representation of normalized pY511 levels from the ITK kinase assays shown in (a). Normalization was done as before in Figure 4(c and d), except that the value for ITK in the absence of any phosphoinositol

compound was set to1. Experiments were run in triplicate. (c) In vitro ITK kinase assay in solution (lane 1), in the presence of PIP_3 containing liposomes (lane 2) and control liposomes that lack PIP_3 (lane 3). PC indicates 1,2-dioleoyl-sn-glycero-3-phosphocholine (DOPC) and PS is 1,2-dioleol-sn-glycero-3-[phosphor-L-serine] (DOPS). ITK concentration, reaction time, and detection of activation loop phosphorylation and total enzyme levels are as described for panel (a). (d) Histogram representation of normalized pY511 levels from the ITK kinase assays shown in (c). Normalization was carried out as in panel b above. Experiments were run in triplicate.

Figure 7. The activation loop in the ITK kinase domain is sterically blocked by the PHTH domain in autoinhibted ITK**.** (a) Domain constructs of ITK and LCK. Full length ITK and the fragment lacking the PHTH domain (ITK SH3-SH2-Kinase) are FLAG-tagged at the C-termini and the LCK kinase domain carries a His6 tag at the N-terminus. Full length ITK and the ITK SH3-SH2-kinase fragment contain the K390R mutation rendering both inactive(24) . (b) In vitro LCK kinase assay in solution (lanes 3 and 4), in the presence of PIP_3 containing liposomes (lanes 5 and 6) and control liposomes that lack PIP_3 (lanes 7 and 8). ITK SH3-SH2-Kinase (K390R) (1 μM, lanes 3,5,7) and full length ITK (K390R) (1 μM, lanes 4,6,8) serve as substrates for LCK (200 nM). Lanes 1 and 2 are no enzyme (LCK) controls. Phosphorylation of ITK Y511 is detected using anti-BTK pY551 and total substrate and enzyme levels are detected using anti-FLAG and anti-His6 antibodies, respectively. (c) Histogram representation of normalized pY511 levels from the LCK kinase assays shown in (b). Normalization was done as in Figure 4 (c and d) with the value for ITK in the absence of liposomes set to 1. Data for the ITK SH3-SH2-Kinase

(K390R) substrate is on the left and the full length ITK (K390R) substrate is on the right. Experiments were run in triplicate.

Figure 8. The ITK PHTH domain contacts its cognate kinase domain in a manner that differs from the current model of autoinhibted BTK**.** (a) The structure of tethered BTK PHTH-Kinase domain (PDB ID: 4Y93) where the ITK PHTH domain has been superimposed with the BTK PHTH domain (BTK PHTH not shown for clarity). R133 in the BTK PHTH domain makes contact with the BTK kinase domain. R111 is the corresponding residue in the ITK PHTH domain but mutation of R111 does not affect the ITK PHTH/Kinase interaction. The ITK PHTH interface residues located in and around the β3-β4 loop (colored red) are not located at the interface with the kinase domain defined in the crystal structure for the tethered BTK domains but are close to the IP(1,3,4,5)P_4 binding site (circled). (b) left, Model of closed, autoinhibited ITK in a resting T cell (arrangement of the SH3 and SH2 domains is based on the BTK crystal structure of the SH3-SH2-Kinase fragment (4XI2)). Right, model of an open form of ITK (based on SAXS structure of full length BTK(32) in the presence of membrane anchored PIP_3 revealing Y511 for phosphorylation by LCK. (c) The ITK kinase domain presents a large negatively charged surface that spans the N-lobe and activation loop and may serve as a binding site for the positively charged region of ITK PHTH defined in this study. The highly basic stretch of residues on the β3-β4 loop are shown and labeled. (d) The BTK kinase domain shares the acidic patch across the N-lobe and activation loop. (e) Autoinhibitory ITK PHTH surface defined in this study. Residues shown in red are those side chains mutated in the current study that have an effect on the inhibitory interaction

with the ITK kinase domain, those in yellow, ball and stick are ITK residues listed in the COSMIC database. F30 is shown in red with ball and stick to indicate that it both affects the PHTH/Kinase interface and is mutated in the database of somatic mutations in cancer.

Figures

Figure 1

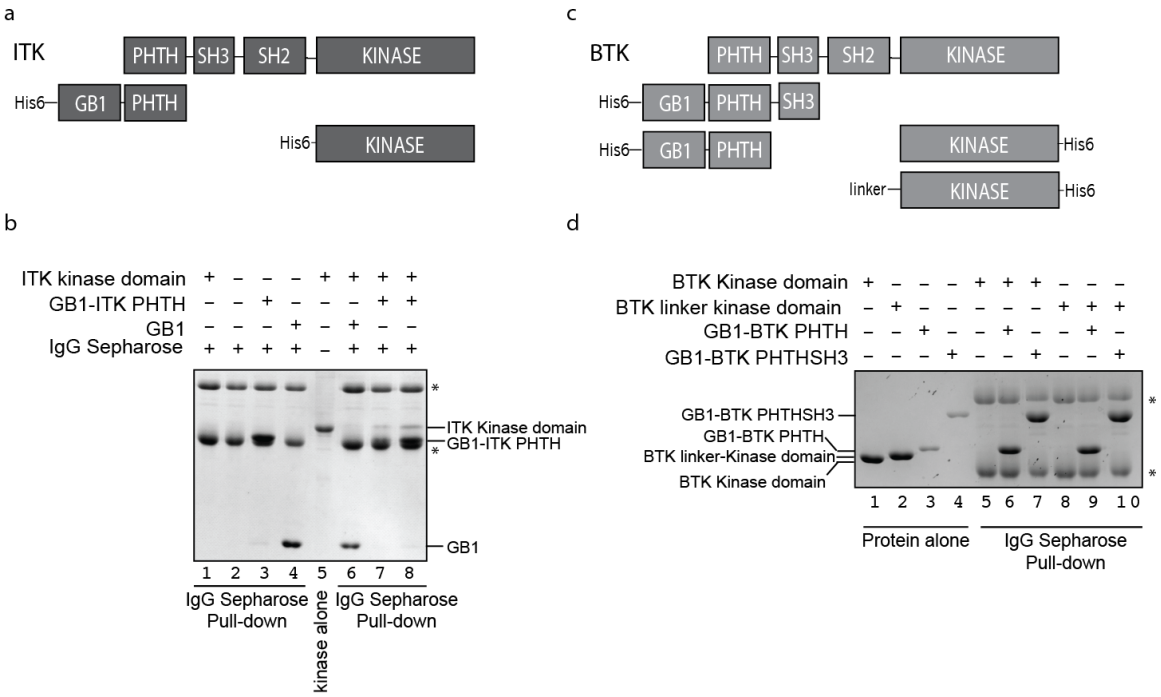

Figure 2

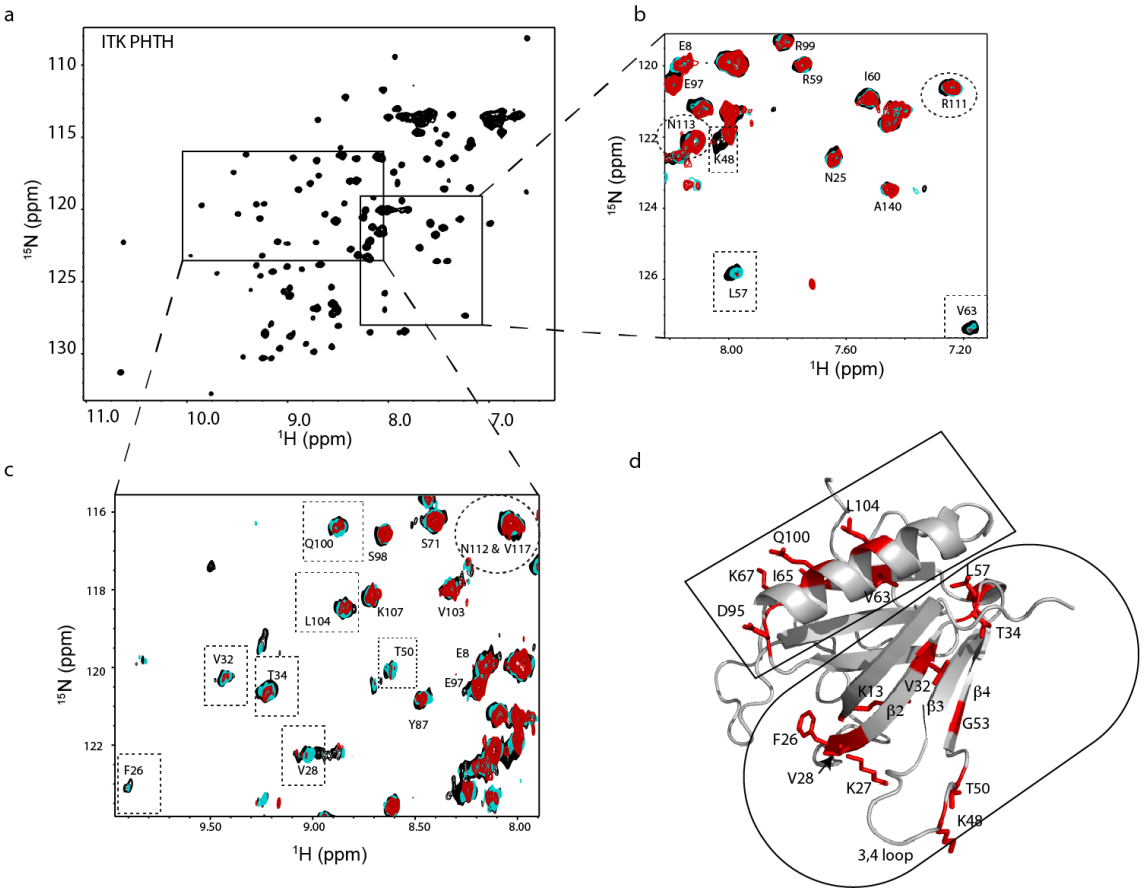
a
ITK PHTH
^{15}N (ppm)
^{1}H (ppm)
b
E8
R99
E97
R59
I60
R111
N113
K48
N25
A140
L57
V63
^{15}N (ppm)
^{1}H (ppm)
c
Q100
S98
S71
N112 & V117
L104
K107
V103
V32
T34
T50
E8
E97
Y87
F26
V28
^{15}N (ppm)
^{1}H (ppm)
d
L104
Q100
K67
I65
L57
V63
D95
T34
K13
V32
β4
β2
β3
G53
F26
V28
K27
T50
K48
3,4 loop

Figure 3

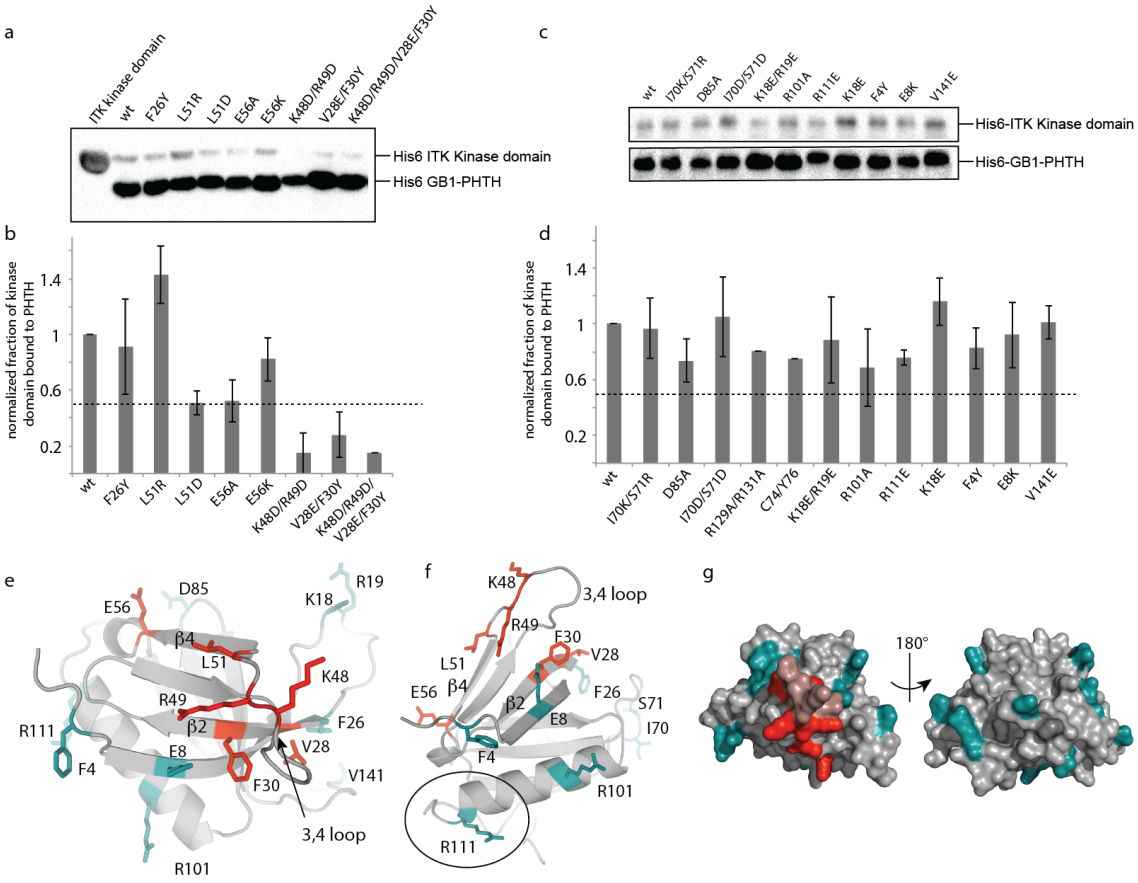
a
ITK kinase domain
wt
F26Y
L51R
L51D
E56A
E56K
K48D/R49D
V28E/F30Y
K48D/R49D/V28E/F30Y
His6 ITK Kinase domain
His6 GB1-PHTH
b
normalized fraction of kinase domain bound to PHTH
1.4
1
0.6
0.2
wt
F26Y
L51R
L51D
E56A
E56K
K48D/R49D
V28E/F30Y
K48D/R49D/V28E/F30Y
c
wt
I70K/S71R
D85A
I70D/S71D
K18E/R19E
R101A
R111E
K18E
F4Y
E8K
V141E
His6-ITK Kinase domain
His6-GB1-PHTH
d
normalized fraction of kinase domain bound to PHTH
1.4
1
0.6
0.2
wt
I70K/S71R
D85A
I70D/S71D
R129A/R131A
C74/Y76
K18E/R19E
R101A
R111E
K18E
F4Y
E8K
V141E
e
E56
D85
R19
K18
β4
L51
K48
R49
β2
F26
R111
E8
V28
F4
F30
V141
3,4 loop
R101
f
K48
3,4 loop
R49
F30
V28
L51
E56
β4
F26
S71
β2
E8
I70
F4
R101
R111
g
180°

Figure 4

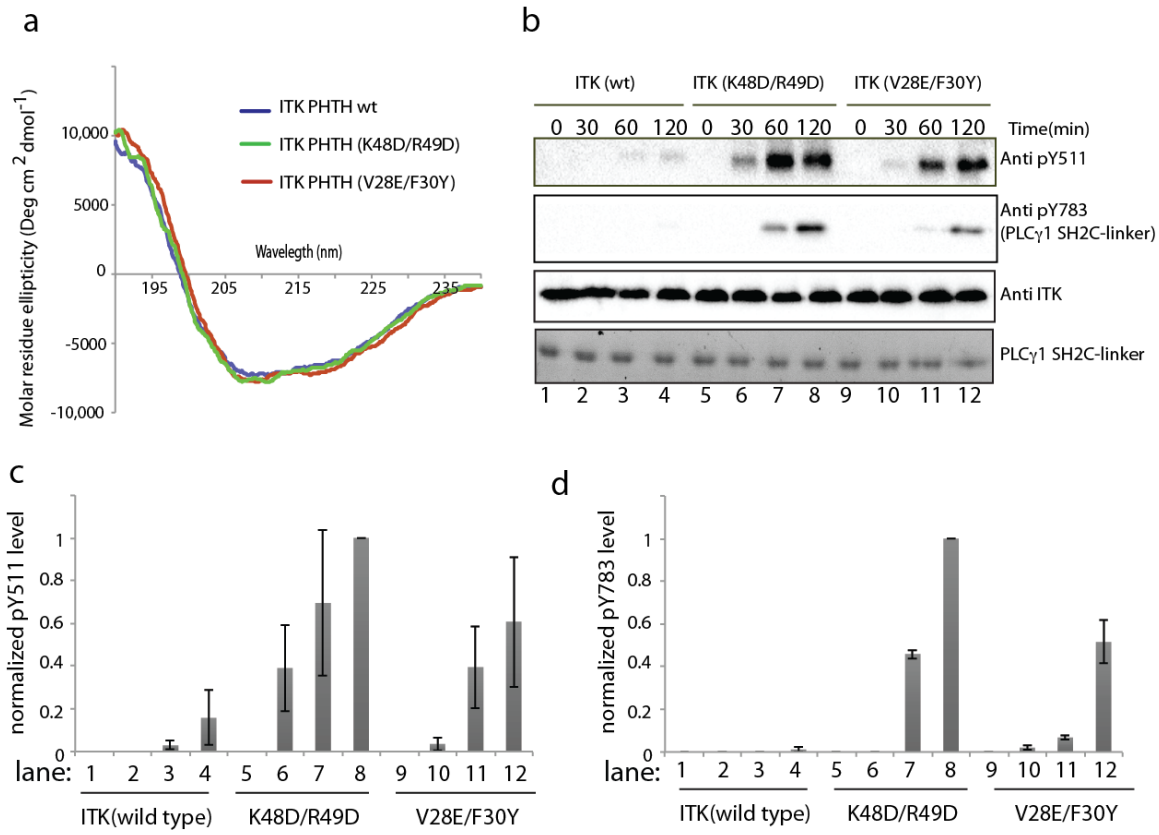
a
b
ITK PHTH wt
ITK PHTH (K48D/R49D)
ITK PHTH (V28E/F30Y)
Molar residue ellipticity (Deg cm 2 dmol-1)
Wavelegth (nm)
ITK (wt)
ITK (K48D/R49D)
ITK (V28E/F30Y)
Time(min)
Anti pY511
Anti pY783
(PLCγ1 SH2C-linker)
Anti ITK
PLCγ1 SH2C-linker
c
d
normalized pY511 level
normalized pY783 level
lane:
ITK(wild type)
K48D/R49D
V28E/F30Y

Figure 5

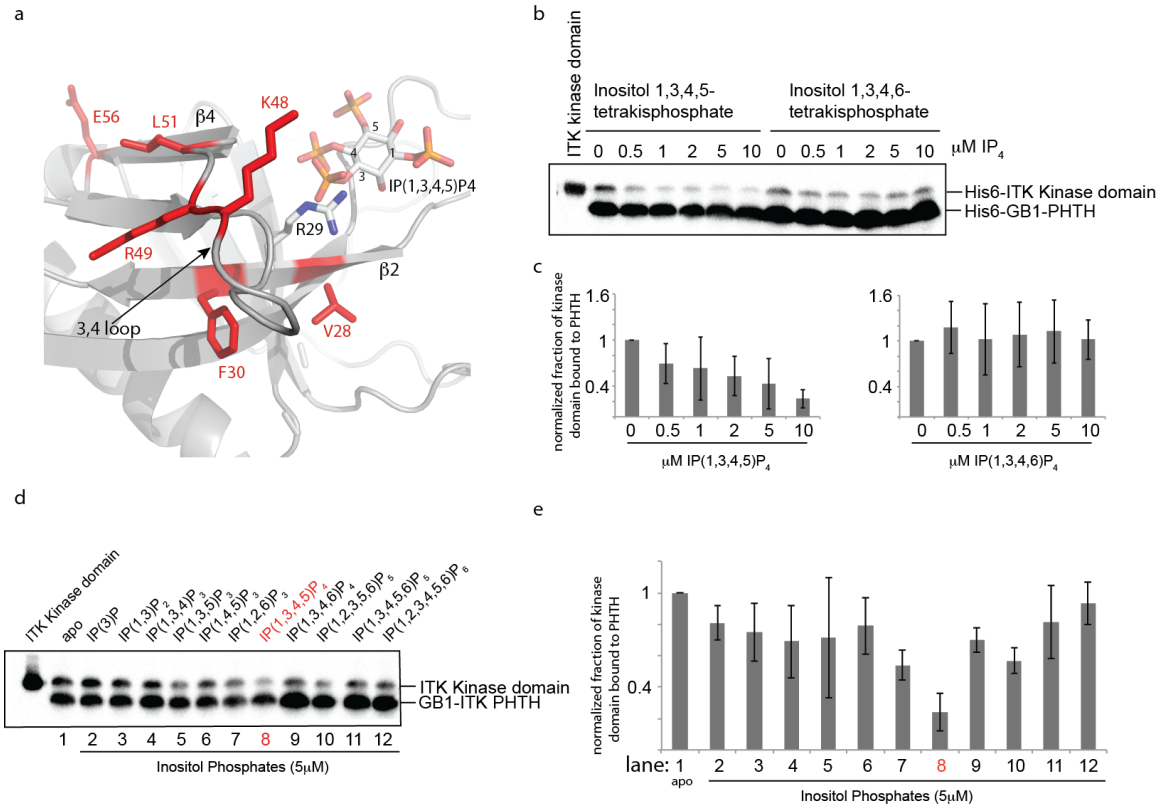
a
E56
L51
β4
K48
IP(1,3,4,5)P4
R29
R49
β2
3,4 loop
V28
F30
b
ITK kinase domain
Inositol 1,3,4,5-tetrakisphosphate
Inositol 1,3,4,6-tetrakisphosphate
0 0.5 1 2 5 10 0 0.5 1 2 5 10 μM IP4
His6-ITK Kinase domain
His6-GB1-PHTH
c
normalized fraction of kinase domain bound to PHTH
1.6
1
0.4
0 0.5 1 2 5 10
μM IP(1,3,4,5)P4
μM IP(1,3,4,6)P4
d
ITK Kinase domain
apo
IP(3)P
IP(1,3)P2
IP(1,3,4)P3
IP(1,3,5)P3
IP(1,4,5)P3
IP(1,2,6)P3
IP(1,3,4,5)P4
IP(1,3,4,6)P4
IP(1,2,3,5,6)P5
IP(1,3,4,5,6)P5
IP(1,2,3,4,5,6)P6
ITK Kinase domain
GB1-ITK PHTH
1 2 3 4 5 6 7 8 9 10 11 12
Inositol Phosphates (5μM)
e
normalized fraction of kinase domain bound to PHTH
1
0.4
lane: 1 2 3 4 5 6 7 8 9 10 11 12
apo
Inositol Phosphates (5μM)

Figure 6

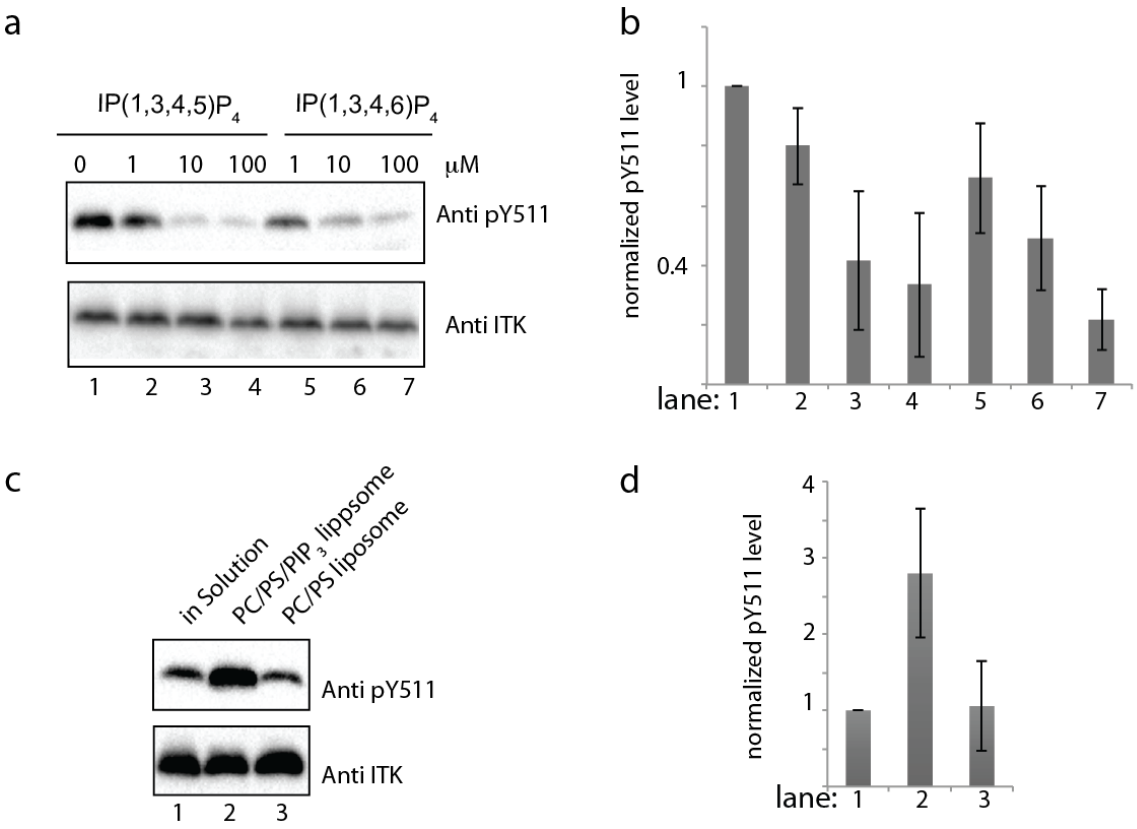
a
IP(1,3,4,5)P4
IP(1,3,4,6)P4
0 1 10 100 1 10 100 μM
Anti pY511
Anti ITK
1 2 3 4 5 6 7
b
normalized pY511 level
1
0.4
lane: 1 2 3 4 5 6 7
c
in Solution
PC/PS/PIP3 lippsome
PC/PS liposome
Anti pY511
Anti ITK
1 2 3
d
normalized pY511 level
4
3
2
1
lane: 1 2 3

Figure 7

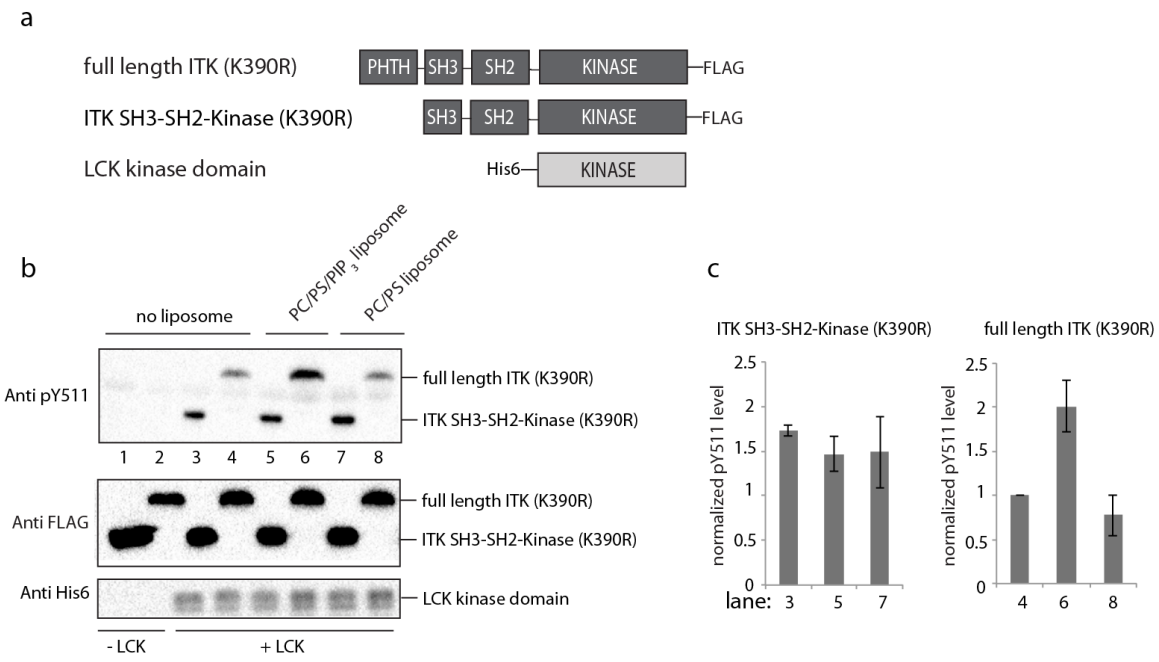
a
full length ITK (K390R)
PHTH
SH3
SH2
KINASE
FLAG
ITK SH3-SH2-Kinase (K390R)
SH3
SH2
KINASE
FLAG
LCK kinase domain
His6
KINASE
b
no liposome
PC/PS/PIP3 liposome
PC/PS liposome
Anti pY511
full length ITK (K390R)
ITK SH3-SH2-Kinase (K390R)
1 2 3 4 5 6 7 8
Anti FLAG
full length ITK (K390R)
ITK SH3-SH2-Kinase (K390R)
Anti His6
LCK kinase domain
- LCK
+ LCK
c
ITK SH3-SH2-Kinase (K390R)
full length ITK (K390R)
normalized pY511 level
2.5
2
1.5
1
0.5
0
lane: 3 5 7
4 6 8

Figure 8

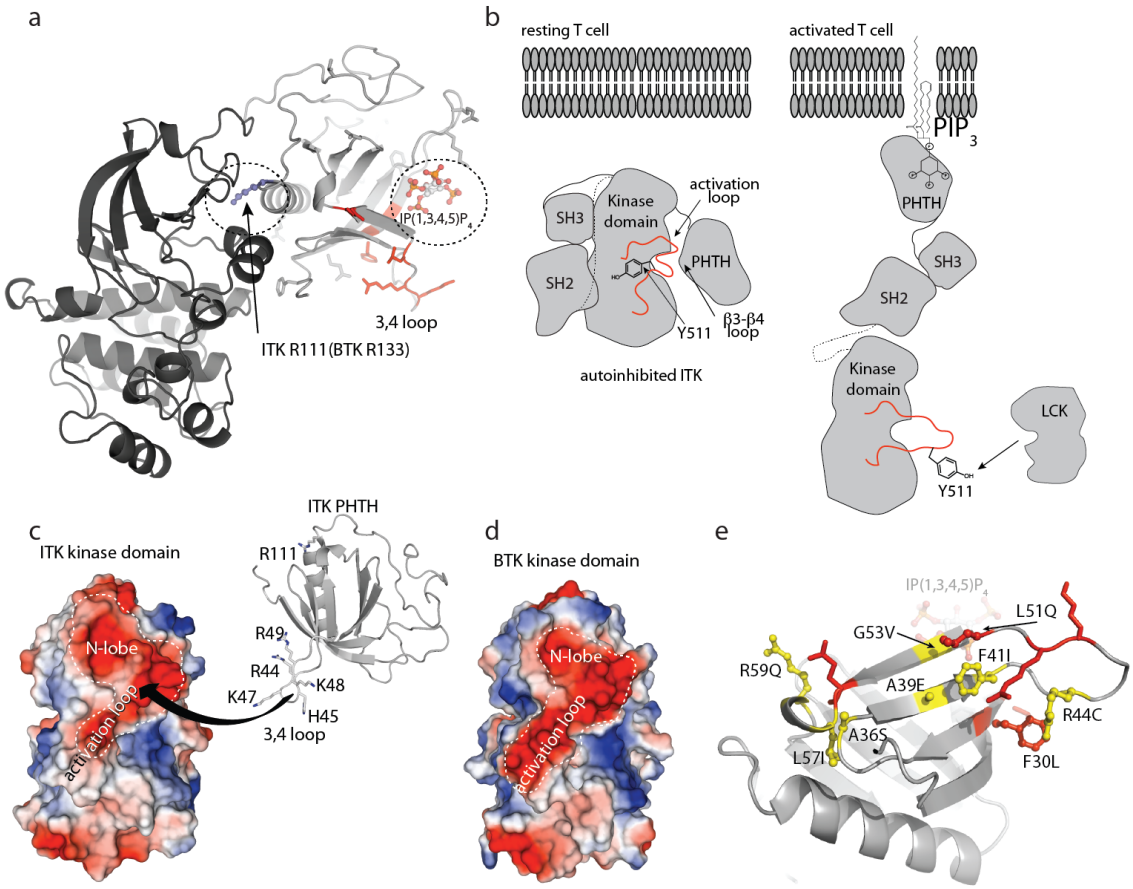
a
IP(1,3,4,5)P4
3,4 loop
ITK R111(BTK R133)
b
resting T cell
activated T cell
PIP3
PHTH
SH3
SH2
Kinase domain
activation loop
PHTH
Y511
β3-β4 loop
autoinhibited ITK
SH3
SH2
Kinase domain
LCK
Y511
c
ITK kinase domain
ITK PHTH
R111
R49
R44
K48
K47
H45
3,4 loop
N-lobe
activation loop
d
BTK kinase domain
N-lobe
activation loop
e
IP(1,3,4,5)P4
L51Q
G53V
F41I
R59Q
A39E
R44C
A36S
L57I
F30L

CHAPTER 4

STUDY OF THE INTERACTION OF ITK PHTH WITH ITK KINASE DOMAIN USING BIMOLECULAR FLUORESCENCE COMPLEMENTATION ASSAY

Abstract

Interleukin-2 inducible T cell kinase (ITK) functions in immune response mediated by T cells, and is a attractive drug target for autoimmune diseases and allergies. Regulatory intramolecular interaction surface of ITK could serve as small molecules target. Our studies have found that the ITK PHTH/Kinase domain intramolecular interaction keeps ITK in the autoinhibited state. Two sets of mutations in the ITK PHTH domain, K48D/R49D and V28E/F30Y, disrupt this autoinhibitory interaction hence increasing the catalytic activity of ITK. Hence, this interaction interface is a plausible allosteric target for small molecules that regulate kinase activity. With the ultimate goal of developing a high-throughput assay to target ITK PHTH/Kinase interaction site, we developed the cell based bimolecular fluorescence complementation (BiFC) assay. In the BiFC assay, the ITK Kinase domain was fused to the non-fluorescent N-terminal fragment of YFP variant Venus while the ITK PHTH domain-containing construct was fused to the non-fluorescent C-terminal fragment of Venus. The ITK PHTH/Kinase interaction allows for the two N- and C-terminal fragments of Venus to structurally complement forming functional fluorophore and BiFC to occur hence, giving rise to fluorescence. The BiFC signal was detected on wildtype ITK PHTH/kinase pair but in the

case of the PHTH domain mutant (K48D/R49D), which disrupts the ITK PHTH/kinase interaction, BiFC signal was reduced. This study lays the groundwork for a highthrough put assay for small molecule screening that modulates the ITK PHTH/Kinase interaction

Introduction

Interleukin-2 inducible T cell kinase (ITK) is non-receptor tyrosine kinase primarily expressed in T cells, which plays a crucial role in propagating signals downstream of the T cell receptor (TCR). Upon TCR engagement, ITK is responsible for phosphorylation of Phospholipase C γ1 (PLCγ1), leading to PLCγ1 activation. Activated PLCγ1 then catalyzes the hydrolysis of phosphatidylinositol-(4,5)-bisphosphate (PIP_2) in the membrane to inositol (1,4,5)-triphosphate (IP_3) and diacylglyecrol (DAG). IP_3 and DAG mediate signaling that eventually lead to expression of various cytokines that are responsible for appropriate immune responses. ITK is a key modulator of T cell responses, and is therefore an attractive target for small molecule intervention that tunes ITK activity.

ITK has been linked to various diseases. Loss of function mutations in ITK leads to fatal Epstein-Barr virus induced lymphoproliferative diseases (EBV-LPD) (1). Also, ITK has been linked to a hyperactive immune response in asthma and autoimmune diseases. ITK deficient mice have been shown to be resistant to ovalbumin induced asthma (2). In addition, autoimmune diseases like multiple sclerosis and inflammatory bowel diseases are linked to ITK (3). Hence, this has generated significant interest in ITK as therapeutic target against EBV-LPD, asthma and various autoimmune diseases. Small

molecules, that break autoinhibition of ITK could treat EBV-LPD and small molecules that stabilize the ITK PH/Kinase interaction could treat hyperactive immune response like asthma and autoimmune diseases.

There has been significant effort in targeting the ITK active site for competitive ATP binders (4, 5). However, all kinases share similar structural features in their active site hence, developing the small molecule binders that do not cross-react with other kinases can be very challenging (6). One to overcome this challenge is to look for and target allosteric regulatory sites specific to ITK. Along with the active site, ITK can also be targeted at various binding interfaces between its domains, since the non-catalytic PHTH, SH3 and SH2 domains regulate ITK kinase activity by directly interacting with the kinase domain. In chapter 3, we have characterized the specific autoinhibitory interaction between the ITK PHTH domain and ITK kinase domain and we have shown that K48D/R49D and V28E/F30Y mutations in the PHTH domain disrupt this interaction making ITK more catalytically active. Hence the ITK PHTH/kinase domain interaction surface could be very plausible target for small molecule intervention. Small molecules that could influence the kinase activity of ITK by modulating ITK PH/kinase domain interaction will be useful in treating various disease conditions.

A cell based bimolecular fluorescence complementation (BiFC) assay has been used previously in a high-throughput format to screen small molecules that target protein-protein interactions (7). In the BiFC assay, two interacting proteins are fused to complementary non-fluorescent N-terminal and C-terminal fragments of the Green

fluorescent protein (GFP) or yellow fluorescent protein (YFP)(8, 9). When two interacting proteins are co expressed in cells, their interaction brings the complementary non-fluorescent fragments of GFP or YFP together allowing for structural complementation to occur and the formation of the functional fluorophore (9). Hence, protein interactions inside cells can be visualized directly using a fluorescence microscope. Here, we set out to test whether the BiFC assay is suited to detect the interaction between the ITK PHTH domain and kinase domain and whether this technique can be adapted to high throughput screening of the small molecules targeting the ITK PH/kinase interaction. Our preliminary result suggests that ITK kinase domain and ITK PHTH domain interact in cells giving rise to BiFC signal. Furthermore, the BiFC signal is diminished when the ITK PHTH mutant (K48D/R49D), which disrupts kinase domain binding, is co expressed with ITK kinase domain. These data indicate that the BiFC complex forms only when the ITK kinase domain interacts with the ITK PHTH domain.

Results and Discussion

In chapter 3, we provided evidence for a specific interaction between the ITK kinase domain and ITK PH domain in vitro using NMR titration and pull down assays. To probe whether this interaction occurs in cells, we developed a BiFC assay specific to the ITK domains of interest. For the BiFC experiments, separate expression vectors containing the ITK PHTH-SH3 construct fused with the C-terminus (VC 154-238) of Venus (YFP variant) and the ITK Kinase domain fused with the N-terminus (VN 1-154) of Venus were created. The constructs used in our BiFC assay are shown in Figure 1.

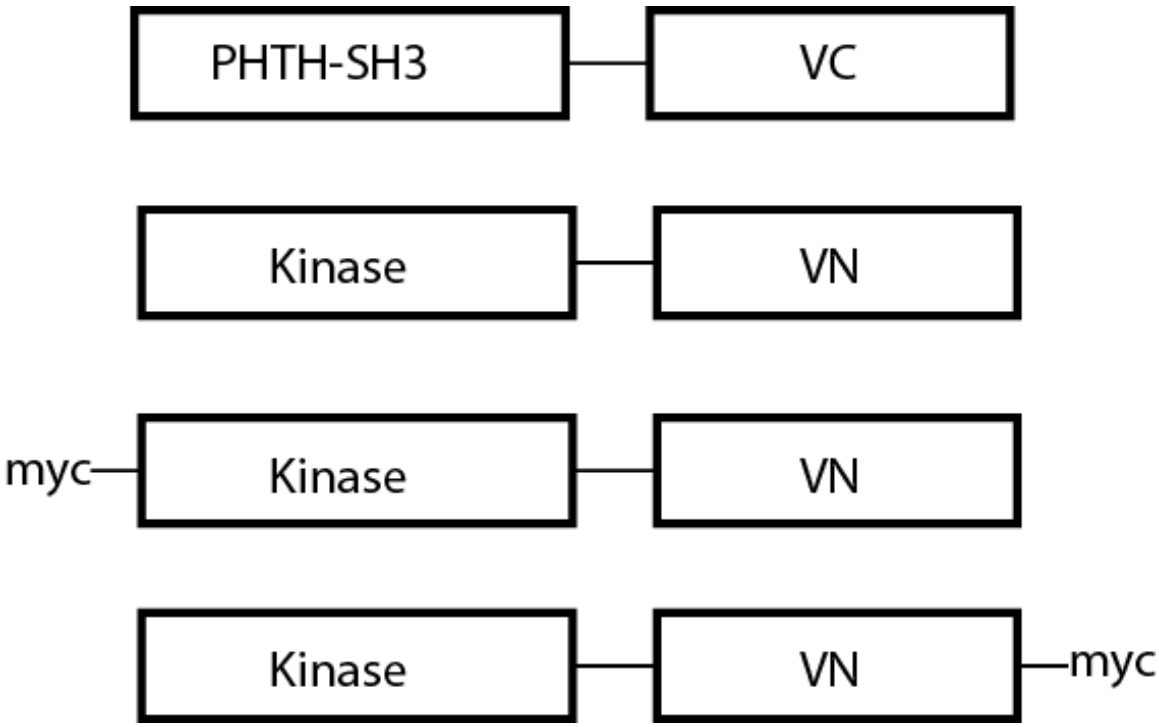

Figure 1. Fusion constructs of the ITK PHTH domain containing construct with Venus C terminal fragment (VC) and three fusion constructs of the ITK kinase domain with Venus N terminal fragment (VN). The three kinase domain constructs are untagged, N terminal myc tagged and C terminal myc tagged.

When co expressed in HEK 293T cells, the ITK kinase domain/PHTH domain interaction should bring two non-florescent Venus fragments in close proximity, resulting in structural complementation of the two non-fluorescent fragments of Venus leading to the fluorescent signal as shown in Figure 2.

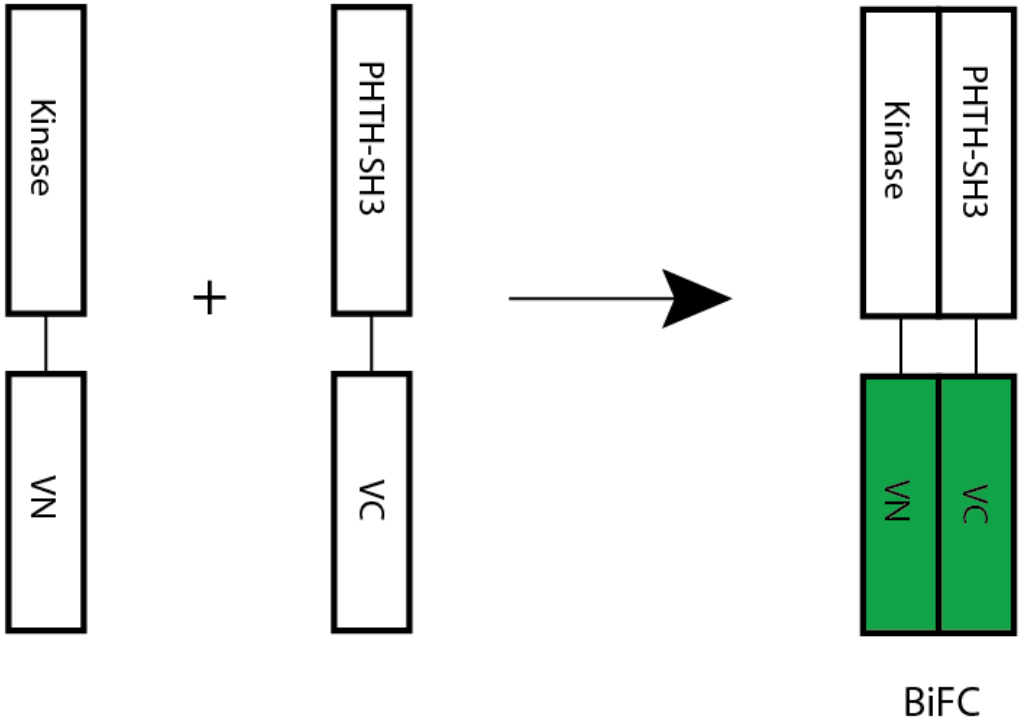

Figure 2. Principle of BiFC. Non fluorescent fragments of YFP variant Venus denoted by VN and VC are fused to the ITK kinase domain and ITK PHTH-SH3 respectively. Co-expression and interaction between two proteins also brings VN and VC together giving rise to the green fluorescence signal.

We monitored and compared three different ITK kinase domain constructs shown in Figure 1, for their ability to give BiFC signal when co-transfected with ITK PHTH containing construct (Figure 3). All three construct tested gave rise to comparable BiFC signal for 72 hours post transfection. For all three fusion construct tested, the BiFC signal increased from 24 hours post transfection to 48 hours post transfection. However, no significant increase in BiFC was observed, from 48 hours to 72 hours post transfection as shown in Figure 3.

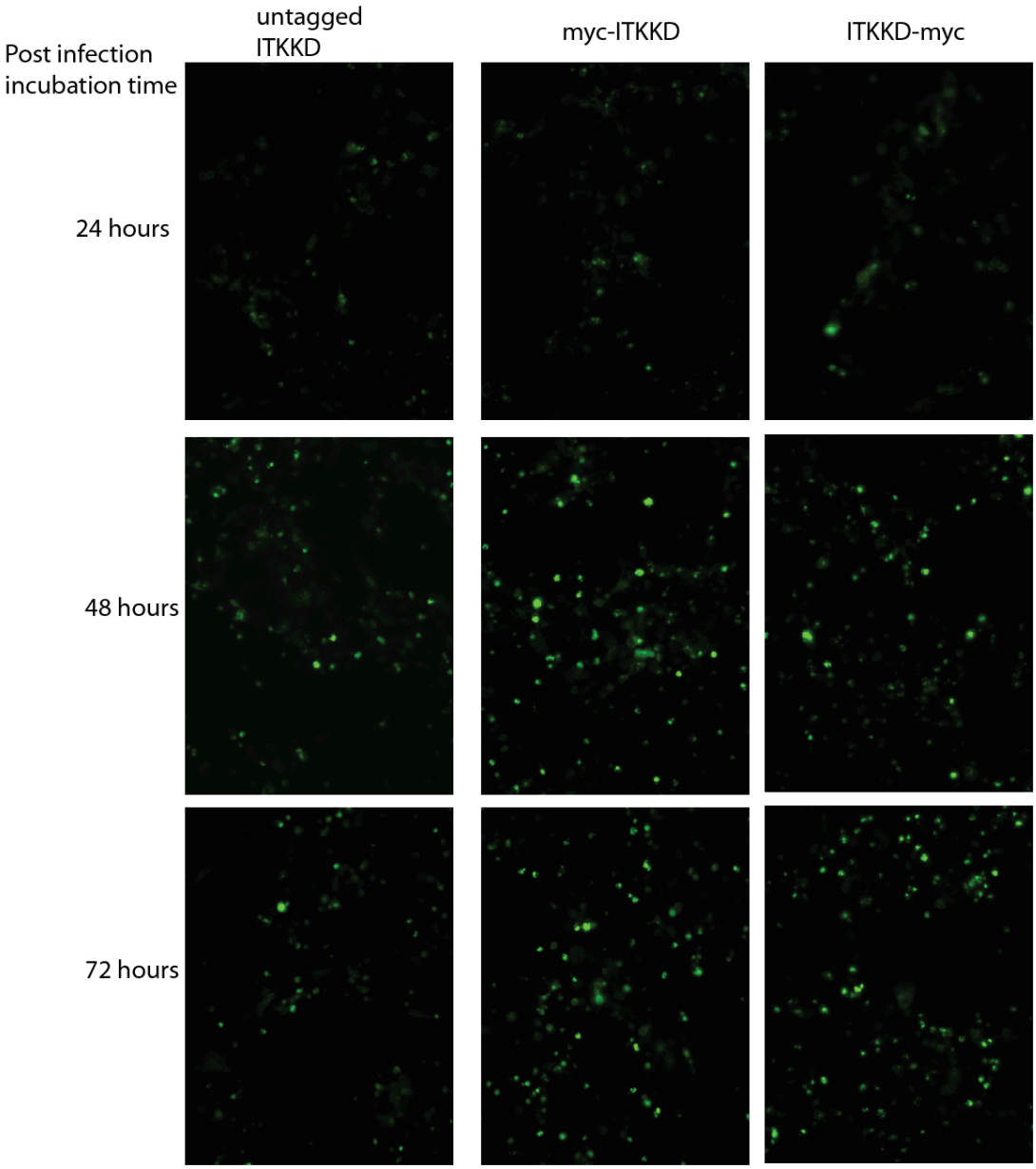

Figure 3. BiFC images captured using fluorescence microscope. BiFC constructs containing untagged, N terminal myc tagged and C terminal myc tagged ITK kinase domain fused to VN and ITK PHTH-SH3 fused to VC were co-transfected and monitored for BiFC signal post 24, 48 and 72 hours after transfection.

To confirm that BiFC signal is dependent on the interaction between ITK kinase domain and ITK PH domain, the assay was repeated with the ITK PH mutant where arginine 48 and lysine 49 were mutated to aspartic acid. This construct is denoted as K48D/R49D. This ITK PH domain mutant is shown to be incapable of binding ITK kinase domain in our previous in vitro pull down studies. Co-expression of the ITK PH mutant with ITK kinase domain shows reduction in the BiFC signal intensity compared to wildtype as shown in Figure 4, which is consistent with our previous in vitro results.

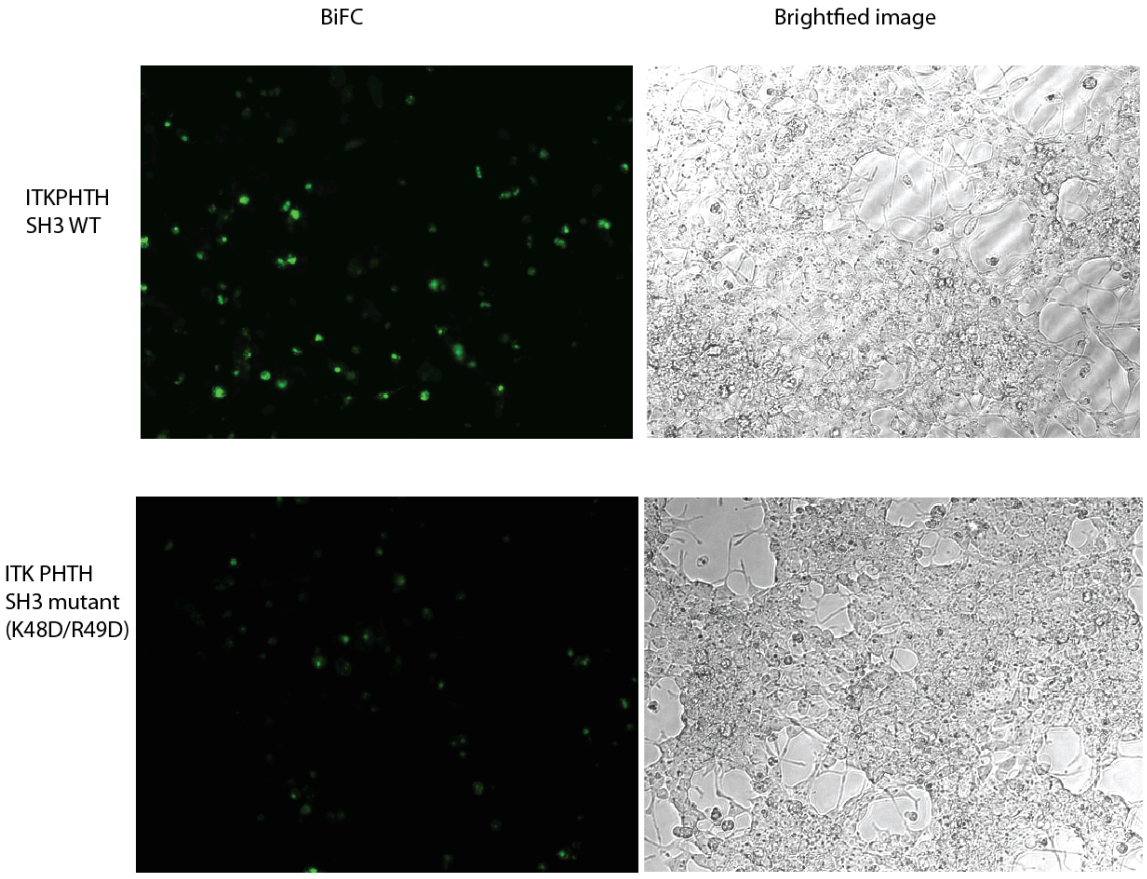

Figure 4. BiFC images comparing fluorescence signal for wildtype and interaction deficient mutant (K48D/R49D) mutant of ITK PH domain (left). Brightfield images show similar cell density in both BiFC image areas. (right).

However, for this experiment total ITK PHTH and its mutant needs to be determined since the reduction in BiFC in mutant protein could also be due to lower expression level than wildtype protein. This experiment will be repeated and total protein expression level of all proteins will also probed along with BiFC. Total protein expression level will be probed by immunofluorescence microscopy. ITK kinase domain will be probed by anti myc antibodies while PHTH domain will be probed with anti ITK antibodies. After further confirmation that the BiFC signal is dependent upon ITKPHTH/kinase domain interaction, this assay will be adapted in high throughput format. In addition, by simultaneously monitoring the BiFC signal and total protein expression level, in the presence of small molecules, we will be able to screen small molecules that modulate ITK PHTH/kinase domain interaction. Wildtype PHTH constructs was used in this study, However, previous studies in our lab suggest that ITK PHTH domain is very unstable in vitro and two mutations C96E/T110I increases the stability of the protein (10). The BiFC assay with this solubilizing mutant will also be tested in future.

Materials and Methods

BiFC expression vectors

Mammalian expression vector pcDNA3.1(-) with Nef VN and ITK PHTHSH3-VC was kindly provided by Dr. Tom Smithgall laboratory at University of Pittsburgh. ITK kinase domain was cloned into the pcDNA3.1(-) Nef VN vector using EcorI and HindIII restriction sites.

Cell culture

Human HEK 293T cells purchased from ATCC were thawed at 37^0 C water bath and transferred to centrifuge tube containing 9 ml of complete media. Complete media consist of Dulbecco's Modified Eagle's Medium (DMEM) supplemented with 10% fetal bovine serum (Gibco). The cells were spun at 125 x g for 10 minutes and the cell pellet was resuspended in 5ml complete DMEM media pre-equilibrated in incubator with 5% CO_2 for 15 minutes to allow the media to reach its normal pH (7-7.6). The culture was transferred to 25 cm^2 culture flask (Corning) and incubated at 370C incubator with 5% CO_2 in air atmosphere. After 2 days, the cells were subcultured to 75 cm^2 flask (corning). The culture medium was removed and the cells were washed briefly with PBS buffer to remove traces of trypsin inhibitors from the medium. After that, 0.6 ml of Trypsin-EDTA solution was added to the cells to disperse the cell layer. After 5 minutes, 5 ml of complete growth medium was added to the flask and cells were aspirated gently by pipetting. The cells were transferred to the 75cm^2 flask with 13 ml complete growth medium. After that, the cells were subcultured in 1:3 ratio every 3 days.

BiFC assay and fluorescence microscopy

In each 35mm dish, $8X10^5$ cells were plated and were incubated for 24 hours. Next day, transfection mixture consisting of X-tremeGENE 9 DNA Transfection reagent (Roche) and plasmid DNA was prepared for transfection. Firstly, X-tremeGENE 9 DNA was diluted with serum free DMEM medium to a concentration of 3ml reagent/100 ml medium for 3:1. 1μg of plasmid DNA was added to 100ml of diluted X-tremeGENE DNA reagent and incubated in room temperature for 15 minutes. The 35 mm dishes were

removed from the incubator and transfection mixture was added to the cells in drop wise manner. BiFC was monitored for 3 days post transfection, using fluorescence microscope (Zeiss.) from Iowa State hybridoma facilities.

References

1. Linka RM*, et al.* (2012) Loss-of-function mutations within the IL-2 inducible kinase ITK in patients with EBV-associated lymphoproliferative diseases. *Leukemia* 26(5):963-971.
2. Mueller C & August A (2003) Attenuation of immunological symptoms of allergic asthma in mice lacking the tyrosine kinase ITK. *J Immunol* 170(10):5056-5063.
3. Waite JC & Skokos D (2012) Th17 response and inflammatory autoimmune diseases. *Int J Inflam* 2012:819467.
4. Sahu N & August A (2009) ITK inhibitors in inflammation and immune-mediated disorders. *Curr Top Med Chem* 9(8):690-703.
5. Vargas L, Hamasy A, Nore BF, & Smith CI (2013) Inhibitors of BTK and ITK: state of the new drugs for cancer, autoimmunity and inflammatory diseases. *Scand J Immunol* 78(2):130-139.
6. Fabbro D, Cowan-Jacob SW, & Moebitz H (2015) Ten things you should know about protein kinases: IUPHAR Review 14. *Br J Pharmacol* 172(11):2675-2700.
7. Poe JA, Vollmer L, Vogt A, & Smithgall TE (2014) Development and validation of a high-content bimolecular fluorescence complementation assay for small-

molecule inhibitors of HIV-1 Nef dimerization. *J Biomol Screen* 19(4):556-565.

8. Miller KE, Kim Y, Huh WK, & Park HO (2015) Bimolecular Fluorescence Complementation (BiFC) Analysis: Advances and Recent Applications for Genome-Wide Interaction Studies. *J Mol Biol* 427(11):2039-2055.
9. Kerppola TK (2009) Visualization of molecular interactions using bimolecular fluorescence complementation analysis: characteristics of protein fragment complementation. *Chem Soc Rev* 38(10):2876-2886.
10. Boyken SE, Fulton DB, & Andreotti AH (2012) Rescue of the aggregation prone Itk Pleckstrin Homology domain by two mutations derived from the related kinases, Btk and Tec. *Protein Sci* 21(9):1288-1297.

CHAPTER 5

GENERAL CONCLUSIONS

Summary

Interleukin-2 inducible tyrosine kinase (ITK) is a member of Tec family kinase that is expressed in T cells and is a key mediator of T cell signaling pathway. In this pathway, ITK is activated by phosphorylation by SRC family kinase LCK (1). Activated ITK then mediates activation of the Phospholipase Cγ1 (PLCγ1) by phosphorylating at tyrosine 783. This phosphorylation activates the PLCγ1 and its lipase activity. PLCγ1 hydrolyses phosphatidylinositol (4,5)-bisphosphate (PIP_2) to produce second messengers inositol-(3,4,5)-triphosphate (IP_3) and diacylglycerol (DAG). ITK has been linked with various disease states ranging from immunodeficiency, autoimmune diseases and allergies (2-4). Hence, ITK has been putative drug target to treat these human maladies. To target ITK for small molecules, understanding of its regulation mechanism is important. Hence, the main goal of this thesis is to understand the underlying regulatory mechanism of ITK that influences the phosphorylation of its PLCγ1 substrate.

Phosphorylation target for the ITK in PLCγ1 is tyrosine 783 which is located within 33 amino acid long linker between PLCγ1 C terminal Src homology 2 (SH2C) domain and Src homology 3 (SH3) domain. Crystal structure of the PLCγ1 SH2N-SH2C-linker shows, the intramolecular interaction between the PLCγ1 SH2C and linker (5). This PLCγ1 conformation makes Y783 inaccessible to ITK for phosphorylation and

keeps PLCγ1 in autoinhibited state. This autoinhibitory interaction needs to be disrupted to make Y783 in the linker accessible to ITK.

In chapter 2, I investigated the mechanism that disrupts this autoinhibitory conformation of the PLCγ1. Our result elucidates the role of scaffold protein SLP-76 to disrupt the PLCγ1 autoinhibition. SLP-76 phosphotyrosine 173 (pY173) interacts with SH2C domain of PLCγ1. NMR titration and fluorescence titration studies suggest that peptide containing SLP-76 pY173 interacts with PLCγ1 SH2C with higher affinity than SH2C-linker construct suggesting SLP-76 pY173 and the linker compete with SH2C binding. SLP-76 pY173 interaction with SH2C ultimately makes PLCγ1 a better substrate for the ITK. ITK mediated phosphorylation of PLCγ1 783 was increased with the addition of SLP-76 pY173 peptide in kinase assay mixture. We describe this role of SLP-76 as substrate priming as it primes PLCγ1 the substrate ITK for phosphorylation. Together, our study provides the understanding on disruption of autoinhibitory conformation of the PLCγ1 and recognizes the new role of the scaffold SLP-76, along with co-localizing enzyme and substrate.

In chapter 3, I study the autoregulatory intramolecular interaction within ITK. ITK consist of four domains PHTH, SH3, SH2 and Kinase domain. PHTH, SH3 and SH2 domains are regulatory domains of ITK as they regulate the catalytic activity of the ITK. However, due to the lack of the full length structure of the ITK, precise mechanism on how these non-catalytic domain regulate kinase activity is not fully understood. This dissertation studies the role of PHTH domain on regulating kinase activity. Previous

studies in our lab has have shown that k_{cat} for ITK lacking PHTH domain, is fivefold higher than the full length ITK (6).

In this thesis, I have expanded our understanding on this observation and characterized the regulatory role of PHTH domain in detail. Our studies shows that ITK PHTH domain and ITK kinase domain interact intramolecularly and this interaction keeps ITK in an auto inhibited state. First of all, pull down assay shows ITK PHTH domain interacts with ITK kinase domain in trans. To map the ITK interacting surface on the ITK PH domain, NMR titration experiment was carried out where ITK kinase domain was titrated into ^{15}N labeled ITK PHTH domain. Using the ^{1}H-^{15}N NMR assignment of the ITK PHTH domain, I was able to map the ITK interaction surface on ITK PHTH domain. NMR titration experiment detects changes on the resonance of the PHTH residues when ITK PHTH/kinase complex is formed. Refining of the binding interface was done by mutagenesis and pull down studies. Using this method, I was able to identify two sets of residues (K48/R49 and V28/F30) in ITK PHTH domain, when mutated resulted in abrogation of ITK kinase domain binding. These, sets of residues, when mutated in the context of the full length ITK led to increase in the activity of the ITK.

The ITK kinase domain-binding interface in PHTH domain is adjacent to phosphatidylinositol (3,4,5)-triphosphate (PI (3,4,5) P_3) binding pocket of the PHTH domain. Inositiol (1,3,4,5)-trisphosphate (IP (1,3,4,5) P4), the soluble head group of the of PI (3,4,5) P_3, competes with the ITK kinase domain for binding ITK PHTH domain. Also, liposome containing PI (3,4,5) P_3 increases the catalytic activity of the ITK. Hence,

PI (3,4,5) P_3 binding of PHTH domain releases its interaction with kinase domain leading to the activation of the enzyme. ITK PHTH domain interaction with PI (3,4,5) P_3 also exposes the activation loop Y511 of full length ITK making this residue more accessible to LCK for phosphorylation. This study, have significantly expanded our understanding PHTH domain mediated regulation of the ITK activity. An ITK PHTH/Kinase regulatory interaction site has been identified and can be targeted for small molecule to modulate kinase activity.

In an effort to develop the cell-based assay to monitor ITK PHTH/Kinase interaction, and ultimately to use this assay to screen small molecules, bimolecular complementary fluorescence (BiFC) assay was developed (Chapter 4). Two complementary non-fluorescent fragment of Venus (yellow fluorescent protein variant) when fused to ITK PHTH domain and ITK kinase domain and co expressed in cells, gave rise to fluorescence signal. ITK PHTH/Kinase interaction brings two non-fluorescent fragments of Venus closer and allowing for the structural complementation to occur, and forming functional fluorophore, giving rise to fluorescence. This assay will be further developed and adapted to high throughput format so that it can be used to screen for small molecules that modulate ITK PHTH/Kinase interaction.

This thesis, characterized the ITK kinase domain binding surface in ITK PHTH domain however, the complementary surface on ITK kinase domain is not known. So, further investigation must be carried out to identify the ITK PHTH binding surface on

ITK kinase domain. Co-crystallization of ITK PHTH and kinase domain will shed light into this interaction. Other way to characterize the binding surface is by mutagenesis and pull down experiments. Here, panel of mutant ITK kinase domain could be screened for their ability to disrupt its interaction with ITK PH domain using pull down assay.

References

1. Heyeck SD, Wilcox HM, Bunnell SC, & Berg LJ (1997) Lck phosphorylates the activation loop tyrosine of the Itk kinase domain and activates Itk kinase activity. *J Biol Chem* 272(40):25401-25408.
2. Linka RM*, et al.* (2012) Loss-of-function mutations within the IL-2 inducible kinase ITK in patients with EBV-associated lymphoproliferative diseases. *Leukemia* 26(5):963-971.
3. Mueller C & August A (2003) Attenuation of immunological symptoms of allergic asthma in mice lacking the tyrosine kinase ITK. *J Immunol* 170(10):5056-5063.
4. Waite JC & Skokos D (2012) Th17 response and inflammatory autoimmune diseases. *Int J Inflam* 2012:819467.
5. Koss H, Bunney TD, Behjati S, & Katan M (2014) Dysfunction of phospholipase Cgamma in immune disorders and cancer. *Trends Biochem Sci* 39(12):603-611.

6. Joseph RE, Min L, & Andreotti AH (2007) The linker between SH2 and kinase domains positively regulates catalysis of the Tec family kinases. *Biochemistry* 46(18):5455-5462.